# Cortical hyperactivity beyond immune attack: pivotal role of TNF-α in early Multiple Sclerosis

## Dissertation

Submitted to the

**Faculty of Biology**

In partial fulfillment of requirements for the

**Dr. rer.nat.**

Johannes Gutenberg-Universität Mainz, Germany

By

**Gautam Kumar Pramanik, M.Sc**.

Mainz, 2016

Tag der mündlichen Prüfung: 09.05.2017

Tag der Einreichung: 08.11.2016

# Contents

# ABBREVIATIONS

| | |
|---|---|
| MS | Multiple Sclerosis |
| EAE | Experimental Autoimmune Encephalomyelitis |
| CNS | Central nervous system |
| RRMS | Relapse remitting multiple sclerosis |
| RR-EAE | Relapse remitting EAE |
| SPMS | Secondary progressive MS |
| PPMS | Primary progressive MS |
| BBB | Blood-brain-barrier |
| CD8+ | Cluster of differentiations 8+ |
| CFA | Completes Freund's adjuvant |
| PTX | Pertussis toxin |
| MOG | Myelin oligodendrocyte glycoprotein |
| PLP | Proteolipid protein |
| CD4+ | Cluster of differentiations 4+ |
| VLA-4 | Very large antigen-4 (Integrin α-4 β-1) |
| VCAM-1 | Vascular cell adhesion molecule 1 |
| LFA-1 | Lymphocyte function-associated antigen 1 |
| ICAM-1 | Intracellular adhesion molecule 1 |
| APCs | Antigen presenting cells |
| DCs | Dendritic cells |
| MRI | Magnetic resonance imaging |
| MHC | Major histocompatibility complex |

| | |
|---|---|
| Th | T helper |
| IL | Interleukin |
| IFN-γ | Interferon-γ |
| TNF-α | Tumor necrosis factor-α |
| TGF-β | Transforming growth factor-β |
| IP-10 | Interferon gamma-induced protein |
| HLA | Human leukocyte antigen |
| Treg | Regulatory T cell |
| Foxp3 | Fork-head box p3 |
| mDC | Myeloid dendritic cell |
| pDC | Plasmacytoid dendritic cell |
| Tr1 | Type 1 regulatory T cell |
| CSF | Cerebrospinal fluid |
| NK | Natural killer |
| BDNF | Brain-derived neurotrophic factor |
| NT-3 | neurotrophin-3 |
| iNOS | Inducible nitric oxide synthase |
| ROS | Reactive oxygen species |
| $H_2O_2$ | Hydrogen peroxide |
| ATP | Adenosine triphosphate |
| $Na^+$ | Sodium ion |
| $K^+$ | Potassium ion |
| ATPase | Adenosine triphosphatase |
| $Ca^{2+}$ | Calcium ion |
| NAA | N-acetylaspartate |

| | |
|---|---|
| NMDA | N-methyl-D-aspartate |
| AMPA | α-amino-3-hydroxyl-5-methyl-4-isoxazolepropionic acid AMPAR AMPA receptor |
| ONOO/ONOOH | Peroxynitrous acid, free radicals |
| $PGE_2$ | Prostagladin 2 |
| CX3CR1 | CX3C receptor 1 |
| CCR2 | Chemokine receptor type 2 |
| NF- κB | Nuclear factor- κB |
| MAPK | Mitogen-activated protein kinases |
| TNF-R1 | Tumor necrosis factor-α receptor 1 |
| TNF-R2 | Tumor necrosis factor-α receptor 2 |
| LTP1 | Lipid-transfer protein 1 |
| CA1 | Region 1 hippocampus |
| LTD | Long-term depression |
| GM-CSF | Granulocyte macrophage colony-stimulating factor |
| GA | Glatiramer acetate |
| FTY720 | Fingolimod |
| S1PR | Sphingosine 1-phosphate receptor |
| GPCR | G protein coupled receptor |
| GABA | Gamma-aminobutyric acid |
| sEPSCs | Spontaneous excitatory postsynaptic currents |
| EPSPs | Excitatory postsynaptic potentials |
| IPSPs | Inhibitory postsynaptic potentials |
| Cl- | Chloride ion |
| LGN | Lateral geniculate nucleus |

| | |
|---|---|
| PFC | Prefrontal cortex |
| PV | Parvalbumin |
| CR | Calretinin |
| FC | Frontal Cortex |
| TPLSM | Two-photon laser scanning microscopy |
| NA | Numerical aperture |
| Ti:Sapphire | Titanium: Sapphire |
| PMT | Photon-multiplier tube |
| fMRI | Functional MRI |
| AP | Action potential |
| 2D/3D | 2 dimension/ 3 dimension |
| BAPTA | 1, 2-bis-[2-aminophenoxy]-ethane-N,N,N’,N’-tetra-acetic acid |
| OGB-1 | Oregon Green BAPTA 1 AM Ester |
| AM | Acetoxymethyl ester |
| SR101 | Sulforhodamine 101 |
| AP | Anteroposterior |
| ML | Mediolateral |
| PBS | Phosphate buffer saline |
| Brpm | Breath-rate per minute |
| mM | Millimolar |
| DMSO | Dimethyl sulfoxide |
| aCSF | Artificial cerebrospinal fluid |
| ROIs | Region of interests |
| MBP | Myelin basic protein |
| LFB-HE | Luxol fast blue-hematoxylin eosin |

| | |
|---|---|
| APP | Amyloid precursor protein |
| RT | Room temperature |
| DAB | 3,3'-Diaminobenzidine |
| RT-PCR | Real-time polymerase chain reaction |
| qPCR | Quantitative polymerase chain reaction |
| GADPH | Glyceraldehyde 3-phosphate dehydrogenase |
| Actb | Actin-beta |
| PFA | Paraformaldehyde |
| GAD | Glutamate decarboxylase |
| CamKII | Ca2+/calmodulin-dependent protein kinase II |
| DAPI | 4',6-diamidino-2-phenylindole |
| VD | Visual Discrimination |
| EPM | Elevated plus maze |
| OF | Open field |
| FC | Fear Conditioning |
| MCBL | Multicell Bolus Loading |
| VC | Visual cortex |
| SNR | Signal-to-noise ratio |
| DV | Dorso-ventral |
| mV | Microvolt |
| DNQX | 6,7-dinitroquinoxaline-2,3-dione |
| GFAP+ | Glial fibrillary acidic protein |
| ANOVA | Analysis of variance |
| SEM | Standard error mean |

## ABSTRACT

The central nervous system (CNS) is the primary target in both multiple sclerosis (MS) and the animal model of experimental autoimmune encephalomyelitis (EAE). The disease is mainly driven by infiltrating myelin specific T cells that are peripherally activated by antigen presenting cells (APCs), yet little known about how the disease itself affects neuronal activity patterns in the different cortices *in vivo*. In the last decades, growing advancement in functional imaging has been successfully applied in several other CNS diseases but its real-time application in CNS autoimmunity has not been achieved. Here, we employed *in vivo* two-photon $Ca^{2+}$ imaging to study the activity patterns of neurons in the visual cortex of mice with different phases of the EAE. By using this method, we identified spontaneous activity of the network in the visual cortex that had drastically increased followed by increased hyperactive cells in remission (disease phase with no or mild symptoms present) rather than in relapse where the disease symptoms were less prominent. In addition, frontal cortex also displayed similar activity pattern supporting that it is a cortex-wide phenomenon and such alteration of activity is independent of demyelination or cellular infiltration. Furthermore, cortical TNF-α level had significantly elevated throughout the cortex in remission mice and a reversal of increased cortex activity was achieved by intraventricular injections of infliximab, a monoclonal antibody specific against TNF-α. CamKII+ excitatory neurons were found to be surrounded by soluble TNF-α. Taken together, this thesis furnishes advances of two-photon microscopy to enable functional studies of visual and frontal cortices neuronal activity *in vivo* in different disease states of EAE.

# ZUSAMMENFASSUNG

Das zentrale Nervensystem (ZNS) ist sowohl bei Multipler Sklerose (MS) als auch im Tiermodel der experimentellen autoimmunen Encephalomyelitis (EAE) das primäre Ziel. Die Krankheit wird vor allem durch myelin-spezifische T-Zellen, die in der Peripherie durch Antigen-präsentierende Zellen (APZ) aktiviert werden, vorangetrieben. Dennoch ist relativ wenig darüber bekannt, wie das die neuronalen Aktivitätsmuster in den verschiedenen Kortizes *in vivo* beeinflusst. Die Fortschritte im funktionellen Imaging in den letzten Jahrzehnten konnten erfolgreich in anderen Erkrankungen des ZNS angewandt werden, jedoch wurde der Einsatz dieser „real-time“ Methoden bei Autoimmunerkrankungen des ZNS noch nicht umgesetzt. Hier haben wir *in vivo* 2-Photonen-Kalzium-Imaging eingesetzt um das Aktivitätsmuster der Neuronen im visuellen Kortex der Mäuse in den verschiedenen Phasen der EAE zu untersuchen. Durch diese Technik war es uns möglich eine drastische Erhöhung der spontanen Aktivität des neuronalen Netzwerkes im visuellen Kortex festzustellen, gefolgt von einem Anstieg hyperaktiver Zellen während der Remissions-Phase (Krankheitsphase mit keinen oder sehr schwachen Symptomen). Im Gegensatz dazu traten die Krankheitssymptome in der Relaps-Phase weniger auf. Zusätzlich zeigte auch der frontale Kortex ein ähnliches Aktivitätsmuster. Dies unterstützt die Annahme, dass es sich um ein Phänomen handelt, welches im gesamten Kortex auftritt und dass die Änderung der Aktivität unabhängig von der Demyelinisierung oder der zellulären Infiltration ist. Außerdem war das kortikale TNF-α bei Mäusen in der Remission im gesamten Kortex signifikant erhöht und die gesteigerte kortikale Aktivität konnte durch eine intraventrikuläre Gabe von Infliximab, ein monoklonaler Antikörper gegen TNF-α, rückgängig gemacht werden. Besonders außergewöhnlich war, dass CamKII+ exzitatorische Neuronen von löslichem TNF-α umgeben waren. Zusammengenommen zeigt diese Arbeit neue Wege der 2-Photonen-Mikroskopie auf, die es

ermöglichen funktionelle Studien der neuronalen Aktivität in frontalen und visuellen Kortizes in den unterschiedlichen Krankheitsstadien der EAE durchzuführen.

## OBJECTIVES OF THE THESIS

Recent technical progress in the field of two-photon imaging opens a real opportunity for intravital $Ca^{2+}$ imaging to detect suprathreshold activity of affected neurons in the diseased CNS. In the present thesis, we ask what are the changes in dynamics of cortical network activity in absence of clinical symptoms in the early phase of MS pathology. We employed *in vivo* $Ca^{2+}$ measurements in different disease phases of EAE mice and the findings are discussed in details. In this context, the key points of this thesis are furnished as follows:

- Reason of the study and what does the study establish?
- Why two cortical regions in remission animals were chosen for the *in vivo* experiments?
- Does CNS inflammation or demyelination impact on the neuronal activity?
- Is there any behavioral phenotype of those animals reported in the study?
- What are the mechanisms tested for neurodegeneration?
- Is there any clinical relevance of this study?

## SUMMARY OF THE RESULTS

Based on the current knowledge in the MS field and results from our study, we report the following findings in the thesis:

- No functional study available about the state of functional network activity in EAE. Hence for the first time, our study establishes altered activity pattern in the first remission (disease phase with no or mild clinical symptoms) by *in vivo* two-photon $Ca^{2+}$ imaging.

- Cortical demyelination or inflammation is not predominant in early remission and no obvious cognitive or sensory related behavioral deficits are observed in those animals.
- We report, increased cortical TNF-α expression is the key modulator for altered neuronal activity in early remission state which may trigger a cascade of pathways that are related to neurodegeneration in the later phases of disease.
- TNF-α has been identified as potential target in this study and treating it with anti-TNF-α restores back network activity to normal level. Hence, administering anti-TNF-α can be considered as prospective therapeutic agent in early phase of Relapse-remitting MS (RRMS).

# INTRODUCTION

Multiple sclerosis (MS) is the most common chronic disabling neurological autoimmune disease of the central nervous system (CNS) in young adulthood. It affects approximately 500,000 individuals in Europe alone and more than 2 million people world-wide (Flachenecker and Stuke, 2008). MS is a chronic neuroinflammatory disease that involves multifocal demyelination, axonal injury, and lesion formation. These alterations are preceded by neuronal damage in the CNS which distorts and disrupts action potential conduction thereby causing clinical manifestation. The symptoms are discrete and recurrent attacks of visual impairment, lack of coordination, motor, sensory and cognitive dysfunction, and many others strongly impacting the quality of patients' life (Smith and McDonald, 1999, Baranzini et al., 2009). The etiology of MS including its initial event remains unknown and there are several causative factors responsible for MS. Subjects with genetically predisposition and with a critical contribution of environmental effect or encephalomyelitis viruses are mostly responsible factors considered by the MS society (Ascherio and Munger, 2007, Hoglund and Maghazachi, 2014). Furthermore, increasing evidence in the field suggest that epigenetic influences also play a role (Burrell et al., 2011). Specialists agree that a combination of these factors might be necessary in order to develop MS (Fig. 1).

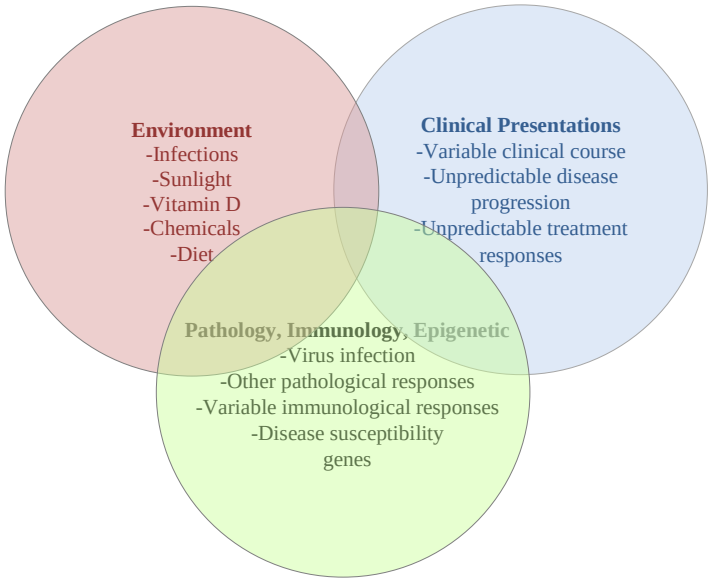


Figure 1: Complexity of the causes of the MS. All Causes are enlisted in color-coded circles. Specific to a combination of causes are considered as responsible factors for developing MS.

The course of the disease is very heterogeneous. After an initial acute episode, the majority of the MS patients (85%) display a relapsing course or symptoms over a short span of time followed by recovery (a form known as relapse-remitting MS or RRMS) (Fig. 2) (Sospedra and Martin, 2005). However, the relapse-remitting course blends into a slow, but permanent progression, and recovery is less effective (secondary progressive; SPMS). The other prominent form is primary progressive MS (PPMS), in which about 10% patients present a steady progression of the disease over time. In all MS types, the clinical course spans over several decades and patients show less inflammation rather more axonal loss in the CNS at earlier time point of the disease (Bashir and Whitaker, 1999, Compston and Coles, 2008, Leray et al., 2010).

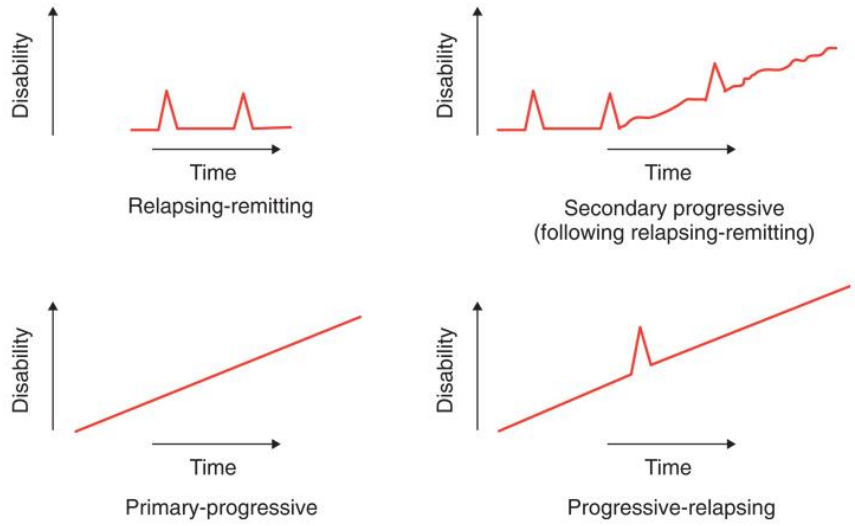


Figure 2: Clinical subtypes of MS. Relapse-remitting: characterized by discrete attacks that evolves over days to weeks followed by some decree of recovery. Secondary progressive: indicative of initial relapses, followed by gradual deterioration. Primary progressive: characterized by steady function decline from the onset of the disease. Progressive relapsing: characterized by steady functional decline from onset of the disease with later superimposed acute attacks. Adapted from (Lublin and Reingold, 1996).

The underlying pathomechanisms in MS is very complex and believed to be mediated by immune-mediated loss of blood-brain-barrier (BBB) integrity and massive infiltration of

immune cells (mainly specific subtypes of T cells and mononuclear cells e.g. monocytes, macrophages and resident microglial cells) via a cascade of signaling pathways causing persistent inflammation and demyelination. Inflammation is predominantly dominated by CD8+ T cells and activated macrophages or microglia. Activated CD8+ T cells are frequently found in close to destructed myelin and axonal damage area in white matter lesions. These processes lead to further production of proinflammatory cytokines and chemokines locally by different immune cells (CD4+ T cells, macrophage/ microglia etc.). Recent data suggests a direct interaction between T cells and neurons via cell adhesion molecules could possibly lead to axonal injury in experimental model of MS (Fig. 3) (Liblau et al., 2013). There is also a release of free radicals, and glutamate-mediated excitotoxicity or direct cytotoxicity including demyelination and neuronal death are common in progressive form of the disease. Demyelination is followed by axonal damage and further grey matter degeneration, caused by autoreactive and inflammatory factors giving rise to clinical symptoms. Whereas extensive remyelination occurs in 20% MS patients, the continuous demyelination and remyelination seems to exhaust the repairing capability of perishing neurons (Patrikios et al., 2006).

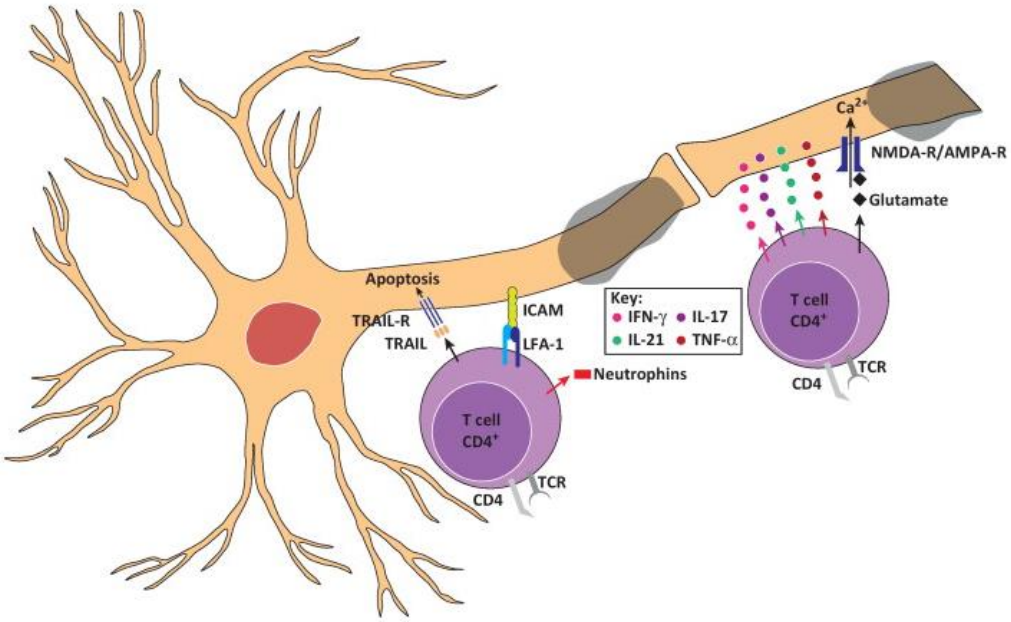

Fig 3: Schematic illustration of interaction between T cells (violet) with axons (maple gold) via lymphpcyte function-associated antigen-1 and cell adhesion molecules expressed on neurons. Adapted from (Liblau et al., 2013).

Animal models are essential in order to understand the underlying disease pathology and develop therapeutic approaches. The most commonly used animal model for MS is experimental autoimmune encephalomyelitis (EAE), providing an attractive setup of studying clinical, neuropathological and immunological aspects of MS, and testing possibilities for therapeutic treatments. Besides, due to the limited access to *ex vivo* MS patients' material as well as the disease heterogeneity, animal models for MS are required. The histopathological hallmarks of EAE also resemble several aspects of the pathology of the human disease (Podojil et al., 2006, Lassmann, 2007, McFarland and Martin, 2007, Denic et al., 2011). EAE was developed following Louis Pasteur's trials to produce vaccine against rabies virus that contained spinal cord and brain tissue. Following the injections, patients developed an immune response towards their own myelin, an active component of axons, causing encephalomyelitis (Freund and McDermott, 1942, Baxter, 2007). Since then, EAE was refined and reproduced in a variety of animals (rodents, rabbits, monkey etc.) (Constantinescu et al., 2011) by active immunization with myelin antigens in conjugation with completes Freund's adjuvant (CFA) and pertussis toxin (PTX) (Hofstetter et al., 2002) or by transfer of myelin specific encephalitogenic T-helper lymphocytes also known as passive EAE (Gold et al., 2006, Croxford et al., 2011, McCarthy et al., 2012). The classical antigens shown to amplify EAE are myelin oligodendrocyte glycoprotein (MOG) in C57BL/6 while proteolipid protein (PLP) in SJL/J mice and, non-myelin antigens (S-100β, a glial specific protein expressed in astrocytes) induce EAE as well (Wekerle et al., 1994, Pollinger et al., 2009, Miller et al., 2010, Stern et al., 2010, Constantinescu et al., 2011). Moreover, in mice,

different strains respond differently depending on the age, gender and have various phases of disease progression (Stromnes and Goverman, 2006).

In active EAE, the clinical symptoms start with the progressive loss of functions in the caudal to rostral direction. Symptoms begin with loss of tail tone followed by hind limb paralysis and then upper limbs, accompanied by intense weight loss. As similar to human form, the disease may spontaneously resolve (acute monophasic) or continue to show developing symptoms (chronic phase). However, the EAE can also exhibit fluctuating course, with progressive disease episodes followed by partial recovery (known as "relapse-remitting"). Depending on the EAE model and the disease severity, there are also uncommon phenotypes observed in some cases e.g. ataxia, spasticity, inability to walk straight or rolling in an axial-rotary manner (Stromnes and Goverman, 2006).

## CLINICAL DEFICITS: COGNITIVE AND SENSORY IMPAIRMENT IN MS

### Clinical characteristics and neuropsychological assessment

MS affects various aspects of cognitive and sensory functioning including efficiency of information processing, verbal and visual-spatial memory, executive functioning, attention and visual perceptual processing at various stages of the disease (Audoin et al., 2003, Chiaravalloti et al., 2005, Chiaravalloti and DeLuca, 2008, Tomassini et al., 2012, Di Filippo et al., 2015). Several MS pathologies seem to contribute to the presence and worsening of such deficits. In many cases, information processing speed and visual learning and memory seem to be mostly affected (Diamond et al., 2008, Genova et al., 2012). Cognitive impairment has been observed irrespective of duration of the disease and is mildly associated with physical disability. However, cognitive disturbances are more severe in patients with chronic phase of the disease compared to early phase or relapse-remitting phase and depression, and fatigues have been identified as important factors to cognitive impairment. Dementia is

another rare but specific and subtle cognitive deficits observed in patients with a substantial variability (Zarei et al., 2003, Leyhe et al., 2005). In the context of information processing, its efficiency refers to the ability to maintain and manipulate the arriving information for a short time in the brain known as "working memory" and the speed with which one can process the information is "processing speed". Most often, reduction in information processing speed is one common deficit in MS which concurrently occurs with other cognitive deficits. Long term memory loss and attention deficits are directly associated with deficits of working memory and processing speed. Furthermore, visual perceptual processing includes recognizing and understanding the pattern of a visual stimulus accurately. In MS, difficulties in primary visual processing (optic neuritis) can show detrimental effect on visual perception process although perceptual deficits are independent of primary visual or other cognitive abnormalities (Nakajima et al., 2010, Burman et al., 2011).

## CNS CELLS – AN OVERVIEW

CNS is the most complex system of the human body composed of neurons and glial cells. These both cell types are directly or indirectly involved in almost all neurological and neurodegenerative diseases. Although, it is estimated that there are more than 100 billion neurons present in the human brain forming a complex network, this is outnumbered by the glial cells by ten times with a steady rise in the total count through the increasing evolutionary complexity of the brain. Four different glial cell types are predominantly observed in the CNS: astrocytes, NG2 cells, oligodendrocytes (having neural origin; i.e. ectodermal) and microglia (non-neuronal origin; i.e. mesodermal). In contrast to other glial cells, microglia originate from invading macrophages during early developmental stages of the brain and settle ubiquitously within the CNS (Verkhratsky and Butt, 2007).

## DISEASE MECHANISM

According to the current understanding, auto-aggressive CD4+ T cells are primed in the periphery which leads to upregulation of its adhesion molecules and chemokine receptors. Once activated, the CD4+ T cells are able to cross the BBB (Fig. 4). Consequently, CD4+ T cells adhere to the endothelium via adhesion molecules, such as VLA-4/VCAM-1 interactions (Charo and Ransohoff, 2006) and crawling on against the blood flow, until they find a site for diapedesis. Further interaction of chemokines with their chemokine receptors induce G-protein-mediated activation of LFA-1/ICAM-1 resulting in diapedesis through endothelium (Engelhardt and Ransohoff, 2005, Engelhardt and Coisne, 2011). Once they reach the perivascular space, CD4+ T cells get reactivated by encountering with local APCs that can be either infiltrating DCs and perivascular macrophages or locally activated microglia and astrocytes (Greter et al., 2005, Dittel, 2008), leading to penetration of the CNS parenchyma through glia limitans (Bechmann et al., 2007).

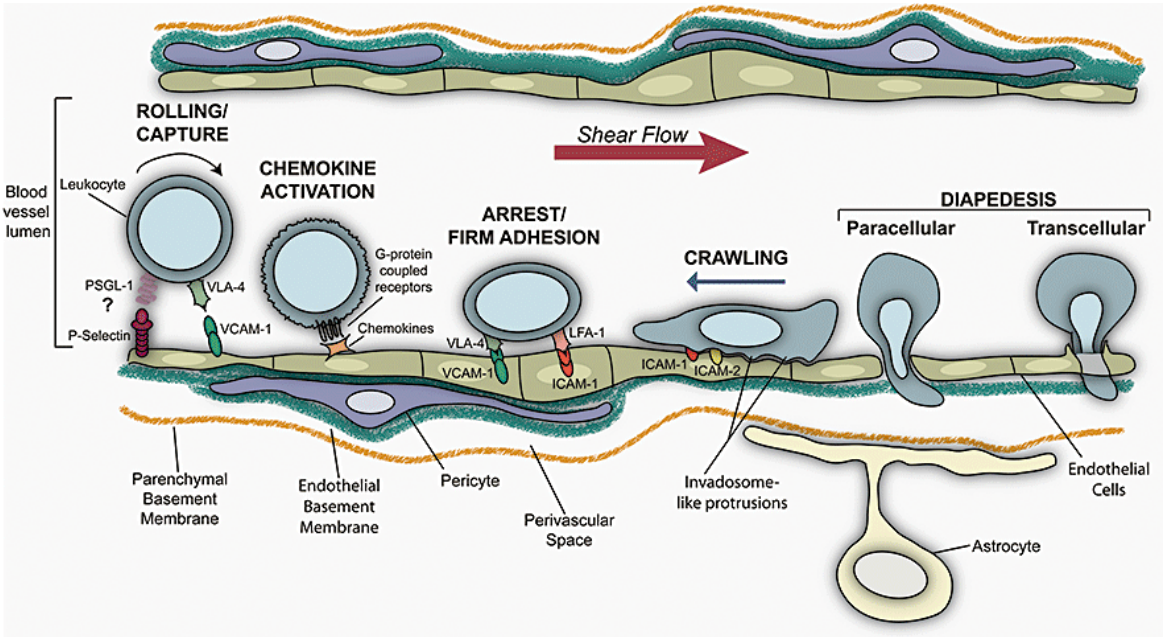


Figure 4: Cartonic demostrations of major phases involved in T cells migration through blood-brain barrier (BBB). Adapted and modified from (Greenwood et al., 2011).

## IMMUNE SYSTEMS IN MS

The innate immune system called self-protective and maintenance machinery part of homeostasis of our body. It is our first line of defense mechanism enabling us to resist infections. It is also known as non-specific immune system. Unlike adaptive immunity, innate immunity has no memory of the encounters, meaning does not remember any specific antigen it encounters, and hence does not provide any protection against future infection. Although these two immune systems (Innate and adaptive) have distinct functions, under circumstances; components of innate immune system influence the adaptive immune system and vice versa. Nonetheless, much has been done to understand the etiology of MS, with major focus on the role of adaptive immune system; the innate immune system can also turn destructive causing autoimmunity. In this part, we will summarize the potential role of the myeloid and lymphoid cells in the pathogenesis of MS and EAE; specially, T cells, dendritic cells or DCs, microglial cells (Wu and Laufer, 2007, Zozulya et al., 2009, Mishra and Yong, 2016).

### T cells

Although the etiology of MS remains to be clearly established, the most widely accepted fact about MS pathogenesis implicates around the cellular immune response against own-self as the central requirement. A major amount studies reported the presence of autoreactive T cells in the perivascular space and parenchyma in the very early phase of the disease. These views are supported by several histopathological observations in the inflammatory lesions and in recurrent sessions seen with MRI (Lucchinetti et al., 2011, Saxena et al., 2011, Ellwardt et al., 2016). A sequence of events involved in the development of inflammatory process in MS and number of factors have been found to be important. The initial sequences of pathological events occur in two phases: (a) priming/activation T cells and (b) subsequent recruitment of other cells followed by the effector phase. Antigen presentation is crucial process for the

generation of T cell mediated responses and professional APCs (DCs, monocytes, microglia/macrophages) are capable of initiating such primary immune response by the representation of antigen to naïve T cells leading to priming of these T cells (Sprent, 2005). CD4+ T cells recognize antigens that are associated with the MHC class II molecules whereas CD8+ T cells are associated with MHC class I molecules. Depending on the co-stimulatory signals from APCs, both CD4+ and CD8+ T cells become fully activated. However, such activation process depends on co-stimulatory signals if those T cells are already primed or exposed to their antigens (Bour et al., 1995, Mangalam et al., 2006). And both CD4+ and CD8+ T cells respond to MS pathogenesis at different steps and have very different roles. Nevertheless, it is well established that myelin-specific CD4+ T cells mainly drives MS and EAE pathogenesis. Earlier studies showed that different subset of CD4+ T cells especially Th1 rather than Th2 cause EAE (268) and more recently Th17 cells, have been identified to cause severe form of EAE (Komiyama et al., 2006, Haak et al., 2009, Jadidi-Niaragh and Mirshafiey, 2011, Ulges et al., 2016). Each of these CD4+ T cells produces large amount of different cytokines (e.g. IFN-γ, IL-6, IL-17, IL-23, TNF-α and TGF-β etc.) and T cells differentiation to direct attack on myelin constituents wildly depends on the variations in cytokine profiles (Lovett-Racke et al., 2011, Petermann and Korn, 2011). In MS, much less is known about CD8+ T cells but they are much better suited to mediate CNS damage compared to CD4+ T cells as because these cells are more prevalent in MS brain tissue, and they secrete chemo-attractants (IL-16, IP-10) for CD4+ myelin-specific T cells (Liu et al., 2001, Dufour et al., 2002, Skulina et al., 2004, Miljkovic and Spasojevic, 2013). CD8+ T cells particularly can recognize antigen presented on HLA class I on neurons (Figure 4) and oligodendrocytes and kill the target cells (Friese and Fugger, 2009, Mars et al., 2011). Another population of CD4+CD25+ T cells (also known as Treg), have been found to inhibit INF-γ production and proliferation of encephalitogenic cells proving it to the regulatory population among the CD4+ family (Arellano et al., 2015). Tregs can also affect APC function directly through

several mechanisms such as inhibiting DC maturation (Liang et al., 2008). Several studies have shown that depletion of Treg cells prior to immunization for active disease could aggravate the disease course to more severe form (Akirav et al., 2009).

## Dendritic cells

Dendritic cells are "professional antigen presenting cells" that play vital role in promoting activation and differentiation of naïve T cells. Based on their surface markers, they are distinguished into two different categories: myeloid (mDC) and lymphoid/plasmacytoid (pDC) (Lipscomb and Masten, 2002). DCs interaction with T cells determines T cell differentiation into either effector T cells or regulatory T cells (Treg and induced Tr1 cells) (Shortman and Heath, 2001, Gilliet and Liu, 2002, Paterka et al., 2016, Wasser et al., 2016). mDCs can selectively activate natural killer (NK) cells and trigger proliferation of its subset. This activated phenotype of DC-mediated inflammation is more commonly pronounced in SPMS patients than RRMS accompanied by increased level of TNF-α, IFN- γ, IL-6 and IL-23 (Huber et al., 2014, Quintana et al., 2015). Conversely, pDCs usually found to be elevated under neuroinflammatory conditions including CSF of MS patients (Stasiolek et al., 2006).

## Demyelination and axonal degeneration

The major determinant of the permanent neurological impairment during MS is the loss of myelin followed by axonal degeneration. Clinical, pathological and MRI reports suggest widespread axonal degeneration occur independent of acute inflammatory lesions and can occur throughout the entire disease course (Lovas et al., 2000, Su et al., 2009). However, several histopathological results revealed the presence of substantial axonal damage in the active lesions (Haines et al., 2011). In other cases, transected and dystrophic axons in the sites

of active inflammation and demyelination confirm partial or total axonal transection (Trapp et al., 1998, Kornek et al., 2000). Axonal damage takes place in every newly formed lesion, and the cumulative loss of axon is considered to be the reason for progressive and irreversible neurological disability in MS (De Stefano et al., 2001). And the extent of axonal injury correlates with the degrees of inflammation in active MS lesions (Bjartmar and Trapp, 2003). In early stage of MS, axonal loss is clinically silent because the human brain has remarkable capability to compensate for it (Bjartmar et al., 2003). The transition of RRMS to SPMS is thought to occur when brain exhausts its capacity to compensate for spreading axonal loss (Bjartmar et al., 2003). Several different mechanisms have been described for the axonal injury in brain and spinal cord including direct attack of cytotoxic CD8+ T cells on myelin constituents of axons (Huseby et al., 2012), or activated CD4+ T cells mediated injury (Mars et al., 2011). Axonal atrophy can also be mediated through innate immunity driven by activated microglia/macrophages, monocytes, proteolytic enzymes (inducible nitric oxide synthase or iNOS), reactive oxygen species (ROS), derivatives of nitric oxide (NO), free radicals ($H_2O_2$) or by proinflammatory cytokines (Fig. 5) (Martins et al., 2011, van Horssen et al., 2011). One of the main structural changes during progressive MS is the loss of myelin that greatly impairs the efficacy of action potential propagation. Demyelinating axons have higher energy demand for ATP and in response, voltage-gated sodium channels become redistributed all along the axon and synthesis is upregulated (Su et al., 2009). The ATP demand exceeds the production capabilities of existing mitochondria, and the $Na^+/K^+$ ATPase pumps crucial for maintaining ionic gradients which begin to fail. As a result, intracellular accumulation of Na+ ions leads to reversal of $Na^+/Ca^{2+}$ exchanger that normally moves $Na^+$ ions into the cell and $Ca^{2+}$ from the cell (Stys et al., 1992, Dutta et al., 2006). Prolonged elevation of intracellular axoplasm' $Ca^{2+}$ levels can stimulate a multiple downstream events (including glutamate-mediated cytotoxicity) that ultimately results in mitochondrial dysfunction and hypoxic-like axonal damage (Mahad et al., 2008a, Su et al., 2009, Mao and Reddy, 2010). In

MS patients, defects of mitochondrial respiration chain complex IV has been associated with hypoxia-like tissue injury and reduced in N-acetylaspartate (NAA), which are signs for neuronal dysfunction and damage (Mahad et al., 2008b). In chronic neurodegenerative conditions, alteration of glutamate homeostasis has been well documented (Pitt et al., 2000, Dutta and Trapp, 2011). A whole genome microarray approach revealed decreased expression of glutamate receptors in demyelinating neurons (Dutta et al., 2011). Alteration in synaptic properties in neurons result in glutamate-mediated excitotoxicity which further lead to death of oligodendrocytes as well as axonal damage (Pitt et al., 2000). Aberrant accumulation of glutamate has been detected in acute MS lesions (Srinivasan et al., 2005, Haines et al., 2011). Several potential sources of glutamate release were found close to dystrophic neurons including activated immune cells such as microglia/macrophages and astrocytes (Groom et al., 2003, Correale and Farez, 2015). Excessive release of glutamate activates ionotropic and metabotropic receptors at the post-synaptic membrane resulting in accumulation of $Ca^{2+}$ at the toxic level and cell death (Su et al., 2009).

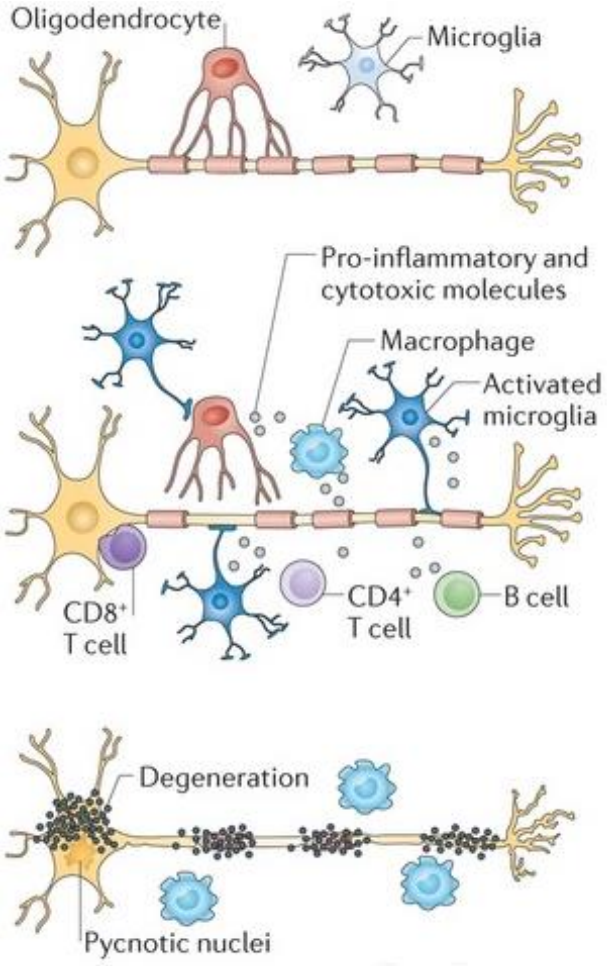


Figure 5: Sequence of inflammatory events in the course of demyelination and degeneration. Adapted from (Calabrese et al., 2015). Infiltration of activated T-cells followed by microglia activation leads to direct or indirect damage of axons in the CNS.

### Activated microglia/macrophage-mediated damage:

As part of CNS resident cells, microglia are immunocompetent in nature forming active defense system by directly contributing to neuronal survival through cellular maintenance and innate immunity. They comprise approximately 10% of all glial cells and have myeloid origin invading the brain during early embryonic development. In the healthy adult CNS, they are defined as resting microglia displaying a small soma and numerous highly branched and mobile processes. The resting microglia take part in maintenance of the CNS. Importantly, mature microglia are highly equipped with several receptors and immune recognition sites.

Hence, upon encountering an antigen i.e. virus, bacteria or foreign peptide substances, these resting microglia turn into activated state and display primary phagocytic function (Polazzi et al., 1999, Raivich, 2005). Under pathological conditions (e.g. CNS injury or neurodegeneration), activated microglia plays different role depending on disease pathology, target area and phase of the disease. In the context of MS pathology, role of activated microglia is still not completely understood. Several studies in neurodegenerative diseases reported that activated microglia can help recruit CD11c expressing activated macrophages/monocytes which can further assist to recruit inflammatory cells including other microglia and dendritic cells (Lull and Block, 2010, Perry and Teeling, 2013, Fenn et al., 2014).

In MS, axonal damage or CNS lesion development has been strongly correlated with the presence of inflammatory cells that include activated microglia/macrophages (Carson, 2002, Fu et al., 2014). During active disease progression these cells express different surface and intracellular markers, which can re-stimulate or activate several other inflammatory cells (Th cells). Furthermore, expression of these markers can help to recruit other resting microglia/macrophages or CNS infiltrating macrophages. Besides, activated microglia/macrophages produce a large array of hazardous molecules in response to disease progress, including proteo- and lipolytic enzymes, cytotoxic cytokines, excitotoxins and reactive oxygen species (e.g. NO, iNOS, ROS, $H_2O_2$, $O_2$ and ONOO/ONOOH) or their intermediates. These molecules have been identified as potential inducers of axonal damage. In particular, mitochondrial aggression followed by the release of ROS has been strongly associated with axonal injury (van Horssen et al., 2011). In case of an over activation, these cells can have much more detrimental effects by releasing diverse cytotoxic molecules including proinflammatory cytokines (e.g. TNF-α, IL1β, IFN-γ, $PGE_2$ etc.) or chemokines (CX3CR1, CCL2) (Block and Hong, 2005).

## Cytokines and Neurotrophic Factors

Cytokines and their receptors play crucial role in the inflammatory process and mediate the pathogenesis of MS. Their relative availability in the healthy individual is usually low or even absent and produced in a small quantities in response to a local stimulus (Ozenci et al., 2002). Based on the mode of action, cytokines have been classified into pro- and anti-inflammatory cytokines and to maintain cellular homeostasis, a dynamic balance between these two cytokines is essential. In MS, key pro-inflammatory cytokines are (IFN-γ, IL-17 and TNF-α) released from Th1, Th17 effector cells in the periphery. At the disease peak of MS, an elevated level of pro-inflammatory IFN-γ and peripheral TNF-α induces inflammation in the CNS followed by drastic increase of IL-17 within the demyelinating MS lesions (Panitch et al., 1987, Hofman et al., 1989). GM CSF, secreted by autoreactive T cells, is another proinflammatory cytokine and an important immunomodulator. Study suggests GM CSF is necessary for the development of autoimmune CNS inflammation (Rasouli et al., 2015).

On the other hand, anti-inflammatory cytokines (TGF-β and IL-4) show distinct role to control the disease progression and inflammation in MS (Soderstrom et al., 1995). In the CNS, IL-4 and TGF-β shows neuroprotective effect; especially an increased production of TGF-β has been found to reduce inflammation in autoimmune disease (Kuruvilla et al., 1991, Guenova et al., 2015). IL-4 production in the CNS is essential for controlling autoimmune inflammation and in several clinical studies, treating patients for IL-4 production has been successful to ameliorate disease severity (Valenzuela et al., 2007). BDNF is another key modulator of the neurotransmitter release and synaptic plasticity, and has been hypothesized to play a role in the neuroprotective mechanisms of some MS therapies (Azoulay et al., 2005, Zuccato and Cattaneo, 2009, Jones et al., 2010).

One of the major cytokine in chronic inflammatory disease is TNF-α. Peripheral TNF-α act as pro-inflammatory cytokine in the innate immune system by activating cascade of pathways including NF-κB, MAPK and the apoptotic signaling pathway (Xu et al., 2015). In the CNS, two different types of TNF-α are found: membrane bound and soluble forms, and act on two different receptors (TNF-R1 and TNF-R2). While soluble form of TNF-α is known to be released from glial cells (astrocytes and microglia) as well as neurons. However, depending on their source of release and receptors interaction each exerts neuroprotective or neurotoxic effect differently (Lieberman et al., 1989, Chung and Benveniste, 1990, Morganti-Kossman et al., 1997, Pickering et al., 2005). In particular, it facilitates glutamate excitotoxicity, both directly and indirectly by inhibiting glutamate transporters on astrocytes. It can directly affect glutamate transmission by increasing surface expression of AMPAR on cortical synapses thereby increasing synaptic strength (Carroll et al., 2001, Beattie et al., 2002, Stellwagen and Malenka, 2006a). TNF-α has been found to play a key role in synaptic plasticity by inhibiting LTP in the CA1 and dentate gyrus regions of hippocampus (Cunningham et al., 1996, Butler et al., 2004, Pickering et al., 2005). Together these cytokines play important role in MS pathogenesis via several direct and indirect mechanisms.

## Current therapies for MS

The first set of drugs approved for the treatment of RRMS was subcutaneous introduction of IFNβ-1b, IFNβ-1a and Glatiramer acetate (GA) which proved to reduce relapse rates by 29 – 34% compared to placebo (Goodin et al., 2002). The main mechanisms of action of IFNβ postulated are through anti-inflammatory process by down-regulating pro-inflammatory cytokines such as IFN-γ while increase in production of anti-inflammatory cytokines and neurotrophic/gliothrophic factors, decrease in migration of T cells across BBB (Ozenci et al., 2000, Sega et al., 2004, Dhib-Jalbut and Marks, 2010).

Glatiramer acetate (GA) is a synthetic mixture of polypeptides and its mechanism of action are not well known. However, studies suggest that GA triggers anti-inflammatory process by Th2 shift of Th1 cells in the periphery through an inhibitory effect on APCs. Several side effects have been reported from severe to mild associated with these agents affecting patients' convenience, quality of life and compliance.

Today, a number of therapies are available with more safety concerns. Mitoxantrone has been approved for the use in severe forms or relapsing MS. It is an antineoplastic and immunomodulatory agent and presumed to induce macrophage-medicated suppression of B, T helper as well cytotoxic T lymphocyte function (Scott and Figgitt, 2004). However, the specificity for this drug in MS is not clear and there are some side effects like cardiac toxicity and leukemia has been documented regarding Mitoxantrone administration (Ellis and Boggild, 2009). One of the most efficient product until today is Natalizumab and it is a monoclonal antibody against α subunit of integrin α4β1 receptors on T lymphocytes. It mainly blocks adhesion of activated T cells with vascular cell adhesion molecules (VCAMs) expressed on laminal surface. Less severe side effects e.g. progressive multifocal leukoencephalopathy or fatal infectious demyelinating disease of the brain has been shown with Natalizumab administration (DeAngelis, 2009).

To overcome the limitations of current therapies and to improve convenience, identifying oral agents has been the greater interests of current researchers considering that the agents should be able to promote endogenous repair via anti-inflammatory mechanisms and prevent neurodegeneration. Fingolimod (FTY720) is a new class therapeutic compound for the treatment of relapsing MS launched in 2010 (Cohen et al., 2010, Kappos et al., 2010). It is believed to act as a modulator for sphingosine 1-phosphate receptor (S1PR) expressed on

lymphocytes via G protein coupled receptor (GPCR) activation pathway. As a functional consequence, migration of lymphocytes in the CNS is prevented and inflammation reduced (Graler and Goetzl, 2004, Matloubian et al., 2004). However, phosphorylated form of FTY710 has been shown to effect on other important functions in regulating physiological and pathophysiological process in various systems.

Given the complex picture of disease pathogenesis of MS, a potent drug should be able to prevent or at least slow down the course of disease progression. Although over last 20 years, a lot of progress was made in therapy regime of MS but it failed to prevent any long term disease progression in human (Killestein and Polman, 2005). The search for more effective approaches is therefore warranted and it has to focus on distinct target mechanism or marker to develop more specified therapeutic strategies for various stages of the disease course.

## THE CORTEX AND ITS FUNCTIONAL ORGANIZATION

### Neurons

Neurons are the core components of the CNS. They are classified based on their architecture and function as well. Each neuron in a network is responsible for different tasks. In the adult cortex, there are two different types of neurons identified based on the receptors present on them: excitatory and inhibitory, and the functional (re)organization of cortical circuitry mediated through the connections between both excitatory and inhibitory cells (Kaas et al., 1990, Yamahachi et al., 2009). At the superficial cortical layers, pyramidal neurons (the primary excitatory populations that release neurotransmitter glutamate; also known as glutamatergic neurons) form long-range connections by projecting axons horizontally. These cells undergo a process of sprouting and synaptogenesis upon altered sensory experience (Chino et al., 1992, Darian-Smith and Gilbert, 1994, Kossut and Juliano, 1999). While the

role of excitatory cells has received most attention, inhibition is also play a critical role in fine-tuning specific firing properties of excitatory neurons, e.g. in the visual cortex, these cells known to heavily involved in orientation selectivity phenomenon (Sohya et al., 2007, Kerlin et al., 2010, Runyan et al., 2010). Inhibitory cells are also known as gatekeeper cells of the brain, use GABA as its neurotransmitter predominantly. In layer 2/3, locally projecting inhibitory interneurons comprise 20-25% of all cortical neurons (Gabbott and Somogyi, 1986, Hendry et al., 1987). One key function of these neurons has been characterized, apart from orientation selectivity phenomenon, is to regulate of experience-dependent plasticity in adult brain (Fu and Zuo, 2011). Excitatory cells in general look very similar in shape and morphology in contrast to inhibitory neurons which vary among themselves and they have different embryonic origins. Moreover, there are many subtypes of inhibitory neurons that express different markers and often have different patterns of firing.

## ANATOMY OF NEURONS

Like other cells, a typical neuron consist of cell body or soma which act as main processing center and carry most common features like other cells including producing enzymes, proteins and other essential chemicals. It functions as a ‘manufacturing’ and ‘recycling plant’. Neuronal membranes with its lipid bilayer properties serves as a barrier to enclose cellular materials, cytoplasm and does not allow ions to freely enter into the cell (Byrne, 1997, Lodish et al., 2000). Diffusion of water and nutrients occurs through aquaporins, a specialized membrane transport proteins, via osmosis. However, neurons are specially equipped with several other important components e.g. filaments like processes from the soma called dendrites which extends for hundreds of micrometers and branches like tree. Dendrites of one neuron connect with the axonal terminal or axonal bouton of another neuron via synapses (Synaptic clefts) forming a highly complex neuronal circuit and transmit information using

pulse frequency modulation of action potentials (Byrne, 1997, Lodish et al., 2000). It is primarily the surfaces of the dendrites called dendritic spines that receive synaptic inputs (chemical signals) from other neurons in the circuit. Every neuron has the capability to contact with many neurons close or long distance via thousands of synapses. Dendrites are the specialized neuronal units that can receive both excitatory and inhibitory synaptic inputs from presynaptic terminals. However, these dendrites cannot generate a local action potential due to low concentration of ion channels, but recent studies show that the dendrites can preprocess the synaptic inputs (Golding and Spruston, 1998, Thome et al., 2014). An excitatory input increases the membrane potential when the net effect of neurotransmitter release is to depolarize the membrane, bringing it closer to the membrane potential threshold (EPSPs). Typically this effect is mediated by opening of ion channels for sodium ($Na^+$) and calcium ($Ca^{2+}$) ions. Conversely, an inhibitory synaptic input decreases the membrane potential by driving it further away from the threshold membrane potential (IPSPs), because the net effect of neurotransmitters release is now to hyperpolarize the membrane, making it more difficult to reach the electrical potential threshold (Purves et al., 2001). These types of inhibitory synapses work by opening different chloride ($Cl^-$) or potassium ($K^+$) ion channels in the membrane. An action potential will result if the potential across the neuronal membrane is equal to the threshold potential. A single presynaptic neuron does not possess sufficient electrical response to generate an action potential in a postsynaptic neuron. However, an action potential can result from the integration of many excitatory post synaptic potential (Purves et al., 2001). In a healthy neuron, EPSPs and IPSPs are summed spatiotemporally. In particular, spatial summation of EPSPs-IPSPs results in more drastic depolarization or hyperpolarization closer to the axon hillock than any other region. This is due to the fact that there is largest concentration of voltage gated ion channels in the axon hillock and hence has the lowest membrane potential (Purves et al., 2001). While temporal summation has an additive effect on the membrane potential. If many EPSP events occur in short period of time

then the individual effects will be summed together which more likely to generate an action potential. At the axon hillock, spatial and temporal inputs are integrated to generate action potentials that propagate down the axon to axonal boutons (Kandel et al., 2013).

The main conducting unit of a neuron is an axon, another longer extension of the soma arising from axon hillock, the site where axon connects with the cell body. Axons are capable of conveying electrical signals or information long distances to different targets. These are usually wrapped with myelin sheaths, specific insulation formed by oligodendrocytes and Schwann cells that enable axons more conductive to travel action potential faster (Lodish et al., 2000, Purves et al., 2001). Multilamellar structure of myelin displays potentially high electrical resistance, which increases the velocity and conduction efficacy of an action potential (Chang et al., 2016). Although, myelin sheath itself does not allow the regeneration of any action potential, the conduction of the electrical signal passively decays approximately 50% of its peak value down the axis of a myelinated axons. Between each pair of successive wrapping there is a gap called Nodes of Ranvier, uniformly spaced at 1 to 2 mm and this exposes the axon directly to the extracellular fluids. The Nodes of Ranvier hosts large number of gated ion channels which helps in regeneration of an action potential, and some of these ion channels are voltage gated or chemically gated that can be excited to exchange ions or chemicals from extracellular fluids once an action potential reaches them. The propagation of an action potential occurs in a leaping fashion from node-to-node, is called salutatory conduction and combination of myelin sheath and the Nodes of Ranvier rapidly increases the conduction efficiency (Chang et al., 2016).There are some neurons which are non-myelinated in the CNS and the action potentials do not decay in these neurons. However, without the myelin sheath the conduction velocity of an action potential is much slower down the length axon. Similarly, in some neurological diseases, there might be a rearrangement of the Nodes

of Ranvier in a non-uniformed manner which may lead to inconsistency in the pulse frequency of the action potentials.

## The primary visual cortex

### Anatomy

The primary visual cortex is responsible for visual information processing and is one of the best understood areas of the cerebral cortex to date. This cortical region is broadly known as V1, Broadmann 17 or striate cortex. It is located at the posterior pole of the occipital cortex in the both hemisphere of the visual systems and process signals independently (Fig. 6). It is considered to be highly specialized region of the cerebral cortex to process visual information about static and moving objects with excellent pattern recognition capabilities. In fact, the concept of strong degree of orientation and direction selectivity was first described in V1 of macaque monkey by Hubel and Wiesel (Hubel and Wiesel, 1968). Apart from V1, there are 20 separate regions (e.g. V2, V3, V4 are named as extrastriate cortex) of visually related cortical areas have been recognized, each of which directly or indirectly contribute to the visual information processing in V1.

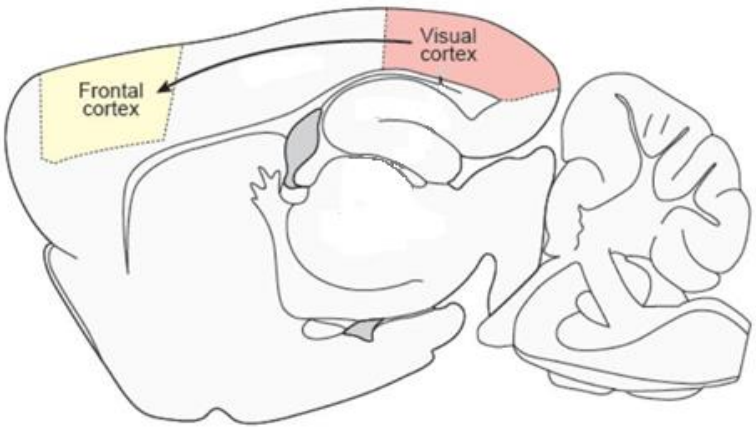


Figure 6: Classical schematic of visual and frontal cortices in the brain. Adapted from (Stroh et al., 2013).

## Basic circuitry and Cellular elements

Area V1 is a cortical area with most well-defined anatomical boundaries shown by previous studies, both histologically and MRI (Carandini, 2012). The estimated number of neurons present in average areas of V1 in human is around 140 million in each hemisphere (Chichilnisky and Wandell, 1995), of which mostly spiny excitatory (pyramidal or stellate) cells and rest are smooth or sparsely spiny interneurons (mostly GABAergic). Layer 1 is nearly aneuronal or represent very few neurons (mostly GABAergic), composed of dendritic and axonal connections (Fitzpatrick et al., 1987). Layer 2/3 is called "supra-granular" layers containing 20% inhibitory interneurons and many excitatory projection neurons to extrastriate layers. Layer 4 is "granular" layer, particularly has the highest density of spiny stellate neurons (Anderson et al., 1998, Douglas and Martin, 1998, Douglas et al., 2008). This layer so compact and myelinated axons from this layer neurons travel to other sub-layers, makes this layer visible by naked eye. Because of this, the V1 is called striate cortex. Layer 5/6 contains many excitatory projection neurons that innervate the LGN and considered as "infragranular" layers. It is also known that these layers contain approximately 20% inhibitory interneurons and receives a direct input from LGN (Hendrickson et al., 1978, Schmolesky, 1995).

Early physiological exploration of V1 supported the view that neurons are arranged in a mosaic of small functionally distinct regions. Because neurons exhibit some of the same functional properties at any one cortical point through several layers in cortical depth, this mosaic was thought of as a set of columns, each with a particular function. We know that each lamina in cortical depth has its own unique properties and functional mosaic, its own pattern of dependency on different inputs from the LGN, and its own efferent relay pattern. The LGN cells are monocular (i.e. respond to stimulation of one eye only) and have concentric receptive fields. The geniculo-cortical pathway is composed of multiple channels,

each of which has different functionalities. The axons of these different types of LGN neurons terminate in different cortical layers or sub-layers of the V1 and then onto different areas of the extrastriate visual cortex. The relays out of V1 to various cortical and subcortical destinations arise from different laminae and cell groups within V1. Each of these efferent relays carries very unique type of visual information derived within the neuropil of V1 from one or more inputs from the LGN. The V1 cortex includes the calcarine cortex, which straddles the calcarine fissure, and extends around the occipital pole to include the lateral aspect of the caudal occipital lobe. Recently, the orientation columns of V1 have been recasted into more complexes geometric such as partial columns (‘slabs’) and pinwheels (Hubel and Wiesel, 1968, Bonhoeffer and Grinvald, 1991).

### Functional organization

In the primary visual cortex, spatial position of each ganglion cells within the retina is preserved by the spatial organization of the neurons within the LGN layers. The topological organization of the receptive fields in the LGN parallels in the organization of the retina and such a spatial layout is called retinotopic organization. The signals from the eyes are retinotopically arranged in V1 (Erwin et al., 1999).

Alike other neocortical area, V1 is divided into six functionally distinct cortical layers, with characteristic distribution of inputs and outputs across layers (Douglas and Martin, 1998, Douglas et al., 2008). Layer 4 receives the feed-forward inputs from LGN, with collaterals to layer 6 and the feedback inputs from other cortical layers mostly arrive in the layer 2/3. While the layer 6 play important role to deliver feedback outputs to the thalamus depart, but outputs to the subcortical targets predominantly depart from layer 5 (Carandini, 2012).

Visual inputs from the eye is carried by the axons of the retinal ganglion cells which further get relayed via different layers of the lateral geniculate nucleus (LGN) in thalamus. More precisely, the main task of V1 is to yield feed-forward connections where V1 process the

visual inputs from LGN cells and then forward the processed information to the higher visual cortical areas or subcortical structures. However, these feed-forward connections, as usual in the cortex, are accompanied by reciprocal feedback connections in a loop fashion. In which, the higher visual areas send feedback response to the V1 and V1, in turn sends feedback response back to the visual thalamus. So the feedback connections from V1 to thalamus target both the LGN and the thalamic reticular nucleus which successively inhibits LGN. However, the functional role of feedback connections are still subjected to research (Alitto and Usrey, 2003, Briggs and Usrey, 2008). Besides, V1 also receives inputs from other cortical regions but the functional roles of these secondary inputs are yet to be explored. In some cases, these secondary inputs are considered to have modulatory effect on V1 (Sherman and Guillery, 1998).

## Frontal cortex anatomy

Frontal cortex plays a critical role in both spatial and non-spatial working memory. It specifically controls behavior with respect to time and place based on the relevant sensory and mnemonic information provided. The anterior part of the frontal lobe often referred as 'pre' frontal lobe in the literature and has been simultaneously quoted as 'frontal granular cortex' and 'frontal association cortex'. Developmental pattern of the anterior portion of the frontal lobe is hierarchical, dynamic and organized by the prefrontal cortex (PFC) on its medial, lateral and orbital surfaces constituting 30% of the cerebral mantle in human (Siddiqui et al., 2008). It is considered to be one last region to undergo full myelination during adolescence in human (Fuster, 1997). In human brain, frontal lobe comprises all the tissue in front of the central sulcus and it has several functionally distinct regions e.g. dorsolateral prefrontal, inferior or orbital frontal and medial prefrontal cortex. Prefrontal cortex (PFC) in mammalian receives projections from the dorsomedial nucleus of the thalamus and these thalamic

projections are being parallel to the projections of the lateral and medial geniculate nuclei to the visual and auditory cortex (Fig. 6). The dorsolateral prefrontal areas receive its main inputs from the posterior parietal cortex and the superior temporal sulcus. The prefrontal areas is the end points of the dorsal (object recognition) and ventral (spatial behavior) visual streams.

### Basic circuitry and Cellular elements:

PFC often attributed as paralimbic (agranular) to eulaminated (granular) cortex, and multimodal receiving sensory inputs from various sensory modalities which is integrated here in a precise fashion to form diverse psychologic and cognitive actions (Masterman and Cummings, 1997). It has been mapped as a heterogeneous entity in adult rhesus monkeys based on the connections and functional attributes. Its' complex and distributed organization reflect the characterization of this brain area, dedicated to rapid computations required to wide range of activities (Morecraft et al., 2002). There are distinct cortical layers having similar features. Laminar density of neurons varies among different prefrontal cortices; estimated to be lowest in caudal orbitofrontal and medial areas while at highest in lateral prefrontal areas. Parvalbumin (PV) positive neurons were most prevalent than calbindin (CB) in lateral prefrontal areas whereas the opposite trend was noted in caudal orbitofrontal and medial prefrontal areas. Neurons positive for calretinin (CR) are fairly present among prefrontal cortices and the differences for the presence of PV and CB neurons are predominantly related to different architectonic types found within prefrontal cortex. The agranular cortices characterized as prominent deep layers consisting lowest neuronal density in general (lowest of PV and highest CB positive neurons) while lateral eulaminate cortices consisting highest density of neurons with a balanced distribution of PV and CB neurons, referring as granular cortices (Dombrowski et al., 2001).

## Functional organization:

Different sub-regions of frontal lobe represent different connections. Inherent connections within the frontal lobe forms a feed-forward and feedback loop circuit similarly like visual cortex. Through the extensive association connections, frontal cortex (FC) is linked with distant and broadly dispersed parts of the associative and limbic cortices. FC undergoes several fold of complex evolutionary progress from embryo stage to adult yielding more intra- or inter-connections within the FC or other cortical areas e.g. with amygdala, hypothalamus, midbrain and pons representing important subcortical linkages of the extended prefrontal neural system. Such broad connections are likely to integrate higher-order cortical functions mediated by PFC such as emotion, autonomic or metacognitive functions (Roberts et al., 1994, Roberts et al., 2000). Except basal ganglia, all prefrontal connections are reciprocal and send unreciprocated direct efferent (Kanki and Ban, 1997). PFC is the only neocortical region known as to project directly to the hypothalamus and septal region (Buchanan et al., 1994). The orbitofrontal region primarily connects with the medial and hypothalamus, ventromedial caudate, and amygdala while the dorsal part connects to the lateral thalamus, the dorsal caudate nucleus with the hippocampus and neocortex (Cummings, 1993).

Lateral and medial prefrontal cortices are commonly involved in memory (meta-memory)-learning, temporal ordering of events and metacognitive processing (Siddiqui et al., 2008). Orbitofrontal cortex functions as a paralimbic ring component involved in different type of functions like autonomic, response inhibition and stimulus significance functions, reward expectations or tastes. Interactions within the FC and with hypothalamus, amygdala or anterior cingulate cortices are intimately associated with such functional outputs (Goldstein, 1999, Onger and Price, 2000).

## *IN VIVO* TWO-PHOTON CALCIUM IMAGING

Optical imaging has been around for decades and considered as a good method for investigation physiological signals in medical research. The first optical microscopes used to image fluorophores were wide-field microscopes. The illumination used in these microscope were an incoherent white light source, generally a mercury or xenon lamp to have uniform light scattering over the field of view. The fluorescent signal is generated from the sample by exciting the fluorescent particle with light of specific wavelength and the diffused emitted light are captured by the detector with the help of mirrors, dichroic filters and lenses. Most useful property of the dichroic mirror is that it can separate the incident light from the emitted light while lenses are used. Filters within the optical path enable the selection of specific excitation and emission wavelengths.

Although, optical imaging has been extensively used for investigating neuronal network in brain cells, because of the compact brain structure and tissue opacity makes it very difficult. Most of the components of our brain are transparent in nature, like lipid, protein and water but the non-homogenous compositions of the cell membranes embedded within a cell, which makes light scattering difficult. And scattering causes photons to change their direction of travel, and after one scattering process, it is no longer possible to determine the origin of the photon. This process rapidly degrades signal quality and hence direct wide-field microscopy is suitable for surface imaging. Researchers around the world have not been successful to acquire images from the deeper layer of the brain until the birth of confocal microscopy in 1961 (Minsky, 1988). A single point is illuminated in this technique (one-photon excitation) and the scattered light is collected through a pin hole allowing increasing the imaging depth for the first time. However, in

practice the imaging depth in biological tissue is about 40µm, and this is still considered as surface region (Ntziachristos, 2010).

In this aspect, the invention of two-photon laser scanning microscopy (TPLSM) was a major breakthrough (Denk et al., 1990). The phenomenon of two-photon absorption was first predicted by Maria Goeppert-Meyer in 1931. Unlike confocal microscopy, instead of blocking signal from out-of-focus planes with a pinhole, excitation of a fluorophore by simultaneous absorption of two photons is made possible just at the focus point, where the density of photons is high enough (Fig. 7) (Helmchen and Denk, 2005, Svoboda and Yasuda, 2006).

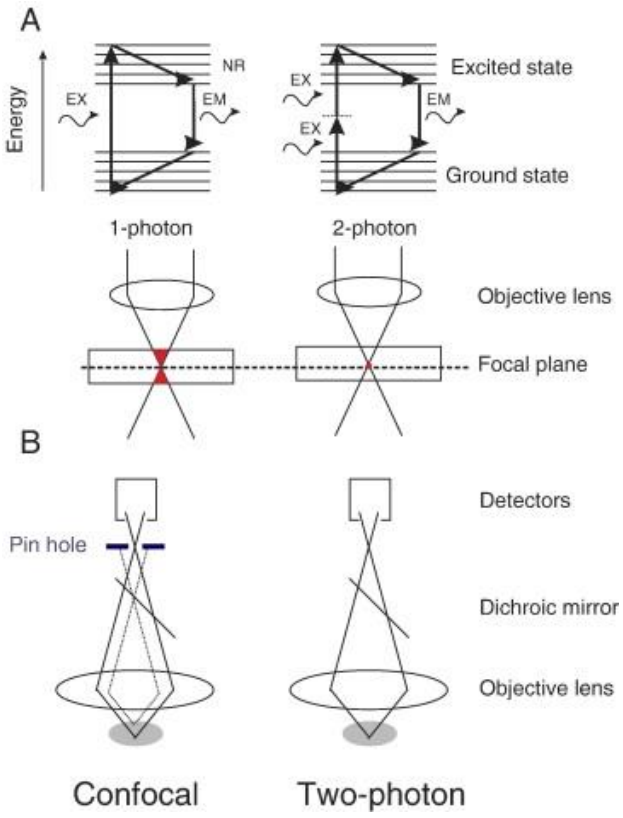


Figure 7: Comparison of conventional confocal (left) and two-photon laser scanning microscope or 2PLSM (right). Adapted from (Flugel et al., 2007).

Typically, this is achieved by using femtosecond-pulse field near infrared laser spatially focusing the beam through a numerical aperture (NA) microscopic lens. Usually, the laser

provides pulses of about 100fs width and 100 MHz repetition rates approximately (matching the nanosecond fluorescence lifetime of many fluorophores). Most widely used laser unit is Ti:Sapphire (Ti:Sa) with (700 – 1000 nm) tunable output and high average power capability of about 1W. Furthermore, without the use of pinhole, all emitted photons from the focal point from the sample are directed to the photo detector (photon-multiplier tube or PMT) using mirrors but the detector is placed close to the objective in order to collect as much light possible. This way scattering process in the detection pathways does not degrade signal quality thereby providing high resolution images. Another great advantage is infrared laser has longer wavelengths, thus have a lower scattering coefficient in tissue allowing deeper penetration depth in the sample. With this technique, we can scan an object in 2D plane upto 1mm imaging depth, which is 25-fold increase than confocal. To get raster image information, movement of the focal spot is necessary and this is achieved by moving the focal spot of light using revolving mirrors (Fig. 8). Moreover, photobleaching is reduced by exciting only at the focal point. Phototoxicity is less of a problem as TPLSM requires less energetic photons allowing the imaging in living animals over extended periods of time without interfering with endogenous processes and cell viability is also improved using infrared light instead ultraviolet light (Helmchen and Denk, 2005). Previously electrical recordings have been commonly used to study neuronal activity, had several limitations when compared with two-photon calcium imaging. In particular, electrical measurements are usually obtained from spatially dispersed neurons and identity of recorded cells were poorly defined (e.g. neuronal subtype or their laminar position) or clueless for hyper, hypo or silent neurons.

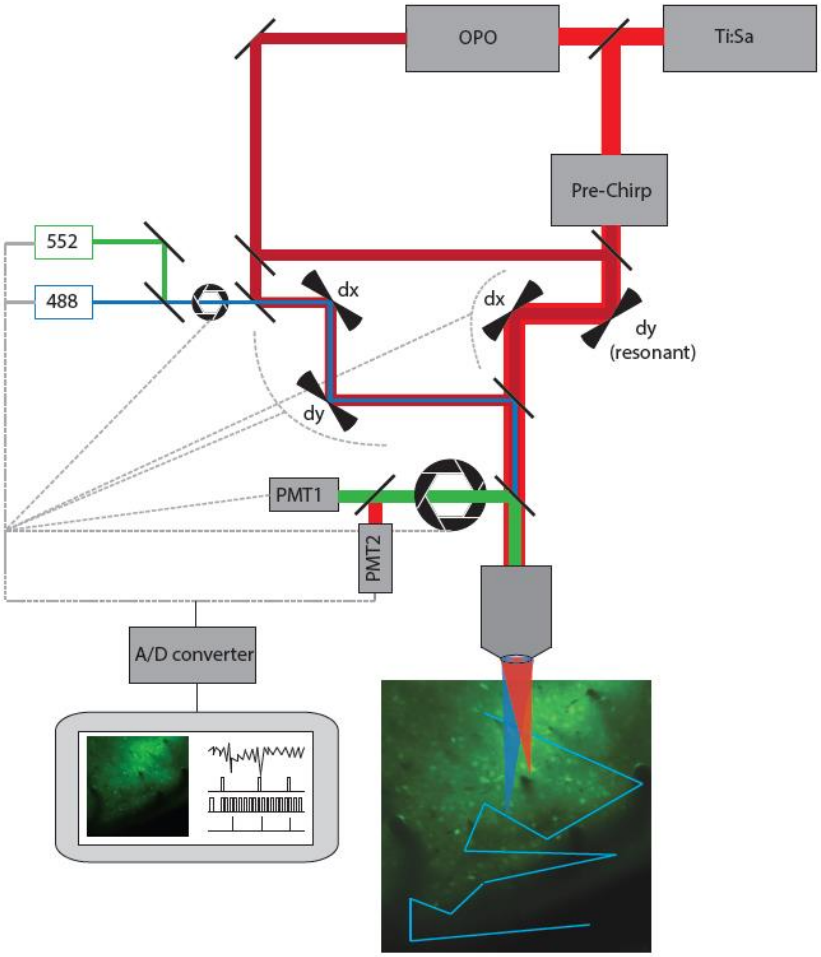


Figure 8: Schematic representation of our custom-built two-photon microscope. Courtesy of Pierre-Hugues Prouvot.

## Resonance mirrors

The main strength of TPLSM is the ability to scan the sample in 2D or 3D plane by moving the focal spot and this is achieved by utilizing revolving mirrors. Functionally, a revolving mirror requires change in orientation angle of a mirror depending on acceleration and deceleration rate. These mirrors oscillate at a very high frequency or resonating frequency which is about 10,000 to 18,000 lines per second and the scan velocity varies with a sinusoidal function, and scanning pattern is bidirectional. The scanning speeds can be increased by about one magnitude, a factor of 10 and this allows for image frequencies upto several hundreds of images per second. However, the faster scanning speed comes with compromising costs such as the change of position with a sinus-function from constant acceleration and deceleration. As their revolving speed changes permanently, the pixel sizes

also changes making the images look a bit distorted, is another disadvantage. Additionally, they remain at the turning points for a while which could potentially damage the sample. To avoid photo damage, "Pockels-cell" an optical element is used that allows fast modulation of the intensity of the laser beam and turn off the turning position.

## Fluorescence imaging

The advent in imaging techniques to assess clinico-pathological relationships between disease progression and lesion formation while reduction in information processing has highly contributed to better understanding of selective dysfunctions in MS. fMRI has been widely used for functional mapping of the brains but the spatial and temporal resolutions are still very poor; whereas optical microscopy is the perfect tool for imaging at the molecular level. Especially, two photon calcium imaging *in vivo* reports accurate information of the firing patterns of individual neurons to its submicron resolution (Garaschuk et al., 2006a). Fluorescence $Ca^{2+}$ indicator are largely used in biological studies because of its versatility and easy labeling method.

The functional analysis of neuronal network requires simultaneous measurements of physiological signals such as the changes of calcium concentrations from many individual neurons in a spatiotemporal manner. By using TPLSM in combination with fluorescent indicators for intracellular calcium, it has become a routine protocol to stain entire local neuronal populations at once and monitor their activity patterns *in vivo*. Calcium is essential for several inherent biological processes to retain cellular homeostasis. Changes of the membrane potential are often accompanied by calcium entry into the cell and therefore, sudden changes in the calcium concentration can impact its electrical activity via series of chain reactions. In resting state, the internal calcium concentration is very low (roughly about 50 – 100 nM), whereas it is several order of magnitude outside the cells, especially several

millimolar in the bloodstream or CSF (Berridge et al., 2000, Grienberger and Konnerth, 2012). Myelinated axons contain different kind of voltage-gated ion channels such as $Na^+$, $K^+$, $Ca^{2+}$ and these opens up differently when a cell produces an action potential. Such events lead to brief influx of calcium and a transient increase in the intracellular calcium concentration. Such calcium transients are reported using fluorescence calcium indicators as they change their fluorescent properties once bind with calcium. Because increase in calcium concentration is tightly coupled with AP firing of the neurons, intensity changes of those fluorescent indicators are an excellent measure of suprathreshold activity (Yuste et al., 2011). Following the rapid rise after AP, a brief surge of intracellular calcium concentration buffered within the cytosol which subsequently decays back to resting level exponentially, reflecting calcium removal from the cytosol (Helmchen, 2009). The decay time constant for a typical calcium transient drastically depends on cytosolic calcium buffering and extrusion mechanisms, ranging from a longer time scale of hundreds of milliseconds for somata (Helmchen et al., 1996). Importantly, the sensitivity varies between cells types. One of the drawbacks is the temporal resolution of determining spike times is limited by the temporal resolution of the laser of the laser scanning, which is usually slow compared to regular electrical recording. However, the optical detection of spiking activity has several advantages, because it enables *in vivo* measurements of spiking patterns of a local network, including those non-active neurons.

## Principals of fluorescence labeling

Fluorescence is a luminescence molecule or fluorophore dye that can be excited by light with a specific wavelength and thereby re-emits light of lower energy (higher wavelength) via electromagnetic radiation. There are two main factors determine the fluorescence efficacy of a given fluorophore indicator at a given wavelength. First, the molecular absorptivity

coefficient, a measure of how efficiently a molecule absorbs light and secondly, the quantum yield, the fraction of absorbed light that is re-emitted as fluorescence (%). In principle, a good fluorescent indicator should have both highly efficient and %. Inversely, photobleaching occurs when the indicator loses its fluorescent properties caused by photochemical reactions with oxygen in its excited state, creating free radicals. Upon photobleaching a fluorophore does not emit light anymore. A downside of photobleaching in live samples can also cause phototoxicity (Patterson and Piston, 2000). Hence, to reduce photobleaching, it is important to limit the duration of excitation and the laser power.

### Calcium indicator

A key aspect of "cellular activity" refers to processes evolving in the temporal domain, whether it is electrical or chemical, turnover of proteins, or alteration in cell morphology. Thus, it was important that an imaging method should be capable of reading out the "dynamics" of brain cells over a given time scale, and the development of a sparse, non-invasive, high-contrast label of functional probe was desirable (Helmchen, 2009). Historically, many targets from several proteins to ions have been tested for optical recording to watch brain cells "at work". But, the successful invention of TPLSM has been fostered by the parallel development of various novel staining techniques for *in vivo* labeling of brain cells (Denk et al., 1990, Yuste and Denk, 1995). In developing novel staining approach, one of the common interests among many researchers was to measure intracellular calcium fluctuations. As calcium ions are universal secondary messengers mediating many essential cellular functions (neurotransmitter release, synaptic plasticity, electrical excitability, gene expression etc.). In neurons, action potentials (APs) trigger large amount of calcium influx rapidly through voltage-gated ion channels resulting elevations of intracellular (somatic) calcium concentration above resting levels (so called "calcium transients") (Gobel and Helmchen, 2007) and these events further mediate synaptic transmission causing calcium

transients in dendritic spines, contributing to propagation of the electrical signals (Katz and Shatz, 1996, Buonanno and Fields, 1999, Spitzer et al., 2004, Adelsberger et al., 2005). So far AP-evoked calcium transients are the predominant signals observed *in vivo* representing suprathreshold population spiking activity and this can be indirectly inferred from either highly localized or more widespread (somatic) calcium signals (Stosiek et al., 2003, Ross et al., 2005, Lin et al., 2007). Ability to image at high speed was a concern for characterizing large-scale activity because spatiotemporal patterns of neuronal spikes on a millisecond timescale. Yet, a fluorescent calcium indicator can indirectly measure spiking activity, although the achievable temporal resolution is limited by their calcium-binding kinetics (Helmchen, 2009). Meanwhile, glial cells especially also have been reported to participate in local network processing (Hirase et al., 2004, Nimmerjahn et al., 2004). However, glial cells are electrically mostly silent, so it is difficult to investigate their electrical potential *in vivo*. On the same note, astrocytic calcium signals have much slower transient (slow rise followed by slower decay time) and they are often linked to the regulation of cerebral blood flow (Takano et al., 2006).

Among, the very first synthetic fluorophores used for monitoring intracellular calcium dynamics was Arsenazo III, an absorbance dye that changes its absorption spectrum as a function of bound calcium (Brown et al., 1975). While Arsenazo III was very useful for *in vitro* experiments but the implementation for *in vivo* delivery was often complicated and tedious. A true breakthrough was the development of more sensitive and efficient calcium specific chelators, such as BAPTA (1, 2-bis-[2-aminophenoxy]-ethane-N,N,N’,N’-tetra-acetic acid) combined with fluorophore (Minta et al., 1989). However, those indicators were particularly not very bright and needed to be used at high concentrations to overcome cellular auto-fluorescence (Tsien and Tsien, 1990, Tsien and Harootunian, 1990). Over the past decades, a wide range of synthetic calcium indicators has been introduced comprising

different binding affinities for calcium (because of calcium concentration changes in large amount: from nanomolar to micromolar level) and excitation spectral properties. Among others, Oregon Green BAPTA and Fluo-4 are widely used exclusively in neuroscience as these are relatively easy to implement and provide large signal-to-noise ratios allowing quantitative measurements of the calcium transients (Stosiek et al., 2003, Sohya et al., 2007, Paredes et al., 2008). Another advantage of these indicators is that they exist in membrane-permeable acetoxymethyl (AM) ester form for *in vivo* experiments (Helmchen and Waters, 2002, Stosiek et al., 2003). Once the dye enters into the cell, trapping of AM occurs through removal of the hydrophobic ester residue by intracellular esterases (Tsien, 1981). The most commonly used method for delivering these indicators is pressured injection through a small skull craniotomy to the targeted brain tissue. This loading procedure is also known as multi cells bolus loading method (Stosiek et al., 2003, Garaschuk et al., 2006b) and can be used for a large spectrum of indicator dyes enabling homogenous staining for wider population of neurons at once in a given cortical layer. Moreover, AM loading is also used in combination with virally transduced transgenic animals having specific cell types fluorescent (Tamamaki et al., 2003, Sohya et al., 2007, Runyan et al., 2010). Functionally active astrocytes also uptake AM ester when bulk loaded but those astrocytes can be identified by either morphological analysis (astrocytes appear much brighter than neurons and their processes can be distinguished) or co-staining with specific glial marker Sulforhodamine 101 (Nimmerjahn et al., 2004). So far such loading method has been extensively used in recent years to stain hundreds of cells in various cortical regions (including cerebellum and spinal cord) in different species, such as rodents, cats, ferrets (Garaschuk et al., 2006a, Grienberger and Konnerth, 2012). However, the bolus loading of any indicator has not proven possible in the deeper layers e.g. hippocampus.

# HYPOTHESIS

Diffusing inflammation in human with MS extends beyond local lesion sites, affecting interconnected regions (Droby et al., 2015). In many cases functional integration of the basal ganglia and thalamus into the motor network reported to be stronger in MS patients compare to healthy individuals (Dogonowski et al., 2013). In RRMS, functional reorganization was hypothesized to compensate for ongoing damages during initial disease stages (Faivre et al., 2012, Bozzali et al., 2013). Using fMRI, it has been shown that common occurrences of demyelinating lesions directly impact on visual system at all anatomical sites from retinal nerve fiber layer to visual cortex (Gallo et al., 2015). Such finding were further strengthened by the explanation of adoptive functional changes taking place at the level of striate and extra-striate visual cortical areas (Rombouts et al., 1998, Langkilde et al., 2002, Toosy et al., 2005, Jenkins et al., 2010). Moreover, increase functional connectivity in frontal regions of the brain was identified to facilitate performance in complex speed-dependent information processing (Wojtowicz et al., 2014). Together these evidence suggests that these changes correlate with the patient's ability to compensate for functional disability (Bozzali et al., 2013).

There is converging evidence that cortical demyelination and axonal loss can cause disruptions of the cortical and subcortical circuits connecting different brain regions in functional network which can lead to cortical reorganization (Helekar et al., 2010, Valsasina et al., 2011). Hence, it is entirely unclear that what are the outcomes of such functional reorganization at single cell level; does the circuit reduce or enhance the efficacy of the network during different disease states (at peak of the disease and in remission) of RRMS? Do cortical demyelination and/or persistent inflammation in different disease phases have direct impact on initiation of cortical neuronal dysfunction followed by deficits in sensory, cognitive and motor learning? What are the molecular mechanism(s) involved in perpetuation

of the functional connectivity in the cortical microcircuit? In this study, examining these questions could help us

to better understand the pathogenesis processes in MS and upon finding signature mechanism or molecule(s) involved will be used as biomarker for the therapeutic development.

# MATERIALS & METHODS

## Experimental Animals

All experimental procedures were performed in compliance with institutional welfare guidelines and were approved by the state of Rhineland-Pfalz, Germany. All animals used for this study were female SJL/J of same age (10 - 12 weeks old) purchased from Charles River Laboratory (Wilmington, USA) and group-housed at the central animal facility, Johannes Gutenberg University-Mainz. For active EAE induction, mice were injected with subcutaneously (s.c.) with 200 µg $PLP_{139-151}$ peptide (Hooke Laboratories, Lawrence, USA) emulsified with complete freund's adjuvant (CFA) supplemented with 4 mg/ml Mycobacterium tuberculosis H37RA. Each mouse received one i.p. injection (500 ng) of pertussis toxin at day 0 and day 2 post immunization. EAE was scored clinically on a daily basis according to a 0-5 scale as follows: 0, no clinical symptoms; 1, tail paralysis; 2, impaired righting reflex and partial hind limb paralysis; 3, complete bilateral hind limb paralysis; 4 total paralysis of hind limbs and partial fore limbs paralysis; and 5, dead (Jolivel et al., 2013).

## Craniotomy preparation of visual and frontal cortices

All experiments were performed in anesthetized animals. For craniotomy preparation, mice were anesthetized by inhalation of 1.5–2.0% isoflurane (AbbVie Inc., Illinois, USA) in pure oxygen and placed onto a warming plate (37°C). The depth of anesthesia was assessed by monitoring the tail-pinch reflex and respiration rate. The stereotactic coordinates of visual and frontal cortices were located accordingly on a stereotactic frame [visual cortex:

anteroposterior (AP)-2.8 mm, mediolateral (ML)–2.8 mm, and frontal cortex: anteroposterior (AP)-2.7 mm, mediolateral (ML)–1.0 mm] (Paxinos and Franklin, 2012). After removing the skin, a cranial window (1 x 1 $mm^2$) was prepared by skull thinning under a dissecting microscope using dental drills and a custom-made recording chamber was glued onto the skull using cyanoacrylic glue (UHU GmbH, Buhl-Baden, Germany) and dental cement (Heraeus Kulzer GmbH, Hanau, Germany). Upon drying the glue, the thinned skull was removed using sharp scalpel and the following area was irrigated with PBS (37°C). The mouse was transferred onto a heating plate of the recording setup and continuously supplied 0.6-0.8% isoflurane in pure oxygen. If necessary, the concentration of isoflurane was adjusted in the course of experiment in order to keep a rather superficial level of anesthesia (respiration rates between 90–120 brpm). The recording chamber was perfused with warm (37°C) artificial cerebrospinal fluid (125 mM NaCl, 2.5 mM KCl, 1.25 mM $NaH_2PO_4$, 26 mM $NaHCO_3$, 2 mM $CaCl_2$, 1 mM $MgCl_2$, 20 mM Glucose, pH 7.4). The fluorescent $Ca^{2+}$ indicator dye OGB-1 AM (500 µM; Life Technologies/ Molecular Probes, Waltham, USA) was bulk loaded in both cortices. Briefly, the indicators dye was dissolved in 20% pluronic F-127 dimethyl sulfoxide (DMSO) and the solution was further diluted with a standard pipette solution to a final concentration of 0.5mM. The diluted dye was pressure-injected (0.6-0.8 bar) 200–300 µm below the dura using micromanipulator (Scientifica Pvt Ltd., Berkshire, UK) using glass pipettes of 4-6 MΩ (Sutter Instrument Inc., Novato, USA) for 4 min. 30–40 min were allowed for the dye to enter into the cells. Astrocytes were identified by bulk-loaded staining with SR101 (100 µM, Sigma Aldrich, Missouri, USA) and further excluded from functional analysis. To reduce any movement or heartbeat related artifact during recordings, the craniotomy was filled with 0.8 – 1% agarose (Sigma Aldrich, Missouri, USA).

## Two-Photon Imaging *in vivo*

For *in vivo* recording, we used a custom-built two-photon microscope based on a Ti:Sapphire (Chameleon; Coherent systems, California, USA) laser equipped with a resonance scanner, operating at 800 nm wavelength (LaVision Biotec, Bielefeld, Germany). The intensity of the laser was modulated with a Pockel's cell and the scanning done using a 40x (1.35 N.A.; Nikon, Japan) or 25x (0.95 N.A.; Olympus, Tokyo, Japan) water immersion objective mounted on an upright microscope. The emitted fluorescence was detected using a photomultiplier tube (PMT). All images acquired were full-frame at 30Hz using custom-written software Imspector Pro from LaVision Biotec. At each focal plane, spontaneous calcium transients of layer II/III neurons were recorded for at least 6 min for each trial. For simultaneous visualization, the emitted fluorescence of OGB1-AM labeled neurons was collected at 515nm (515±20 filter) and SR101 labeled astrocytes at 605nm (620±60 filter).

## Image Analysis

The image analysis was performed off-line using custom-written scripts in MATLAB (Mathworks Corporation, USA). First, regions of interest (ROI) were hand-drawn around individual somata of each neuron by tracing the outlines of cell bodies on a single image and then all pixels within ROIs were averaged to the relative fluorescence change against time course ($\Delta F/F$) across image sequences. A calcium transient was defined as changes of $\Delta F/F$ that were at least three times larger than the standard deviation of the noise band or baseline. A baseline was defined as normalized mean fluorescence of a period of 1-3 sec with no calcium activity within the same ROI. All $\Delta F/F$ signals were plotted against time to analyze calcium transients for all experimental groups. Astrocytes were excluded from analysis upon identifying their specific morphology, typical transients and further by selective staining (Nimmerjahn et al., 2004, Garaschuk et al., 2006b, Nimmerjahn and Helmchen, 2012). All

further analysis of the transients were carried out in Igor Pro software (Wave-Metrics, Inc., Portland, USA).

### Immunohistochemistry and immunofluorescent staining

For immunohistochemical analysis, EAE mice in remission were perfused with 30 ml cold PBS followed by 30 ml 4% PFA in PBS under deep anesthesia. Brains and spinal cords were removed carefully and post-fixed in 4% PFA for overnight in 4°C. To retain the structural preservation, organs were immersed in 15% and 30% sucrose. Tissue were embedded in tissue-tek freezing medium (Thermo Fisher Scientific, Massachusetts, USA) and frozen in -20 °C. Frozen tissues were sliced in 10 µm thick coronal cryosections. Tissue sections were thawed and stained with antibodies against LFB-HE and MBP (Sigma Aldrich, Missouri, USA and Abcam, Cambridge, UK) for myelin loss or CD3 for T-cells infiltration, Mac-3 for activated microglia/macrophages, APP for axonal damage following a standard protocol. For antibody staining, tissue sections were incubated with blocking buffer (Normal goat serum, 0.1% Triton X100, PBS) for 1 hour at room temperature (RT) and further incubated with primary antibody overnight at 4 °C (respective antibodies used for this purpose and their dilution factors are detailed in the table below). Staining were performed for T lymphocytes (mouse-anti-CD3, 1:100, Abcam, Cambridge, UK), activated monocyte/macrophage (Rabbitanti-Mac-3, 1:200, BD Pharmingen, New Jersey, USA), for axonal damage (rabbit-anti-APP, 1:500, Abcam, Cambridge, UK). Incubation with biotinylated secondary antibody was performed for 2 hours in the dark at RT followed by blocking of endogenous Peroxidase and substrate staining using DAB substrate kit (DCS-Innovative Diagnostik-Systeme, Hamburg, Germany) for 30 mins in RT. After successful development of signals, sections were eventually washed and embedded in aqueous mounting medium (Sigma Aldrich, Missouri, USA). All the histological analysis were carried out blinded and images were acquired with Olympus BX51 microscope (Olympus Corporation, Tokyo, Japan) was used

with different magnifications (Olympus 1.25x/0.04, Olympus 10x/0.4, Olympus 20x/0.75, Olympus Corporation, Tokyo, Japan).

For immunofluorescent staining, all brains were fixed in 4% PFA overnight and treated with 30% sucrose later. Using a vibratome (Microtom HM 650 V, Thermo Fisher Scientific, Massachusetts, USA), coronal slices of 40 µm thickness was prepared. Free floating slices were used for all immunostaining. Staining were performed for glial markers (mouse-anti-GFAP, 1:1500, Sigma Aldrich, Missouri, USA), microglia (goat-anti-Iba-1, 1:500, Abcam, Cambridge, UK), TNFα (rabbit-anti-TNFα, 1:500, Abcam) and for neuronal markers (mouse-anti-NeuN, 1:1000, Millipore, Massachusetts, USA), for GABAergic neurons (mouse-anti-GAD67, 1:750, Chemicon), and for glutamatergic neurons (mouse-anti-CamKII, 1:500, Abcam, Cambridge, UK). Overnight incubation with aforementioned primary antibodies was followed by staining with secondary antibodies coupled to different fluorophores for 2 hours. To counterstain all sections were treated with DAPI (Invitrogen, Massachusetts, USA) before being transferred and embedded onto object trays. Imaging were performed using a Leica confocal microscope (Leica TCS SP8, DM 6000CS, Leica Microsystems, Wetzlar, Germany) and sequential scans with a 20x and 63x objectives (Leica, NA 1.4, Leica Microsystems, Wetzlar, Germany).

## Quantitative RT-PCR

| Official gene name | Accession No. | Direction | Primer Sequence | Product length |
|---|---|---|---|---|
| Mus Musculus GADPH | NM_001289726.1 NM_008084.3 | Sense antisense | CAGCAACTCCCACTCTTC TGTAGCCGTATTCATTGTCAT | 101 |
| Mus Musculus ß-actin | NM_007393.5 | Sense antisense | AATCTTCCGCCTTAATACT AGCCTTCATACATCAAGT | 100 |

| | | | | |
|---|---|---|---|---|
| Mus Musculus BDNF | NM_007540.4<br>NM_001048139.1<br>NM_001048141.1<br>NM_001048142.1<br>NM_001285416.1<br>NM_001285417.1<br>NM_001285418.1<br>NM_001285419.1<br>NM_001285420.1<br>NM_001285421.1<br>NM_001285422.1<br>NM_001316310.1 | Sense<br>antisense | AACAATCGCTTCATCTTAG<br>GCATATTCAGTGGTATTCC | 149 |
| Mus Musculus GM-CSF | NM_009969.4 | Sense<br>antisense | GCTACTACCAGACATACT<br>ATATCAGTCAGAAAGGTTT | 105 |
| Mus Musculus IFN-γ | NM_008337.4 | Sense<br>antisense | AGACAATGAACGCTACAC<br>TCCACATCTATGCCACTT | 139 |
| Mus Musculus IL-4 | NM_021283.2 | Sense<br>antisense | TCATCCTGCTCTTCTTTCTC<br>TCCTGTGACCTCGTTCAA | 101 |
| Mus Musculus IL-17A | NM_010552.3 | Sense<br>antisense | GACTTCCTCCAGAATGTG<br>TATCTATCAGGGTCTTCATTG | 140 |
| Mus Musculus IL-17F | NM_145856.2 | Sense<br>antisense | ACTTTCTGGCTTGCTTTA<br>ACTGTGGTCATCATCTAAC | 129 |
| Mus Musculus TGF-β1 | NM_011577.2 | Sense<br>antisense | TACATTGACTTTAGGAAGGA<br>TCCAGGCTCCAAATATAG | 104 |

| | | | | |
|---|---|---|---|---|
| Mus Musculus TGF-β2 | NM_009367.3 | Sense antisense | CCAGAAGACAGACAGAGA TTATACAGAAGTGACAGTGA A | 122 |
| Mus Musculus TNF-α | NM_013693.3 NM_001278601.1 | Sense antisense | TCTTGTGTTTCTGAGTAG GTCTGTATCCTTCTAACTTA | 89 |

In order to analyze the expression of different cytokines and neurotrophic/neuroprotective factors, quantitative RT-PCR of the cortices from EAE remission mice were performed and compared with healthy control. Briefly, on day 17 cortices from EAE remission mice were isolated following perfusion with PBS and later were homogenized. Amplification primers were designed using the Beacon Designer 8 Software (Premier Biosoft International, USA) according to the manufacturer`s guidelines and subsequently tested for amplification efficiency and specificity. Sequences for the primers used are listed below. iQ SYBER® Green supermix (Bio-Rad Laboratories, Germany) in an CFX Connect™ Real-Time Detection System (Bio-Rad) was used for performing RT-PCR. To determine the relative changes in gene expression, the $\Delta\Delta C_t$ method (Livak and Schmittgen, 2001) with glyceraldehyde 3-phosphate dehydrogenase (*GADPH*) and actin-beta (*Actb*) as reference genes.

### Intraventricular injections of Infliximab

Pure infliximab (Remicade®) was first dissolved in sterile PBS and injected at a concentration of 200µg/3µl per animal. Prior to injections, all remission mice (n=10 for each group) were first treated with carprofen (Rimadyl®, 0.4 mg/ml) 300 µl subcutaneously under the neck area. This worked as pain killer for long-term pain-relief. After 30 minutes, mice were anesthetized with a mix solution of ketamine (Ketavet, diluted 1:5 in 0.9%NaCl, Hameln Pharmaceuticals Ltd., Gloucester, UK) and xylazine (Rompun, 2%, diluted 1:40 in 0.9%NaCl, Bayer AG, Leverkusen, Germany) 200-250 µL intraperitonially, adjusted to the body weight.

Next, they were placed on a rodent stereotaxic frame (David Kopf instruments, Tujunga, USA) and heads were fixed at both ears and mouth. Body temperature was monitored using a rectal probe and further temperature was controlled at 36 ± 1 °C using a thermostatic heating pad (NPI Electronic GmbH, Germany) throughout the experiment. The scalp was shaved between the ears towards the nose and a local anesthesia lidocaine gel (Xylocain® 2%, AstraZeneca, London, UK) was applied. To remove head cranial muscles and periost, 30% hydrogen peroxide were used after opening the skin. A blur hole was drilled at the following co-ordinates; 1 mm caudal to bregma and 0.22 mm lateral to the midline. A Hamilton syringe (Hamilton 10 µL) was placed at 2.5 mm depth and 3 µL Infliximab solution in PBS was injected slowly over 3 mins period. All sham control animals received 3 µL of PBS. All Infliximab injected animals were either used for two-photon imaging or electrophysiology. For electrophysiological recordings, 48 hours post injection brains were collected for slicing.

## Electrophysiological recording of spontaneous EPSCs

All electrophysiological experiments were performed in the layer II/III of the visual cortex (V1). For the recordings, mice (N = 30) were deeply anaesthetized by inhalation with isoflurane, and decapitated. Dissection for all brains were done in cold (1 – 4 °C), oxygenated sucrose-based artificial cerebrospinal fluid (aCSF) (in mM: NaCl, 87; KCl, 2.4; $KH_2PO_4$, 1.25; $MgSO_4$, 2.6; $CaCl_2$, 0.5; d-sucrose, 75 and d-glucose, 10; pH: 7.4) and sliced coronally (350 µm) on a vibratome (Microtom HM 650 V, Thermo Fisher Scientific, Massachusetts, USA) from both hemispheres containing the visual cortex. Acute slices were further incubated in a chamber with oxygenated sucrose-based aCSF for 1 h at room temperature. A recording chamber was continuously perfused with standard oxygenated aCSF containing (in mM) NaCl, 124; KCl, 4.9; $KH_2PO_4$, 1.2; $MgSO_4$, 1.3; $CaCl_2$, 2.5; $NaHCO_3$, 25.6 and d-glucose, 10; pH: 7.4 and single brain slices were transferred onto the chamber. The chamber

was located on the fixed-stage of an upright Olympus-BX50WI microscope (Olympus, Tokyo, Japan). All constituents used for the preparation of aCSF were from Sigma-Aldrich (USA). Temperature of the recording chamber was set to 33 °C using heating unit (TC-10, NPI Electronic GmbH, Germany). Layers II/III pyramidal neurons from those acute cortical slices were targeted for whole-cell patch-clamp recordings. AMPA-receptor dominated, sEPSCs were pharmacologically isolated by bath application of picrotoxin (PTX, 50 µM) and D (−)-2-Amino-5-phosphonopentanoic acid (D-AP5, 20 µM) and measured in voltage clamp-mode at -80 mV. The recording glass pipettes (resistance 5-7 MΩ) were filled with an intracellular solution containing 125 Cs-gluconate (in mM), 5 CsCl, 10 EGTA, 2 $MgCl_2$, 2 $Na_2$-ATP, 0.4 $Na_2$-GTP, 10 HEPES and 5 QX-314; pH: 7.3. For recording the electrical signals, an Axopatch-200B amplifier (AXON Instrument, Foster City, USA) operated in the bridge mode. Recorded data were then filtered at 10 kHz and digitized at 20 kHz using a Digidata-1400 system with PClamp 10 software (Molecular Device, Sunnyvale, USA). Data were analyzed off-line using PClamp 10.1 software (Molecular Device, Sunnyvale, USA).

## Behavioral tests

Mice in remission with a score level of ≤ 1 were considered for all behavioral tests and all tests were conducted exclusively during the light phase (6:00am - 6:00pm) in quiet rooms. During behavioral experiments, majority of the tests were recorded using an overhead video camera connected to a computer and animals' behavior were automatically tracked by EthoVision®XT software (Version 8.0, Noldus Information Technology, Wageningen, The Netherlands). Each equipment used for all tests were thoroughly decontaminated with 70% ethanol or cleaned with water at the end of each trial.

## Visual Discrimination (VD) test

We employed visual discrimination test to determine visual performances in EAE remission mice. The diagram of the apparatus is shown in the Fig 9 below and the design of was adapted from Bussey et al. (Bussey et al., 2008). At first, mice were trained in an operant chamber (height 18 cm, width 25 cm, depth 20 cm, Med Associates Inc.; St. Albans, USA), equipped with a touch-screen, enclosed in a sound-attenuating box, and controlled by "K-Limbic" software (Med. Associates, Vermont, USA).

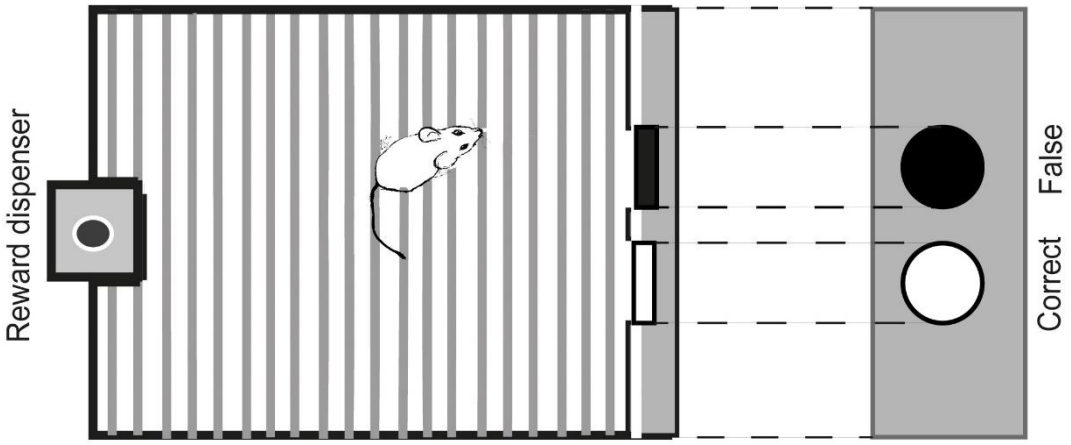


Figure 9: Schema of the visual discrimination task set up. Left panel, top view of the set-up. Right panel, front view of the set-up. A monitor is placed at the end of the unit which simultaneously displays correct or false stimuli. Both wild-type controls were trained to choose correct stimuli and for each correct choice made, reward of food pallet were dispensed from a reward dispenser placed on the other end of the unit.

The touch screen with infrared detection network was installed on one end of the chamber, which was covered by a 23.2 cm × 15.5 cm black metal panel and accessible through two circular windows (Ø 3.2 cm) to allow visual presentation of the stimuli as well as nose poking (touching). A magazine was placed opposite to the wall of the touch screen, equipped with a photocell detector of head entries, in which illumination of the magazine (cue) and dustless precision 14mg food pellets (Bio-Serv Inc, Flemington, USA) were delivered simultaneously. A sufficient distant (32 cm) of house light (2.8 W) was maintained by placing it above the magazine.

In order to keep animals motivated to perform the task, their daily food intake was adjusted to maintain body weight to 85% of their initial body weight and maintained during the course of the experiment (Rowland, 2007), and water was supplied *ad libitum*. The experiment itself consisted of 3 distinct phases.

1. Phase I: At first, all the mice were habituated to the food rewards in their home cage and then trained for 15 min. in the operant chamber for three consecutive days to associate a nose poke in the magazine with food reward and illumination.
2. Phase II: Mice were introduced to the "touch screen training", wherein mice learnt to associate a nose poke through either response window that displayed a bright stimulus with a food pellet as a reward (correct stimulus). More precisely, the screen behind both windows displayed a simple bright field image and was activated to register touch (nose poke). Upon a correct touch response by an animal, a pellet was dispensed and the animal had to collect it before the next trial started after an ITI of 5s. While nose poking into the window displaying a dark image with a punishment by turning off house-light and no food pellet referred as false stimulus. In order to proceed to the next experimental phase, animals had to perform a minimum of 70 out of 100 correct trials within a 30 min session for three consecutive.
3. Phase III: from trial phase II, mice learned to respond to a correct stimulus and/or a false stimulus. The correct or false stimuli were presented left or right in pseudo-random fashion to avoid any learnt biasness. Animals were considered to have learnt the task when a 70% correct choice could be achieved for at least 3 consecutive days. Once this criterion was reached, EAE was performed and the animals tested during remission. See the movie x and y for the demonstration of phase II and III of the rest respectively.

### Assay for motor skills and gait parameters: Rotarod and Cat Walk

To assess the difference in motor coordination and endurance between healthy control and remission mice, a standard rotarod test was performed. Briefly, mice were placed on a motorized rotating cylinder (Ugo, Basile, Italy). The cylinder used for this test was 3 cm in diameter and had a rotational speed of 4 to 40 rpm (rotations per minute), in a total run time period of 5 minutes. A diagram of the apparatus is shown in Fig 10. Basic grip strength and latency to fall from the rotating cylinder was measured.

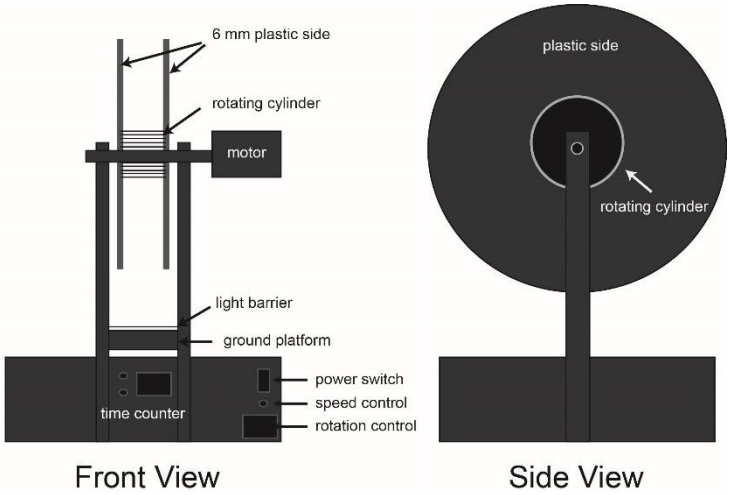


Figure 10: Schematic representation of rotarod apparatus used for assessing motor and gait parameters. Adapted and modified from Hamm et al. (Hamm et al., 1994).

The Catwalk test provided the means to automatically assess gait function more specifically while providing the benefit of measuring a number of locomotor-related parameters simultaneously (Neumann et al., 2009). The apparatus (Catwalk XT, Noldus Information Technology, Wageningen, Netherlands) was made of a 130 cm long glass plate with dimmed fluorescent light beamed into a glass from the side. In a darkened environment (below 1 lx of illumination), the light was reflected downwards and the images of the footprints recorded by a high speed camera (100 fps) under the walkway. Gait and locomotor-related parameters were automatically calculated, including the spatial parameters related to individual paws (e.g. print area), relative spatial relationship between different paws (e.g. stride length) and inter-limb coordination (e.g. walk speed). Mice were subjected to at least three consecutive runs of gait assessment.

### Assay for anxiety-related behavior: Elevated Plus Maze (EPM) and Open Field (OF).

The EPM apparatus consisted of open (length 66 cm) and closed (length 66 cm) arms, crossed in the middle between them and elevated 50 cm above the floor, while a camera was installed directly above. Mice were placed in the central platform (5 cm x 5 cm), facing an open arm of the maze and behavior automatically recorded and tracked for 5 min in a single trial, using the EthoVision software (Noldus Information Technology, Wageningen, Netherlands).

To test the innate tendencies of avoidance of bright light and open spaces and exploring novel environment, the open field (commonly used as anxiety test) test was performed. The OF apparatus consisted a grey Perspex arena (120 cm in diameter). Mice were placed in the center of the arena and their spontaneous behavior recorded over a period of 7 min, also in a single trial, using a camera installed directly above. An illumination of 120 lx was applied in the room for both tests.

### Cognitive performance: Fear Conditioning (FC)

Fear Conditioning, another test for measuring anxiety was performed in a conditioning chamber (transparent acrylic box, length 20 cm x width 20 cm x height 40 cm) having a floor of electricity-conducting metal wires at the bottom. The entire conditioning chamber was housed in a sound-attenuating observation box (Johansen et al., 2011). A video camera was mounted on the ceiling to record behaviors. For an overview of the experimental phases, see Table 1. In brief, phase I (training), on day 1, consisted of placing a naïve mouse in the conditioning chamber in order to measure the baseline amount of freezing (complete immobility except for respiration) during 2 min, before exposing the animal to an auditory cue (10 kHz, 80 dB, 28 s) that was paired with a mild foot shock of 0.4 mA during the last 2s of the auditory stimulus. After a break of 20s, the pairing was repeated. Finally, after a delay of 10s the testing mouse was returned to its home cage. The number of seconds spent freezing

in the test chamber on the training day was considered the reference measure. On the second day, phase II, the mouse was transferred in the same conditioning chamber and allowed to explore its environment for 2 min. while neither a foot shock nor a tone was applied. The number of seconds spent freezing was the measurement of contextually conditioned fear. A few hours later, during phase III, the mouse's fear conditioned response to the conditioned stimulus, the acoustic cue, was measured for 4 min. in a novel environment, un-related to the original conditioning chamber. Thus, the animal was placed in a round instead of square Plexiglas chamber (Ø 20cm, height 40 cm) that was enriched with visual cues not present in the original chamber. Then, the acoustic cue was presented for 2 min. and freezing was measured during this time.

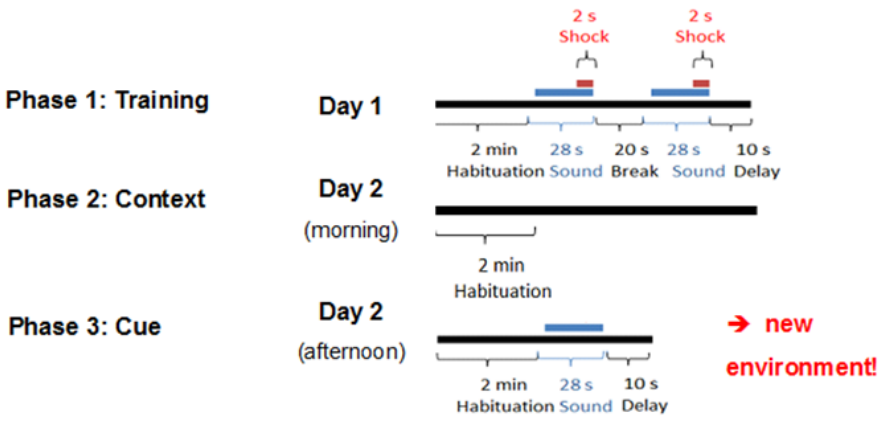


Table 1: Presentation of the fear conditioning test

## Statistical analysis

Statistical analyses were performed using Prism (Graphpad Software Inc., La Jolla, USA) and Matlab (Mathworks, Natick, MA). Statistical significance was assessed using one- or two-way ANOVA measures with Tukey's post-hoc multiple comparison analyses, when criteria for parametric statistics were met. Alternatively, Kolmogorov-Smirnov test was used to

compare distributions between groups and $X^2$ test was employed to compare categorical distributions. Unless otherwise stated, data are represented as mean ± SEM.

# RESULTS

Understanding the neuronal network activity patterns in the cortex of SJL mice at different time point of the EAE disease progress using high resolution *in vivo* two-photon $Ca^{2+}$ imaging was the primary objective of this thesis. To address this, we immunized SJL/J mice with $PLP_{139-151}$ emulsion to cause EAE disease (See Material & Methods). We monitored their clinical symptoms on a regular basis post immunization. Mean clinical scores against time is plotted in Fig. 11. Based on the scores, we determined early disease peak or EAE 'relapse' and 'remission'. Next, we recorded the pattern of spontaneous activity from layer II/III visual cortex (V1) during relapse and in remission. Thereafter, we compared our data with wild-type animals of same age and sex.

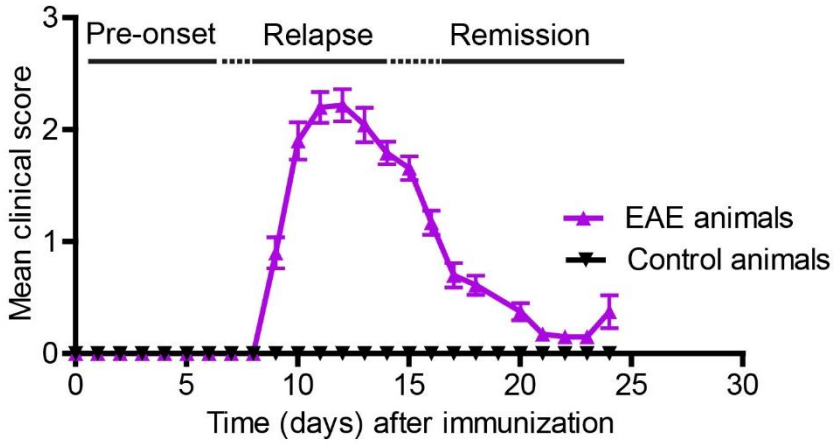


Figure 11: Representative clinical score graph for relapse-remitting EAE of mice immunized with $PLP_{139-151}$ shown. Noticeable clinical symptoms occur around day 7 onwards increasing to a mean clinical score of 2 or above, which is considered as disease peak or relapse. Score reaching to 0.5 or below after day 17 is considered as EAE remission. Color codes define clinical scores of different group of animals (EAE animals' score in purple and wild-type controls in black). Representative data of 4 independent experiments are shown (n = 10 in each group for each experiment).

## *In vivo* visualization of cortical neurons by two-photon imaging

In both hemispheres, V1 is an easily accessible cortical region below the dura for functional imaging at the cellular-level *in vivo*. To achieve labeling in broad area, we adapted a well-established protocol from Garaschuk et al. (Garaschuk et al., 2006b). After drilling, we carefully removed the piece of skull attached to access the V1 area shown in Fig. 12(a & b) and bolus loaded (MCBL or Multicell Bolus Loading) fluorescent calcium indicators to label neurons for *in vivo* imaging (See Materials & Methods). In our experimental approach, the bolus loading procedure is based on pressure injection of membrane permeable OGB-1 BAPTA calcium indicator which is commonly used for *in vivo* two photon calcium imaging in the brain region of interest (Stosiek et al., 2003, Garaschuk et al., 2006b).

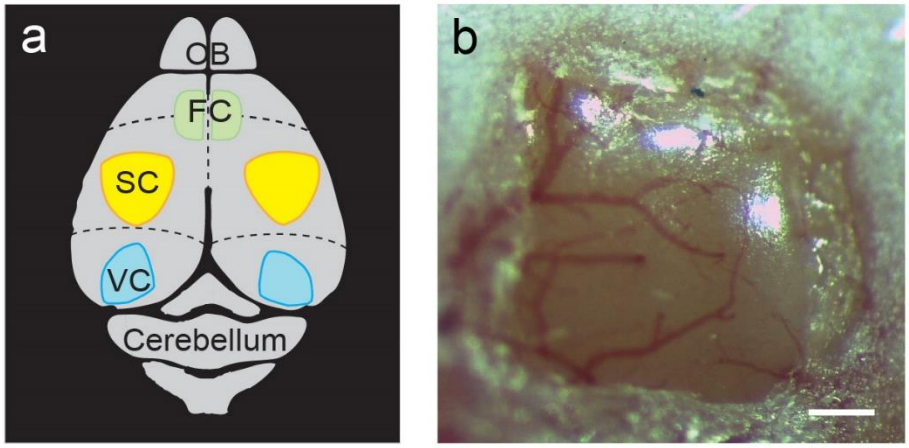


Figure 12: (a) Location map of the visual cortex (VC) in the brain. (b) Bright field image of cranial window opening of the V1 area in the visual cortex (Scale bar= 200µm).

Using our custom built two-photon microscope, we found densely packed neurons at the depth of 200µm below the surface in layer II/III visual cortex. Equipped with a fast resonant scanner our microscope allows us to image at 30 Hz in full field optical view (Fig. 13a).

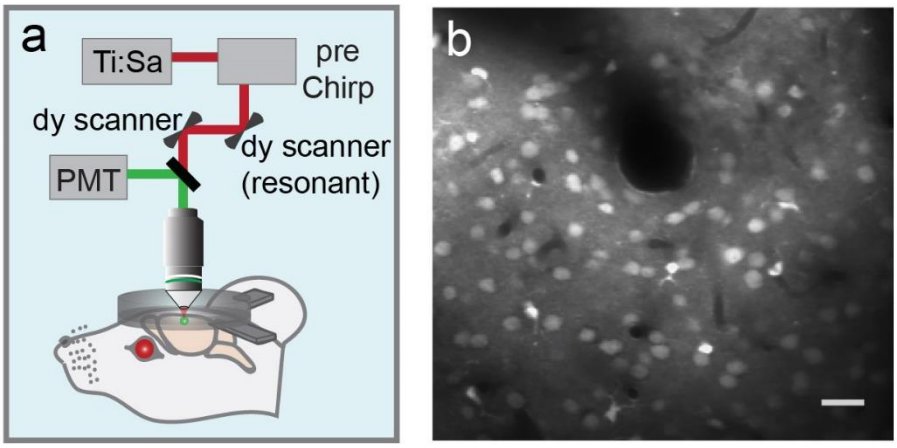


Figure 13: (a) Left, detailed view of Ti:Sa imaging *in vivo*. (b) Right, *in vivo* image of OGB-1 BAPTA stained neurons and astrocytes in V1 of a wild-type SJL mouse. Brightly labelled cells with processess are astrocytes (Scale bar= 25µm).

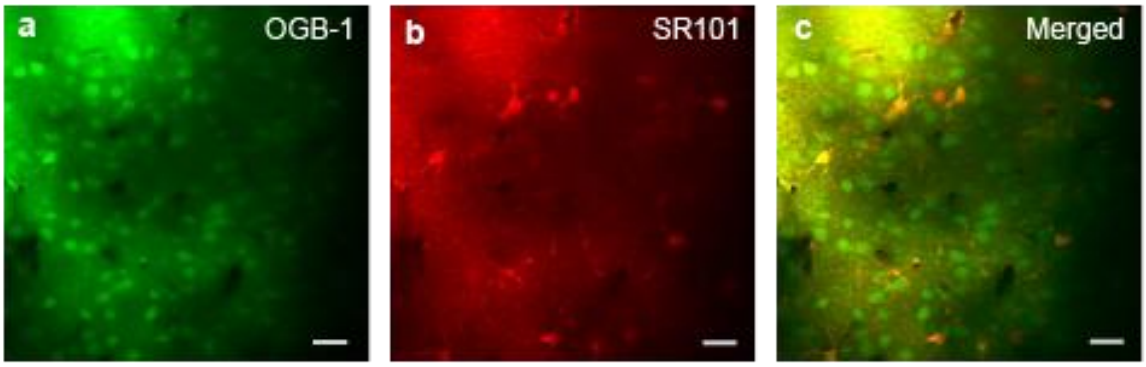


Figure 14: (a) Left, *in vivo* image of OGB -1 BAPTA labelled neurons and astrocytes in mouse visual cortex. (b) Middle, *in vivo* micrograph of SR101 labelled astrocytes. (c) Right, merged image of (a) & (b) (Scale bar= 25µm).

In a typical OGB-1 BAPTA staining, homogeneously labeled neurons and astrocytes (~250 cells) could be observed when excited at 800nm wavelengths (Fig 13b). In parallel, we also co-stained for astrocytes with Sulforhodamine 101 (SR101) along-side of OGB-1 BAPTA injection to confirm the identification of astrocytes (Fig. 14a, b & c). However, from previous studies, SR101 was found to have an effect on neuronal excitability and hence, staining for astrocytes using SR101 was abolished for subsequent functional experiments (Kang et al., 2010, Rasmussen et al., 2016). In addition, kinetics of astrocytes' $Ca^{2+}$ transients are very different than neuronal counterpart: typical $Ca^{2+}$ transients from astrocytes show slow rise as

well as slow decay time response curve (Nimmerjahn et al., 2004, Thrane et al., 2011). We performed ROIs analysis in the above imaging area and displayed spontaneous $Ca^{2+}$ transients (Fig 15). Those transients were identified by a time course consisting sharp rise and exponential decay response suggesting that they were resultant from neuronal action potential (AP) firing (Rochefort et al., 2009, Kang et al., 2010).

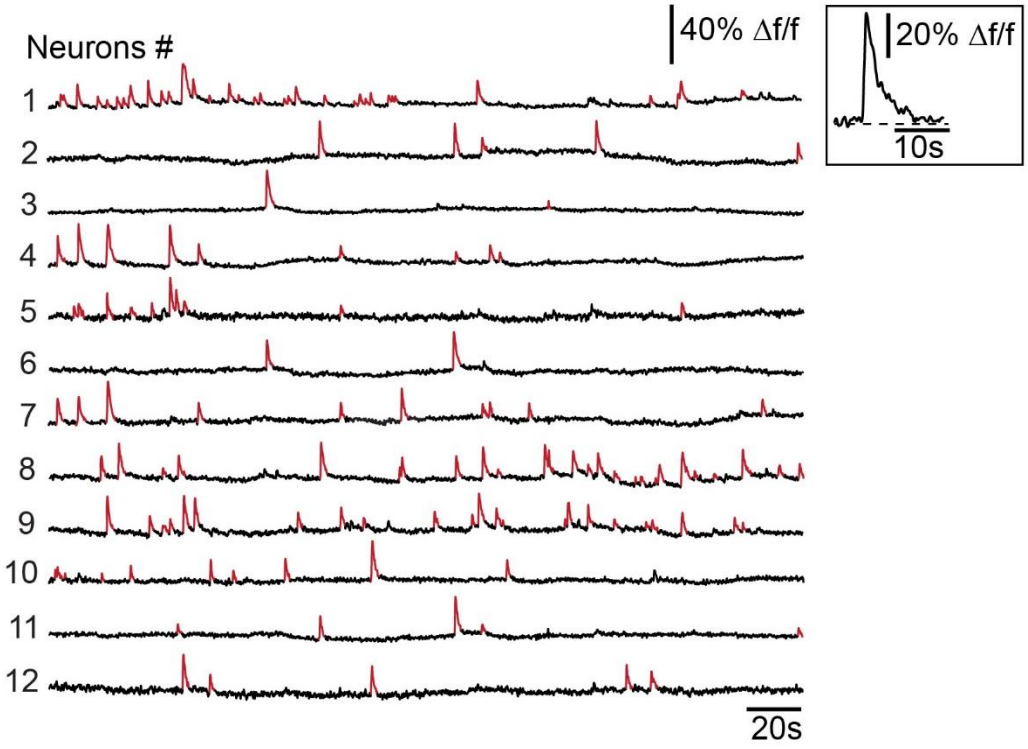


Figure 15: Two photon *in vivo* recording of spontaneous $Ca^{2+}$ transients from OGB-1 BAPTA labeled neurons of a wild-type animal. $Ca^{2+}$ transients are marked in red and baseline in black.

Action potentials firings lead to a brief surge of calcium ions into the cell resulting in an increase of intracellular calcium concentration which is detected as a rapid fluorescence change (Kerr et al., 2005, Yuste et al., 2011). The decay time constant of such transient typically ranging in few hundred milliseconds depending on the calcium buffering and extrusion mechanisms from the cell soma (Markram et al., 1995, Scheuss et al., 2006). Clearly, $Ca^{2+}$ transients and APs are well documented to linearly correlate with each other and

transients appear only after AP firing, shown in earlier studies by combining cell-attached recording with calcium recording (Rochefort et al., 2009). For our two-photon imaging experiments, we chose to label neurons with OGB-1 as it shows much greater photostability and in terms of absolute response and signal-to-noise ratio (SNR), it provides substantially better SNR compared to other indicators (See Materials & Methods). It is also a very sensitive reporter of neuronal activity allowing optical detection of single APs (Rochefort et al., 2009, Garaschuk and Konnerth, 2010). Here, we show spontaneous $Ca^{2+}$ transients from visual cortex neurons stained with OGB-1 AM from wild-type animal (Fig. 15). To differentiate the $Ca^{2+}$ transients from baseline, color codes were used where each transient is marked in red and baseline in black.

### Imaging spontaneous neuronal activity in the visual cortex

To monitor neuronal activity in the different cortical region, as discussed before, a widely used multi-cell bolus loading (MCBL) method of fluorescent calcium indicators has been used (Stosiek et al., 2003, Busche et al., 2008, Garaschuk and Konnerth, 2010). All these studies have revealed a fundamental finding, that individual neurons and neuronal population in the layer II/III exhibit sparse activity in absence of external stimuli (also known as "sparse spontaneous activity") (Kerr et al., 2005, Busche et al., 2008, Busche et al., 2012). Depending on the cortical layer, from a single spike of $Ca^{2+}$ transient to spike-burst has been observed. We found some neurons tend to be co-active repeatedly over the course of time in wild-type controls. This is shown in a short segment of data from 12 cells in Fig: 15. Such co-activation of neuronal ensembles in the layer II/III visual cortex may suggest that the functionally related cells are organized into distinct sub-networks. To be noted here, hippocampal neurons display more dense activity patterns as compared to the sparse activity we observed in the layer II/III visual cortex (Busche et al., 2012)

Under pathophysiological conditions, a very different activity pattern of those neurons could be observed depending on the disease type, affected area, phases of the disease etc. One of the common neurological disorders of human central nervous system is MS; a disease in young or middle aged female that last for several years causing from focal lesions to CNS-wide neurodegeneration (**see** Introduction). To fathom the neurodegeneration process and its' clinical relevance during MS development, a basic understanding of activity pattern of cortical neuronal network were mandatory. So far, the precise pattern of neuronal activity within different cortical regions during MS development has not been studied *in vivo*. To address this issue, we performed *in vivo* two-photon calcium imaging in the visual and frontal cortices in two different disease phases in EAE induced mice.

To attain homogenous fluorescent labeling with OGB-1 in layer II/III visual cortex's neurons in EAE animals, we followed the same MCBL protocol as previously described. Staining of each cortical layer at different cortical depth (100 & 140 µm below the surface representing layer I while 200 & 260 µm representing layer II/III) is shown in Fig 14. Next, we qualitatively assessed for any morphological differences of neuronal cell bodies in all groups. Here, we achieved reliable correspondence between *in vivo* images confirming no changes in morphological properties in either cases (Fig 16). We also observed very homogenous staining across all layers. Additionally, we determined the density of stained neurons from the layer II/III recording plane that resulted in similar values across all the three experimental groups (Fig 17). Astrocytes were excluded from the density analysis and numbers of stained neurons are expressed as neurons per square millimeter, shown in the histogram.

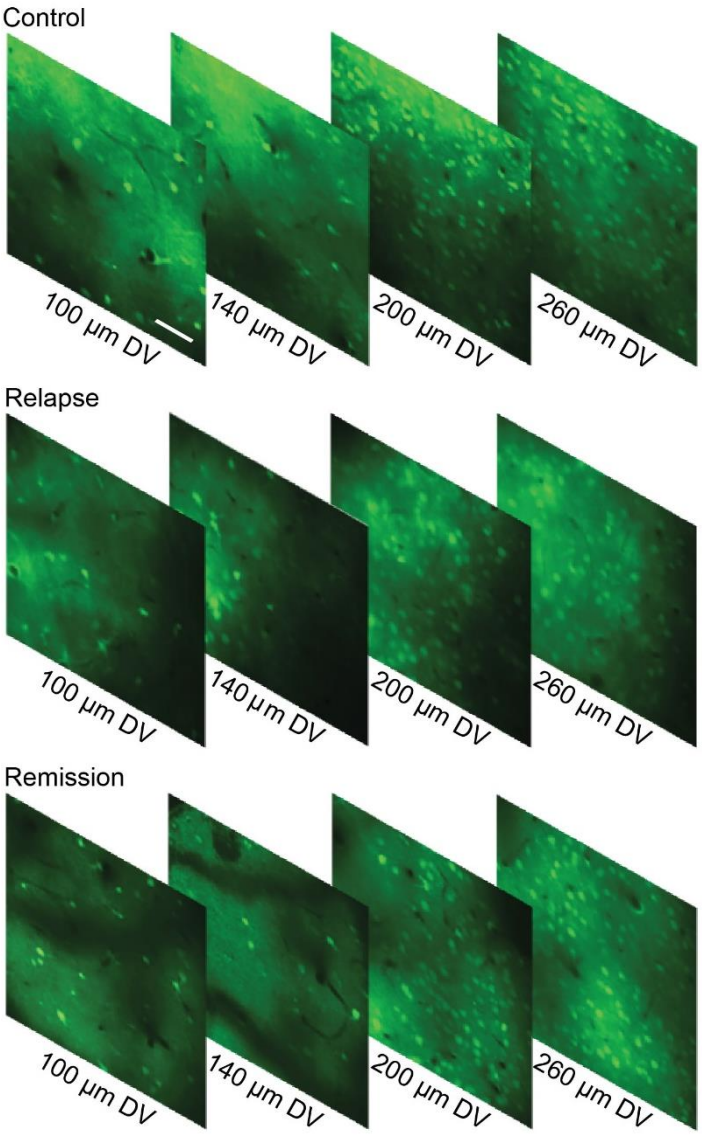


Figure 16: *In vivo* micrographs of different cortical depths from wild-type control, relapse and remission are shown here (scale bar = 25 µm; DV denoted as dorso-ventral.).

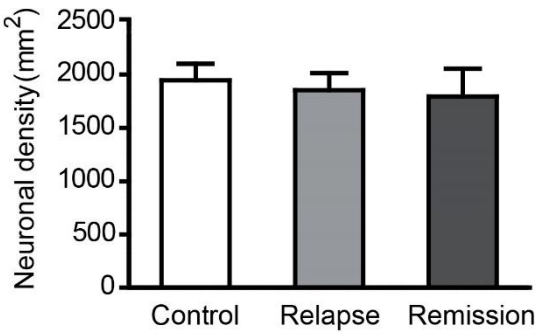


Figure 17: Quantitative analysis of neuronal density based on OGB-1 AM staining from all three experimental groups. Data are represented as mean ± SEM; One-way ANOVA test, N = 6 mice in control and relapse; 5 mice in remission.

## Activity pattern of visual cortical neurons in relapse-remitting EAE mice

In the next step, we used our method to assess spontaneous activity of the functional network in the V1 of EAE relapse and remission mice, and compared with wild-type controls. Note, all animals used for imaging in this study were same sex, age matched, and non-transgenic but with SJL background only as this background closely represent human disease form when immunized with $PLP_{139-151}$ (Miller and Karpus, 2007).

After cranial window preparation and OGB-1 loading, we first imaged layer II/III neurons from mice that were in the peak of the disease or relapse and then in remission. Traces of spontaneous calcium transients of the cortical microcircuit from each experimental group of animals are shown in Fig 18 (a, b, c). These representative traces are fractions of total recording where the total recording time for each session was 6 mins. Clearly, neurons from peak of the disease or relapse as well as wild-type control exhibited sparse spontaneous transients during whole recording period. But there was a drastic shift identified in the pattern of firing in remission mice compared with relapse and wild-type controls. Finding such burst of activity in absence of clinical symptoms or presence of mild symptoms is remarkable.

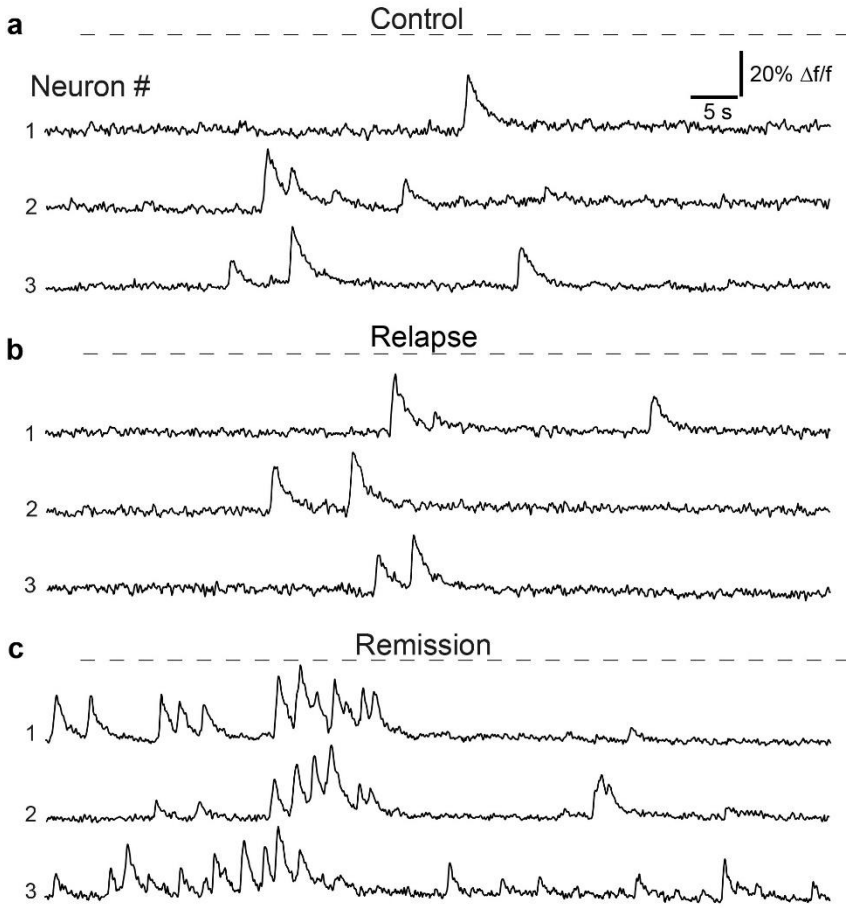


Figure 18: (a, b, c) Example traces of spontaneous $Ca^{2+}$ transients of three neurons from layer II/III visual cortex of all experimental groups. Note, increased activity of spontaneous $Ca^{2+}$ transients observed in remission.

We next performed detailed analysis by quantifying number of active vs. inactive cells present in each group. While there was a slight difference in percentage of active neurons in relapse compared with wild-type control (Control 50% and relapse 56%) but to our surprise, we noticed a drastic increase in active cell population in remission (remission 77%), referred in Fig 19 (Control n = 567 neurons, N = 6 mice; relapse n = 595 neurons, N = 6 mice and remission n = 650 neurons, N = 5 mice). Furthermore, we also identified significant increase in mean firing frequency of those active population only in remission (1.19 ± 0.05 transients/min, n = 500 cells, N = 5 mice) whereas there were no difference noticed in wild-type control vs. relapse, shown in Fig 20 (Control: 0.72 ± 0.04 transients/min, n = 282 cells, N

= 6 mice; relapse: 0.73 ± 0.04 transients/min, n = 332 cells, N = 6 mice). It is critical to mention here that in relapse, clinical symptoms are apparent (at the highest peak) but barely present in remission (from mild to no symptoms).

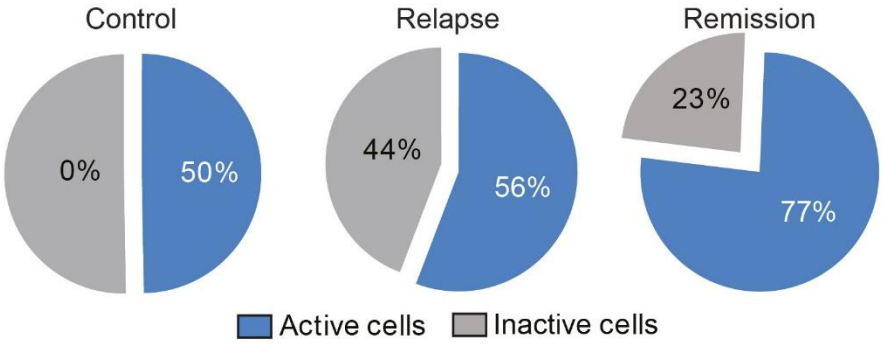


Figure 19: Pie chart depicting the relative proportions of active vs. inactive neurons from each category, respectively (Control n = 567 neurons, N = 6 mice; relapse n = 595 neurons, N = 6 mice and remission n = 650 neurons, N = 5 mice). Significant proportion of active neurons found in remission compared to wild-type control and relapse ($X^2$ test, $p < 0.001$). Separate color codes define the active (blue) vs. inactive (dark grey) population.

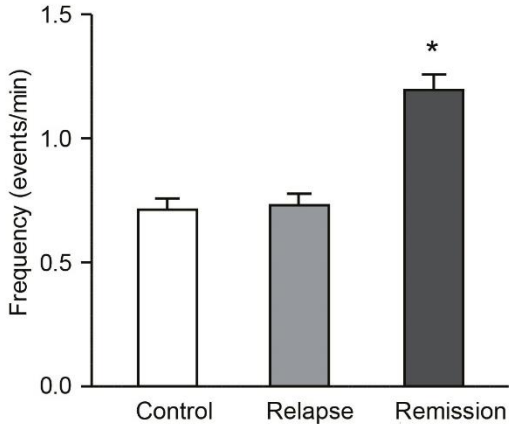


Figure 20: Histogram showing the mean frequency difference of spontaneous $Ca^{2+}$ transients of all active neurons among groups. The mean frequency was calculated from the active population, shown in Fig 17. Note, significantly increased in mean frequency detected in remission only (Data are represented as mean ± SEM; One-way ANOVA test, $p < 0.001$).

For a detailed analysis, all recorded neurons were classified based on their individual activity rate as “inactive” in dark grey (0 transients/min), “hypoactive” in yellow (<0.25 transients/min), “normal” in green (0.25-3.0 transients/min) or “hyperactive” in red (>3.0 transients/min), similar to previous assessment (Busche et al., 2008, Busche et al., 2012, Busche and Konnerth, 2015), traces shown in Fig 21. We then color-coded all four types of neurons based on their frequency response in relation to the three-dimensional place and navigated their spatial distribution (qualitative approach) within the microcircuit (Fig 22). The resultant shows that each neuronal subtype was randomly distributed instead of being clustered to represent their activity phenotype.

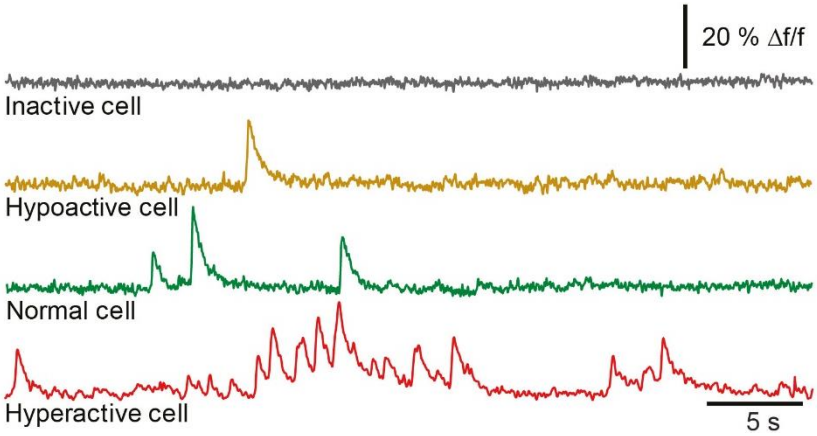


Figure 21: Traces are color coded to categorize based on their calculated frequency response to either inactive in dark grey (0 $Ca^{2+}$ transients/min), hypoactive in yellow (<0.25 $Ca^{2+}$ transients/min), normal neurons in green (0.25–3 $Ca^{2+}$ transients/min) and hyperactive neurons in red (>3 $Ca^{2+}$ transients/min).

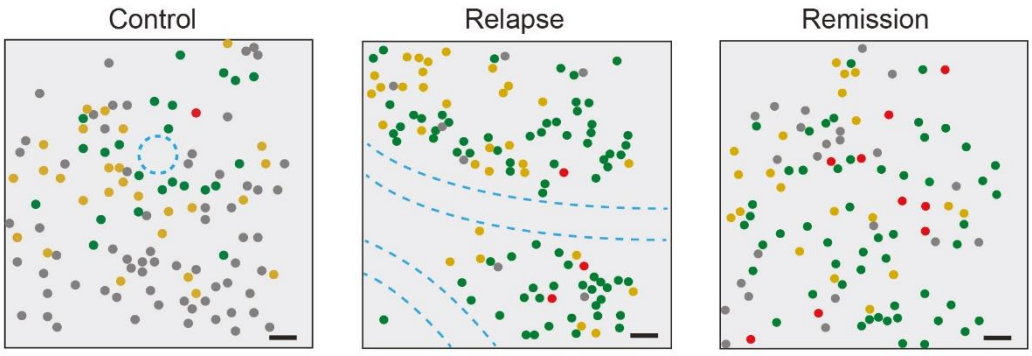

Figure 22: Schematic diagram representing spatial distribution of neurons that are color coded based on their mean frequency rate. All inactive cells in dark grey, hypoactive in yellow, normal in green and hyperactive cells in red. Blue dotted lines are used to mark the blood vessels (Scale bar= 25µm).

In addition, we observed that the proportion of normally active neurons were slightly elevated in relapse animals compared with wild-type controls (control 71%, relapse 78%), and no change in the fraction of hyperactive neurons could be observed in either groups (Fig 23). To our surprise, we found over four-fold increase in fraction of hyperactive neurons in remission mice (control 2%, relapse 2%, remission 9%), shown in Fig 23. This was accompanied by a gradual decrease in fraction of normally active cells in remission.

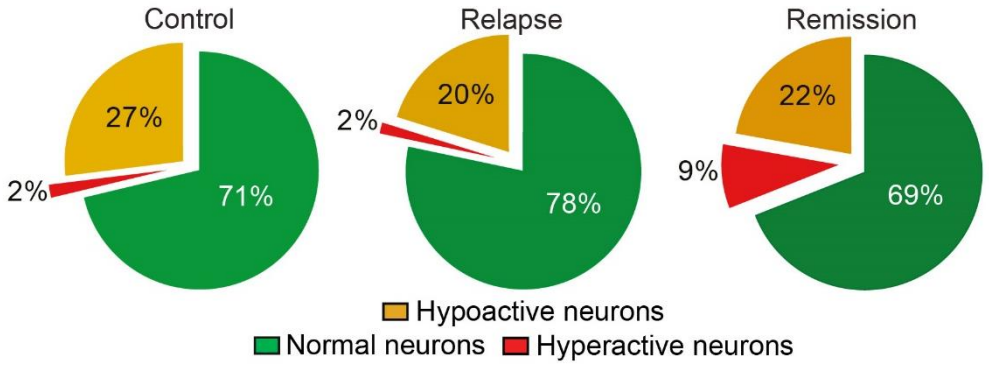


Figure 23: Relative proportions of all different categories of neurons (hypoactive, normal and hyperactive neurons) are shown in pie charts that were calculated from the total number of active cells provided in Fig. 17. All inactive population was omitted out from the current and following analyses. Note, significant increase in hyperactive neurons found in remission group compared with relapse and wild-type controls ($X^2$ test, $p < 0.001$).

Furthermore, we detected a slight difference in overall frequency distribution of normally active neurons in all experimental groups (Fig 24), reaffirming our finding about the total percentages of overall active neuronal population (Fig 23). We also did not find any obvious difference in mean frequency of hypoactive or hyperactive neurons among groups. Then we compared the cumulative frequency distributions of all neurons among groups which revealed

a significant shift towards higher frequencies of $Ca^{2+}$ transients particularly in remission phase (Fig 25).

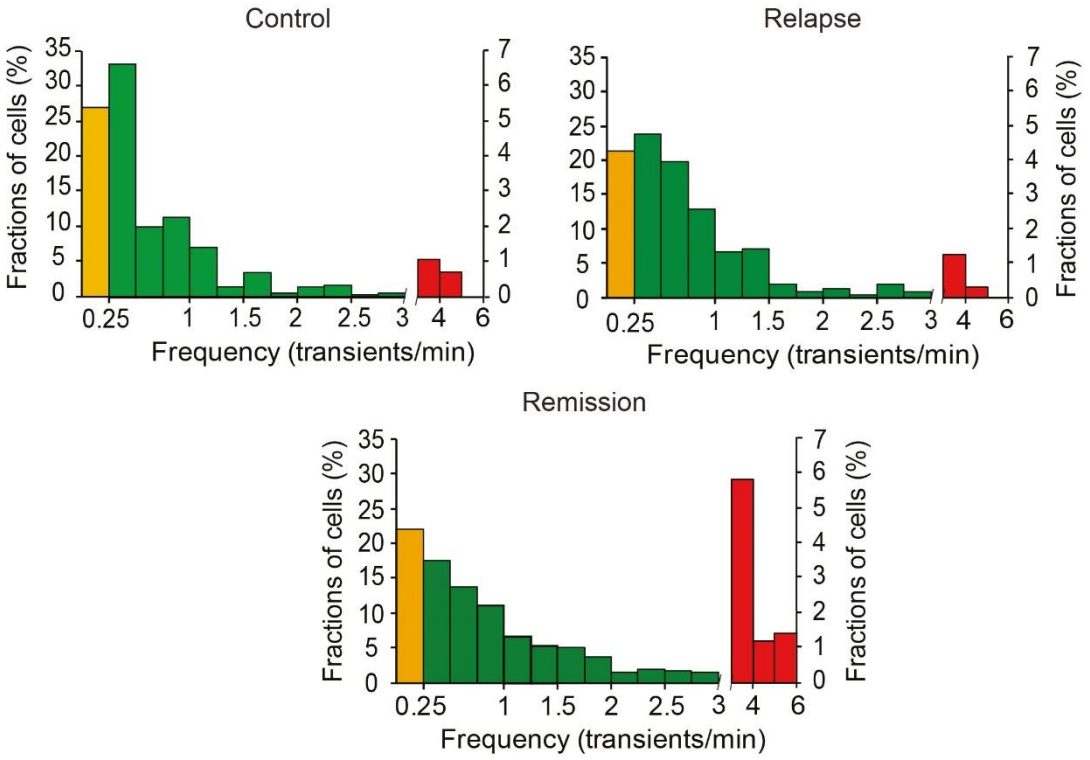


Figure 24: Histogram showing the frequency distribution of $Ca^{2+}$ transients in all three experimental groups. Note, increase in range of firing frequency in remission mice only.

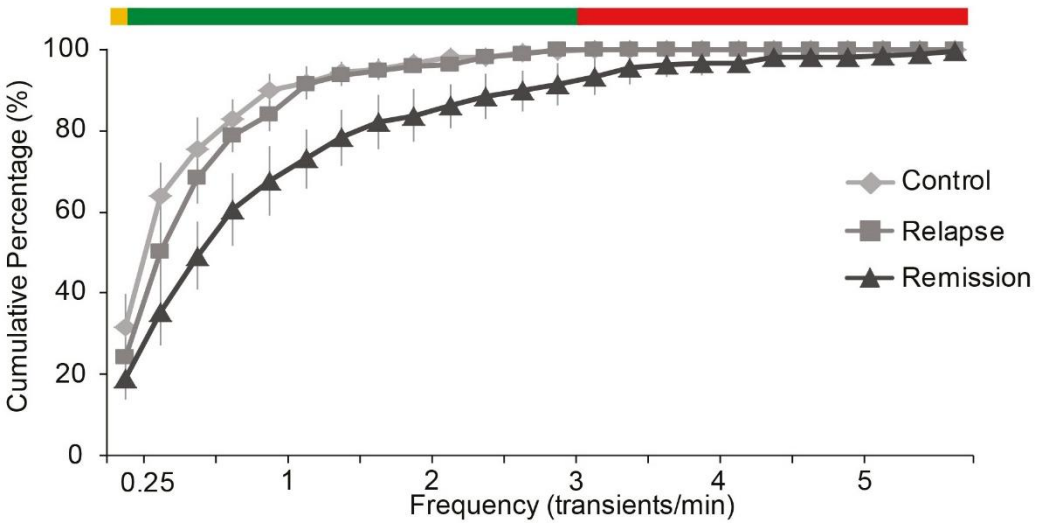


Figure 25: Line chart comparing cumulative normalized frequency distribution between all groups. Line trends are color-coded either in light grey to represent wild-type control, or mid

grey for relapse or dark grey for remission (mean ± SEM, Kolmogorov-Smirnov test, $p < 0.05$).

Together our results suggest that, there is higher proportion of active cells accompanied by increased calcium transient frequency which is due to the emergence of hyperactive neurons in the cortex of remission mice despite lowered clinical scores, and those hyperactive neurons are spatially distributed across the recording plane. On the other hand, despite having increased clinical scores, there was no obvious change in activity pattern observed in relapse mice.

### Patterns of neuronal activity in the frontal cortex of remission

While our observations in the visual cortex were very promising, we set out to understand whether such alteration of activity pattern is specific to a sensory area or it can be present in any other brain region which is not directly associated with any kind of sensory inputs. This would allow us to test whether the alteration of activity pattern is a cortex-wide phenomenon or not in remission phase of the disease. Therefore, we conducted subsequent imaging experiments in frontal cortices in remission; a cortical region that receives no direct sensory inputs from sensory cortical areas.

In order to record neuronal activity in the frontal cortex, cranial window was performed in the respective coordinates in a similar fashion as visual cortex and using MCBL, layer II/III neurons were labeled (refer Materials & Methods). To our surprise, the majority of the frontal cortex (FC) neurons in remission mice exhibited significantly elevated rates of spontaneous calcium transients when compared with age-matched wild-type controls (Fig. 26a). There was over four-fold increase in the fraction of active neurons in remission (21 %, n=106 cells, N = 4 mice) in contrast to wild-type mice (5 %, n=25 cells, N=4 mice). This was also reflected in significant elevation in the mean frequency of calcium transients in remission (0.42 ± 0.03

transients/min, n=106 cells, N = 4 mice, Mann Whitney U test, p<0.05) compared to wild-type controls (0.26 ± 0.03 trans/min, n=25 cells, N=4 mice). Furthermore, all recorded neurons were classified based on their individual activity rates as "silent" (0 transients/min), "hypoactive" (<0.25 transients/min), "normal" (0.25 – 3.0 transients/min) or "hyperactive" (>3.0 transients/min). As similar to the visual cortex, we studied the spatial distribution of each neuronal subtype based on their firing frequency in the activity map (Fig. 26b). In line with our result from visual cortex, we found that the fraction of normal neurons was significantly higher in remission (59%, N = 4 mice) unlike the wild-type (24%, N = 4 mice, p <0.05) (Fig 27a). This was further accompanied by drastic reduction in fraction of hypoactive neurons (41%, N =4 mice) in remission when compared with controls (76%, N =4 mice), suggesting overall increase in excitatory drive in spontaneous activity in the frontal cortex in remission animals. However, no hyperactive neuron was observed in both groups.

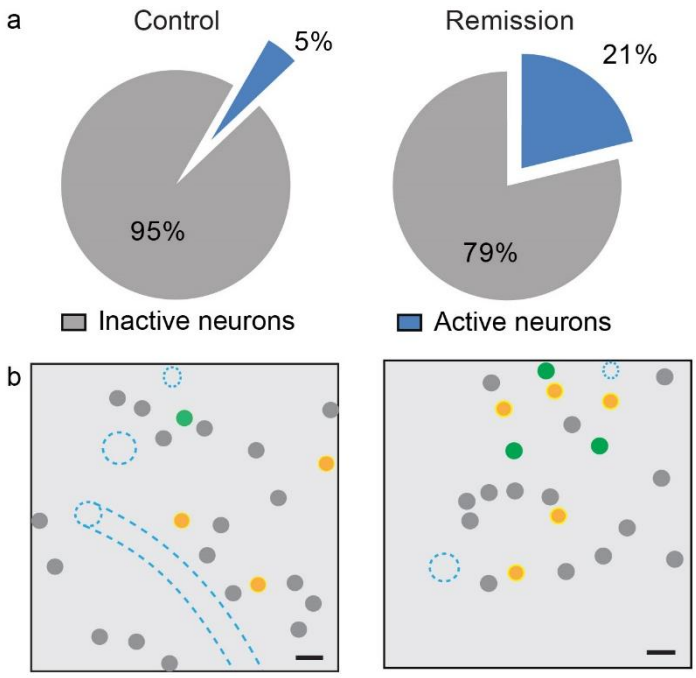


Figure 26: (a) Pie charts depicting relative proportions of active vs. inactive neurons in the frontal cortex from wild-type control and remission groups (n = 543 neurons; N = 4 mice; remission n = 500 neurons; N = 4 mice). Over four fold increase in active neurons found in remission frontal cortices in contrast to wild-type ($X^2$ test, p < 0.001). Dark grey represents

inactive neurons and blue represents active neurons. (b) Activity map is determined by the spatial distribution of neurons that are color-coded based on their frequency, overlaid on the anatomical image. Inactive neurons in dark grey (0 $Ca^{2+}$ transients/min), hypoactive neurons in yellow (<0.25 $Ca^{2+}$ transients/min) and normal neurons in green (0.25–3 $Ca^{2+}$ transients/min). Dotted lines in blue represent blood vessels. Scale = 25 µm.

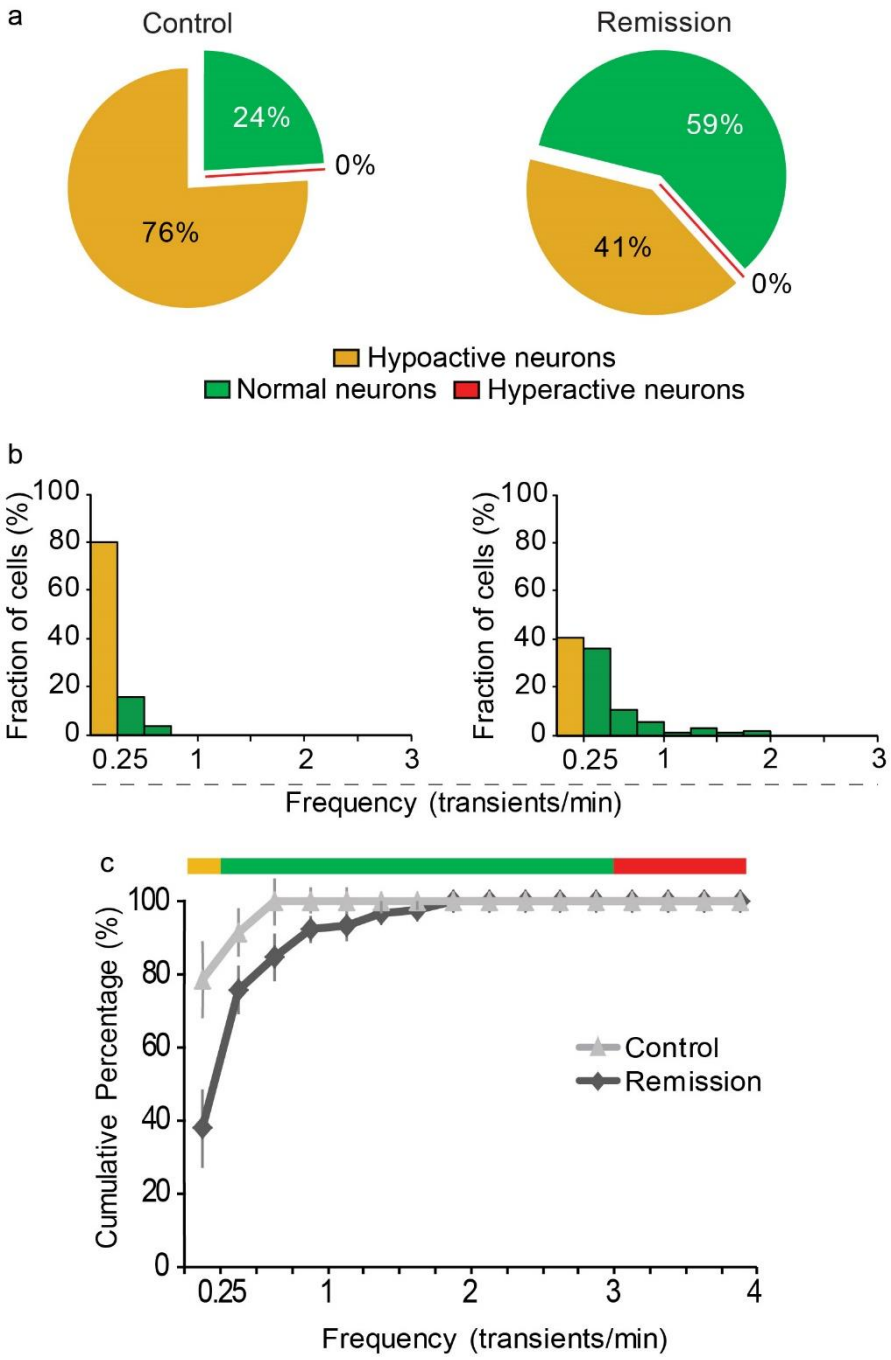


Figure 27: (a) Relative proportions of hypoactive, normal and hyperactive neurons are shown in above pie charts. Color-codes are used to distinguish each category of neurons based on their rate of firing frequency. Inactive neurons were excluded from the following analysis.

Two fold increase in normally active neurons found in remission while reduction in hypoactive neurons ($X^2$ test, $p < 0.001$). (b) Histograms illustrating the frequency distributions of calcium transients in wild-type controls and remission mice. Note, increased fractions of normally active neurons in remission mice. (c) Cumulative frequency distribution of spontaneous calcium transients in remission mice which was significantly shifted from wild-type controls. Data represented mean ± SEM, Kolmogorov-Smirnov test, $p < 0.05$. All error bars denote S.E.M.

In addition, our detailed analyses also confirmed that the frequency distribution of normally active neurons shifted towards higher values in remission (Fig 27b), which was further accompanied by a significant shift in cumulative frequency distribution towards higher frequencies in remission compared with wild-type controls (Fig. 27c).

Together these results clearly indicate that alteration in activity patterns exist in both cortices, suggesting a cortex-wide phenomenon in remission animals.

## Analysis for affected areas in the brain of EAE mice by histology

As we observed overt changes (increased network activity followed by elevated hyperactivity) in spontaneous activity in the visual cortex layer II/III neurons in EAE remission mice, we sought for the responsible factor(s). Our notion was that the transmigrating inflammatory cells e.g. mononuclear cells, lymphocytes infiltrate through BBB. The entry of these cells triggers inflammation and progressive lesion formation, and it could be the key elements for alteration in microcircuit activity. To evaluate their contribution, we performed histology and immunohistochemistry (refer Material & Methods) to stain for myelin loss, microglia/macrophages, T cells and axonal pathology in remission animals (Fig 28). To our surprise, we did not find any myelin damaged area in the cortex from the anti-MBP staining confirming no ongoing myelin damage (Fig 28a.). Furthermore, we did not spot any activated

microglia/macrophage cells in Mac-3 stained or CD3 positive T cells in brain slices (Fig 28b, c). Yet there were small areas of demyelination and infiltrates of mononuclear cells (microglia/macrophage and T cells) spotted in the meningeal area of spinal cords in remission (Fig 29; left panel – demyelination, middle – microglia/macrophages and right panel – CD3+ T lymphocytes). Parallelly, we conducted amyloid precursor protein (APP) staining to determine axonal degeneration in the brain slices from remission mice which revealed no positive APP signal, indicating no obvious neurodegeneration (Fig 28d). Thus, we exclude any possibilities of direct effect of infiltrating or activated CNS-resident immune cells on neuronal activity observed in the cortex in remission mice.

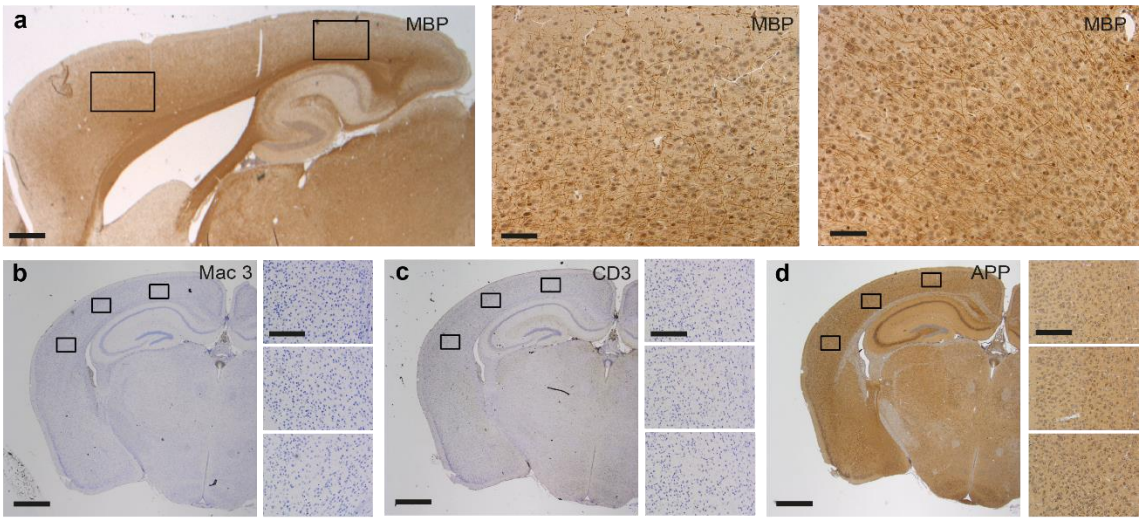


Figure 28: Brain slices from remission mice were stained for myelin damage (with anti-MBP), T-lymphocytes infiltration (anti-CD3 antibody), microglia/macrophage activation (anti Mac-3 antibody), and axonal degeneration (amyloid precursor protein or APP) and imaged by light microscopy. Boxed area on the left panels are enlarged on the right panels (a) no myelin loss, (b & c) inflammatory infiltrates or (d) axonal degeneration were detected in the cortex (N = 4 mice of same age and sex). For all images scale bar = 200 µm.

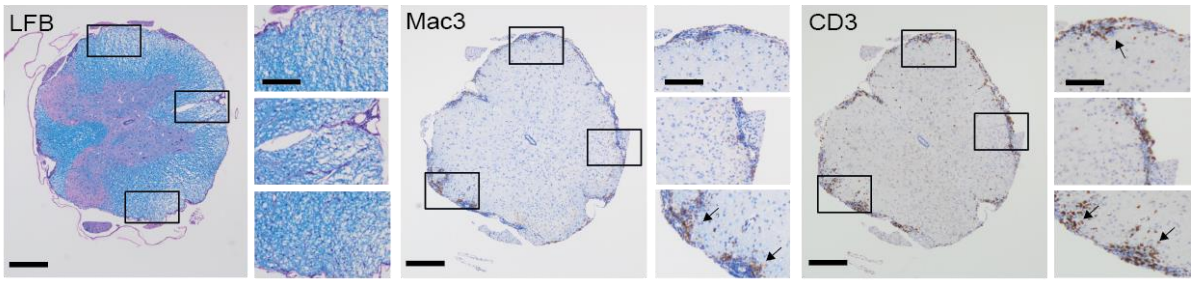


Figure 29: Histology and immunohistochemistry of the lumbar area of spinal cord slices from remission mice. Left panel, demyelination spotted in meningeal area in the white matter, shown in boxed sections and in the right their enlarged views. Center and right panels, locations of microglia/macrophages and inflammatory infiltrates are shown in the box areas and their corresponding enlarged windows on right (Scale bar= 200 µm). In all images above arrow marks are placed indicating the positions of respective positive signals.

## Etology of remission phase EAE mice

While the pathology and prognosis in MS is generally associated with the neurological and neuropsychological deficits ranging from cognitive, memory learning to sensory and motor dysfunctions, such behavioral alterations at the early stage of the disease has also been documented in EAE (see Introduction) (Haussleiter et al., 2009). Hence in our studies, the relationship between increased cortical network activity and any behavioral alteration in remission was desirable.

## Visual discrimination & rotarod task

Next, we asked whether if there is any association of observed cortical hyperactivity and behavioral deficits in remission mice. Since, optical neuritis is a common clinical symptom and often noticed in human patients with MS. Hence, to rule out any effect of peripheral degeneration of sensory afferent pathways on cortical network activity, we conducted visual discrimination tasks in remission and compared with wild-type. In parallel, we also conducted rotarod, open-field, elevated plus maze and fear-conditioning tests to assess their cognitive,

sensory, and motor and memory learning capabilities. Visual discrimination task was conducted to assess the ability to discriminate between a dark (black) and bright (white) screen. A basic diagram of the visual discrimination task set up is illustrated in Fig 9. Note, relatively old SJL/J background mice are known to exhibit retinal degeneration, leading to impaired vision (Chang et al., 2002, Wong and Brown, 2006). Prior to EAE induction, training sessions were carried out for both groups, and mice that made correct choice over 70% at least for three consecutive days, were considered for subsequent EAE induction followed by discrimination analysis (see Materials & Methods). After a period of one week training session, mice were able to perform tasks successfully exceeding the 70% criterion (Fig. 30a). The performance level of both group was comparable to that of Bl6 mice (Fig 30b), which has been used as positive controls because of their normal visual acuity (Wong and Brown, 2006).

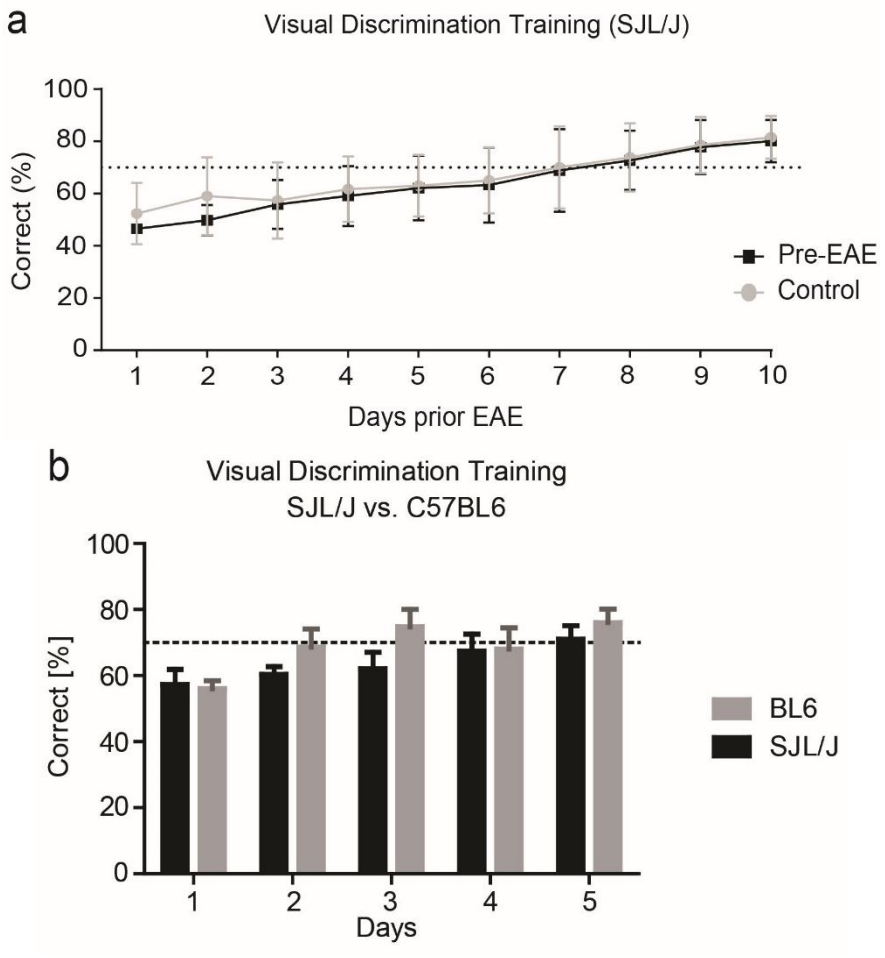

Figure 30: (a) Graph representing time course of the training sessions of each group prior EAE induction. Pre-EAE denotes prior to EAE induction. Note, no statistical difference observed between wild-type control and pre-EAE mice (10 mice per group and 6 training sessions performed for each group; two-way ANOVA test, p=0.56). Mice made 70% correct choice for at least three consecutive days were considered for further tests. Dashed lines denote chances in performance. (b) Comparison of the training results between BL6 and SJL/J mice are shown. Note, the difference between both groups were comparable. Student's t-test, all error bars denote S.E.M.

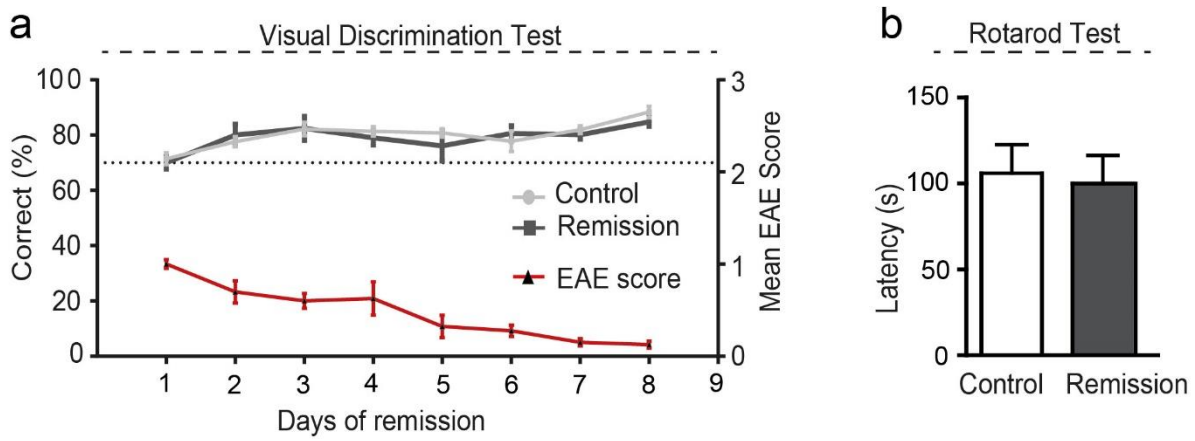


Figure 31: (a) Time course of the performance from both group animals in the visual discrimination task in relation to the clinical score of EAE remission. There was no difference observed between both groups (5 trial sessions per animal, wild-type control N = 10 mice; remission N = 10 mice, Two-way ANOVA, p=0.59). Dashed lines, chance in performance. (b) Rotarod: sensorimotor function and cognitive performance tests of remission and wild-type control mice. Latency to fall from the rotarod for each group are shown (wild-type control N = 10 mice; remission N = 10 mice, p = 0.05). Student`s t-test all error bars denote S.E.M.

After the training period, mice were subjected to EAE induction followed by task performance. Interestingly, visual discrimination ability was not affected in EAE remission mice, as it stayed above the 70% learning criterion and further increased over seven days of testing period during remission period (Fig. 31a). In rotarod test, we tested for motor coordination and cerebral dysfunction. , The performance on the typical accelerating rotarod

was identical in remission and wild-type controls mice, because latencies for falling were similar (Fig. 31b).

## Open-Field, Elevated Plus Maze, Fear Conditioning Tests

To assess locomotor activity in remission animals, we used the B-B-B (Baaso, Beattie and Bresnahan) locomotion scale for evaluation in an open field test (Basso et al., 1995). In our experiment, post EAE induction, all remission animals displayed a severe impairment in locomotor activity in the open field, shown in Fig 32a. In particular, remission mice demonstrated significantly decreased distance travelled, and velocity as compared to wild-type controls (Fig. 32a, left and middle panels). These results indicate that EAE remission mice show impaired locomotor activity. However, both groups spent nearly same time in the central zones of the open field (Fig 32a, right panel)

Using the elevated plus maze paradigm for assessing anxiety, remission mice moved significantly less distance with lower velocity, and demonstrated significantly lesser frequency in entering to the open arms (Fig. 32b). Following the test course, remission mice also demonstrated a significantly higher time spent in the center. These impaired performances suggest an anxious phenotype in EAE remission mice. To ascertain if EAE itself altered fear memory in remission or any association between hyperactivity and fear memory in remission we performed fear conditioning tests, illustrated in Fig 32c. Freezing levels were significantly higher in remission in response to the baseline indicating a fear memory effect compared with wild-type, while no obvious difference observed in response to context or cue. Together these data shows slight behavioral phenotype in remission animals.

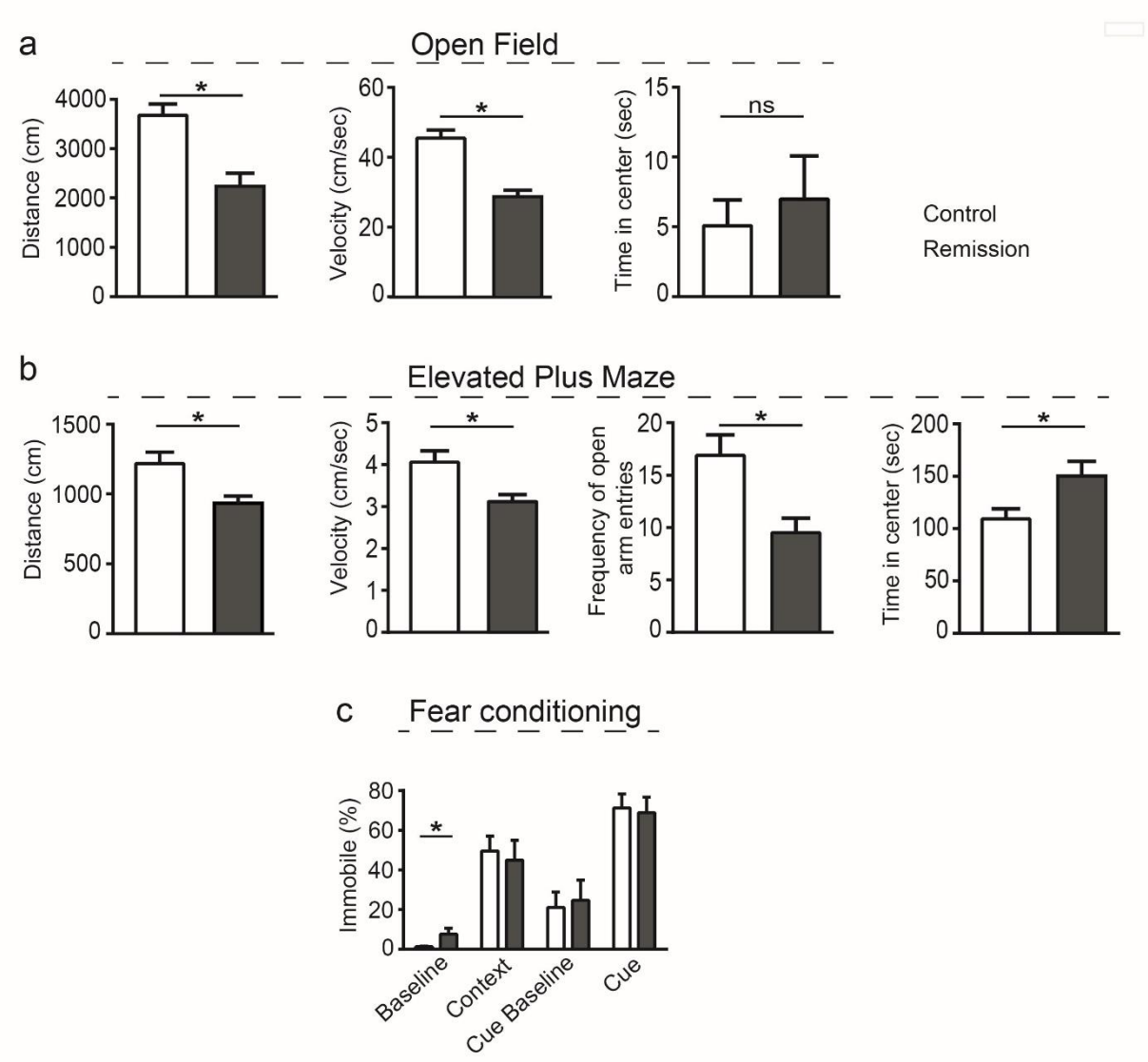


Figure 32: (a) Exploratory activity and time spent in the center in the open-field test comparing remission mice with wild-type controls. Left, remission mice moved shorter distances compared with wild-type mice. Middle, remission mice demonstrated significantly reduced velocity, respectively ($p<0.05$). Right, no significant difference observed in time spent in the center ($p= 0.06$). (b) Bar graphs depicting performance of remission and wild-type groups in elevated plus maze (EPM) task. Each of the parameters in the EPM test performed by remission mice showed significant differences compared with wild-type mice ($p<0.05$). (c) Contextual and cued fear conditioning, data shown in percentage of freezing responses after each treatment (at the beginning and end of the task) monitored in wild-type and remission mice. Note, freezing levels were significantly higher in remission ($p < 0.05$) in response to the baseline. In all above experiments, 10 mice per group and 6 training sessions for each group were performed; unpaired test. Data presented as mean ± S.E.M. ns, not significant.

## Molecular analyses of cytokines and neuromodulatory factors in remission

The finding that increased cortical activity occurred independent of cortical myelin loss or demyelination, inflammatory inflammation or any sensory deficits had indicated that not any peripheral factor rather internal factor(s) of the CNS might play an important role for altering the cortical circuit dynamics. Several earlier studies in developmental neuroscience and neuropathology field reported about the implications of neurotrophic and neuromodulatory factors in remodeling brain function(s), of which cytokines are common. Therefore, to investigate whether cytokine(s) and/or stimulatory factor(s) are responsible for increased cortical activity, we carried out quantitative PCR analysis of cortices only in all three groups (wild-type control, relapse and remission).

## Increased TNFα levels in the cortex during remission

Our qPCR analysis of relevant cytokines and neuromodulatory factors revealed surprising results in relapse and remission (Fig. 33). In contrast to the basal expression in wild-type controls, there was significant increase of TNFα in relapse mice and further five-fold increase in remission mice (Fig. 33a). While the expression of other proinflammatory cytokines such as interferon-γ (IFN-γ), interleukin-17 (IL-17) and stimulating factors e.g. granulocyte macrophage colony-stimulating factor (GM-CSF) remained below the detection threshold (Fig. 33a). In addition, overall expression of neurotrophic and neuromodulatory factors i.e. brain-derived neurotrophic factor (BDNF), transforming growth factor beta 1 (TGF-β1) and interleukin-4 (IL-4) remained unaltered in all group (Fig. 33b). Thus, elevated TNFα level in the cortex could be the key factor responsible for alteration of the cortical hyperactivity in remission mice and this finding is further supported by earlier reports about potential

involvement of TNFα in synaptic plasticity (Beattie et al., 2002, Stellwagen and Malenka, 2006b, Centonze et al., 2009a).

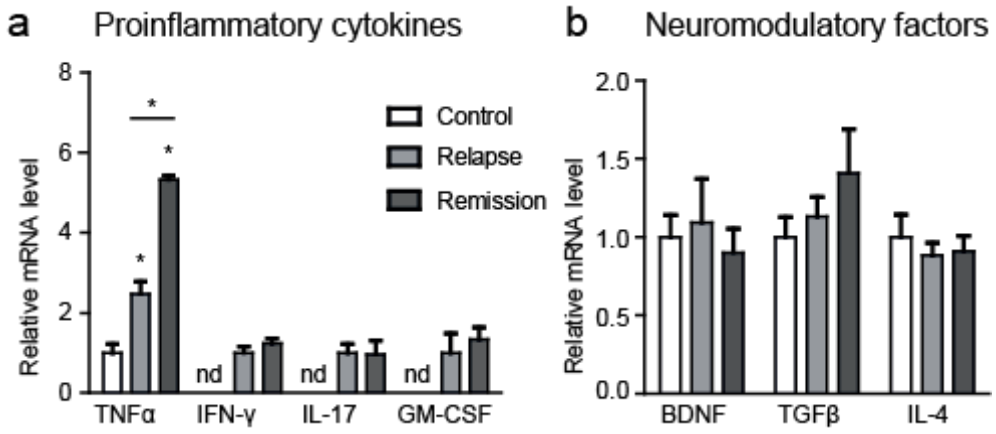


Figure 33: (a & b) Summary graphs from all quantitative PCR (qPCR) experiments illustrating the relative changes in proinflammatory cytokines and neuromodulatory factors' expression in all three groups. Data are representative from 10 mice per group of two independent experiments. Cytokines and neuromodulatory factors expression was normalized to the expression of the housekeeping genes (refer Materials & Methods). Note, we found two fold increase of TNF-α expression in relapse and five-folds increase in remission compared with wild-type controls. All data represented as mean ± S.E.M., one-way ANOVA, $p<0.05$ or $p=0.05$, nd, no difference relative to the control group.

## Rescue of neuronal hyperactivity by infliximab injection

It was shown in previous chapter we show that there is significant increase in TNFα expression in relapse and further in remission, and cortical TNFα is known to play role in synaptic transmission (Beattie et al., 2002). Therefore, we hypothesized that elevated cortical TNFα expression could drive alteration in activity pattern (including hyperactivity) in the layer II/II cortices is in remission mice. Next, we examined whether selective release of cortical TNFα at the trans-synaptic terminals is the only responsible factor for altering neuronal activity. If so, controlling TNFα expression in the cortex could possibly restore the activity pattern in remission mice. In order to seek out this hypothesis, we performed whole-

cell patch clamp recording on acute slices and analyzed AMPA-receptor mediated spontaneous excitatory post synaptic currents (sEPSCs) from remission mice comparing with wild-type controls. In all cases, sEPSCs were isolated pharmacologically at a holding potential of -80 mV. Mean amplitude, frequency and decay time constant were calculated from the recorded sEPSCs. Few example traces are displayed in Fig. 34.

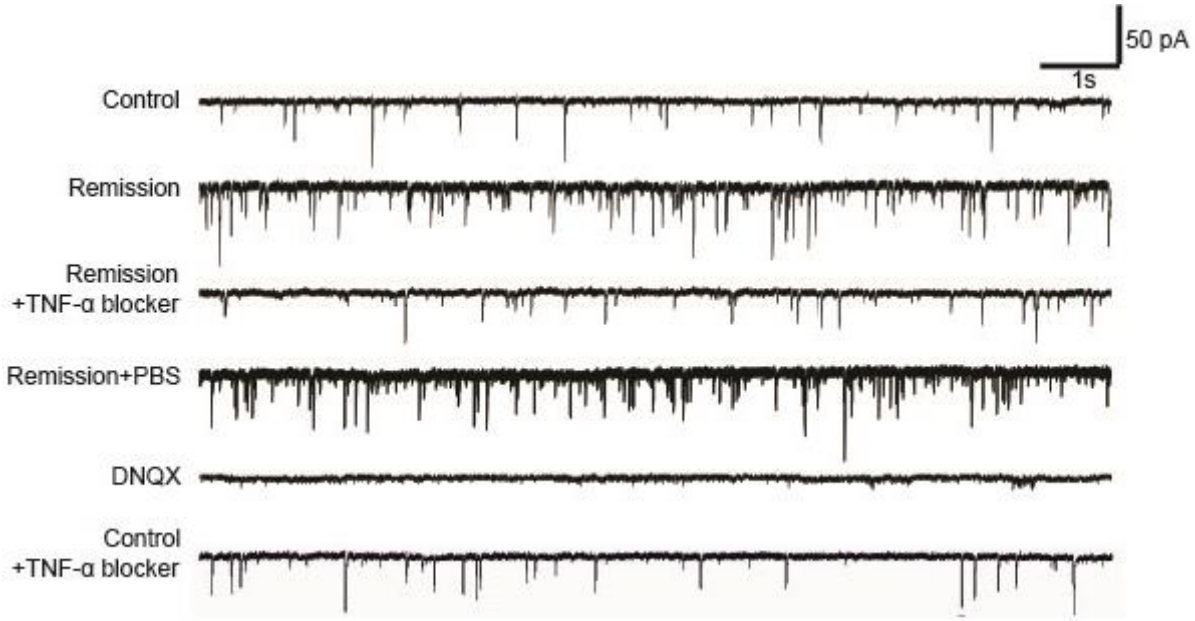


Figure 34: Representative traces of AMPA-receptor mediated spontaneous excitatory post synaptic currents (sEPSCs) under various conditions. The whole-cell patch clamp recordings in voltage-clamp mode were made in acute slices from wild-type untreated control and untreated remission mice or remission mice treated with infliximab, PBS, DNQX, respectively or wild-type controls treated with TNFα blocker (see Materials & Methods for treatment protocol).

From the traces and Fig 35a, it is clear that the mean frequency of sEPSCs were significantly increased in remission animals (8.98 ± 0.8, Hz, N=18 mice) compared with wild-type controls (4.55 ± 0.7 Hz, N=19 mice). But we did not observe any difference in amplitude or decay time constant of those recoded sEPSCs (Fig. 35b & c), suggesting a presynaptic site of action. Subsequently, intraventricular injection of infliximab, a monoclonal antibody for TNFα,

restored sEPSCs frequencies in remission animals (5.4 ± 0.5 Hz**,** N=18 mice) to same levels as wild-type controls (4.6 ± 0.7 Hz, n=19 mice), shown in Fig. 35a. Yet PBS treatment in remission did not restore frequency changes in those animals. Note, we also tested for whether application of TNFα blocker has any effect on sEPSCs and we did not notice any difference in frequency or amplitude but noticeable difference observed in decay time constant. Together this data confirms that TNFα is a key factor in increasing cortical hyperactivity proven at single cell level. However, we also wanted to test whether restoring cortical hyperactivity can be achieved at the network level and to do that we performed *in vivo* $Ca^{2+}$ imaging in remission mice treated with infliximab.

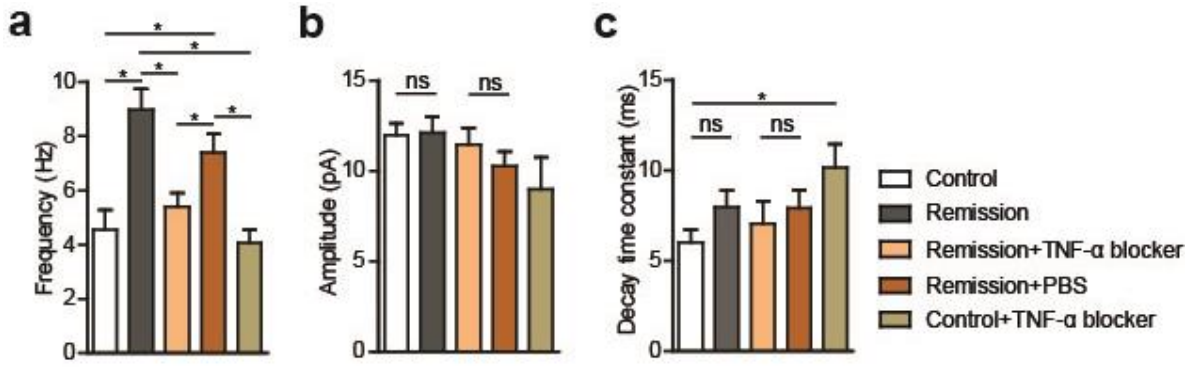


Figure 35: (a) Summary graph depicting changes in mean frequency of sEPSCs relative to the controls from the experiment in fig 34. Note, significant increase in mean frequency revealed in remission which further recovered by infliximab (anti-TNFα antibody) administration. While sham injections (PBS) did not alter sEPSCs frequencies. (b) Histogram illustrates mean amplitude of sEPSCs from all experiments (normalized to controls). No change observed in either group. (c) Summary graph showing decay time constant of the recorded sEPSCs (normalized to controls). No difference observed except in wild-type controls treated with infliximab. Data represented from 60 cells in 18 mice per group. Student's t-test, $p<0.05$, all error bars denote S.E.M.

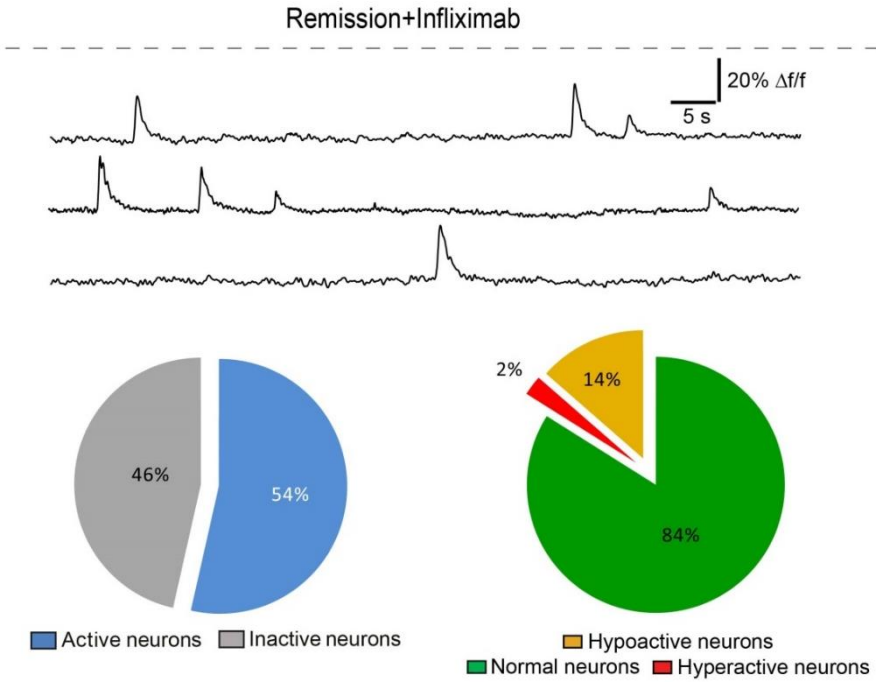


Figure 36: Representative traces of spontaneous $Ca^{2+}$ transients of three neurons of remission animal treated with infliximab are shown above. (Bottom-left) Pie charts depicting the relative proportions of active vs. inactive neurons (Remission treated with infliximab n = 525 neurons, N = 4 mice) and (bottom-right) relative distributions of all different category of neurons (hypoactive, normal and hyperactive neurons) are shown. These distributions were calculated from the total number of active cells from the left. No difference in total number of active cells or hyperactive neurons observed in comparison to wild-type controls, showed in Fig 19 & 23. Separate color codes define the active (blue) vs. inactive (dark grey) population in the left and hypoactive (yellow), normal (green), and hyperactive population (red).

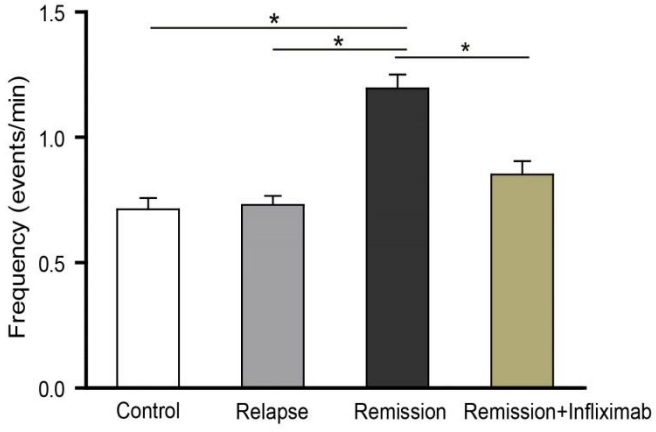


Figure 37: Histogram showing the mean frequency difference of spontaneous $Ca^{2+}$ transients of all active neurons among groups including remission mice treated with infliximab for

increased TNFα. The mean frequency of infliximab treated remission group was calculated from the active population, shown in fig 33. Note, no difference observed between wild-type controls and remission mice treated with infliximab. Data are represented as mean ± SEM; One-way ANOVA test, $p < 0.001$.

Our *in vivo* two-photon results from remission mice treated with infliximab bear a significant resemblance to the finding of whole cell patch recording data. We noticed the percentage of active and hyperactive neuronal population was similar to the wild-type controls (Fig. 36). Furthermore no difference in firing frequency of the active population in infliximab treated remission group was observed comparing with wily-type controls (Fig. 37). It confirms that the observed changes in activity pattern in remission can be restored back to normal at the large network level similar to wild-type controls dynamically by administration of infliximab.

Together these suggest that selective release of cortical TNFα in the trans-synaptic cleft is the key modulator for alteration in firing frequency of cortical neurons and a restoration can be achieved by application of anti-TNFα antibody in remission mice of EAE. However, the source of TNFα release is not yet clearly identified in the cortex in remission.

### Immunofluorescent staining for TNFα

Next, in order to investigate the source of TNFα in the cortex, we performed immunofluorescent staining for TNFα and for different glial and neuronal markers in brain slices of remission animals (Fig. 38 & 39).Results are compared with same age and sex matched wild-type controls (Fig. 40). From qualitative analysis of confocal images, we did not observe any co-localization of TNFα with any of the following markers i.e. GFAP+ astrocytes, Iba-1+ microglial cells and GAD 67+ inhibitory neurons (Fig 38a, b & d). Surprisingly, there were co-localization of TNFα with some NeuN+ neurons, and almost all (under the field of view) CamKII+ excitatory neurons detected (Fig 38, 39c & e). As

expected, overall signal for TNFα was low in wild-type controls (Fig 40) and in contrast to the remission group, we encountered weak co-localization of TNFα with NeuN or CamKII+ neurons in those wild-type controls (Fig 40c & e). Several studies in the past reports that in the mature brain, astrocytes are the main source of soluble TNFα at the pre-synaptic terminals that are involved in synaptic strength and homeostatic plasticity (Beattie et al., 2002, Stellwagen and Malenka, 2006a). However, we did not observe any overlapping signal of TNFα and astrocytes in our co-staining but this does not exclude the possibilities that soluble TNFα released from activated astrocytes could potentially translocate and bind to other cells.

Together these results suggest that soluble TNFα released in the cortex bind to the CamkII+ excitatory neurons and directly induces neuronal hyperactivity by altering cortex-wide network activity, which might initiate early dysfunction of cortical network in EAE mice. Yet, we did not identify the source of soluble TNFα, thus we cannot exclude the possibility that residential cells of the CNS i.e. astroglial cells or different neuronal subtype could be the potential source of TNFα production thereby affecting neuronal activity in the remission.

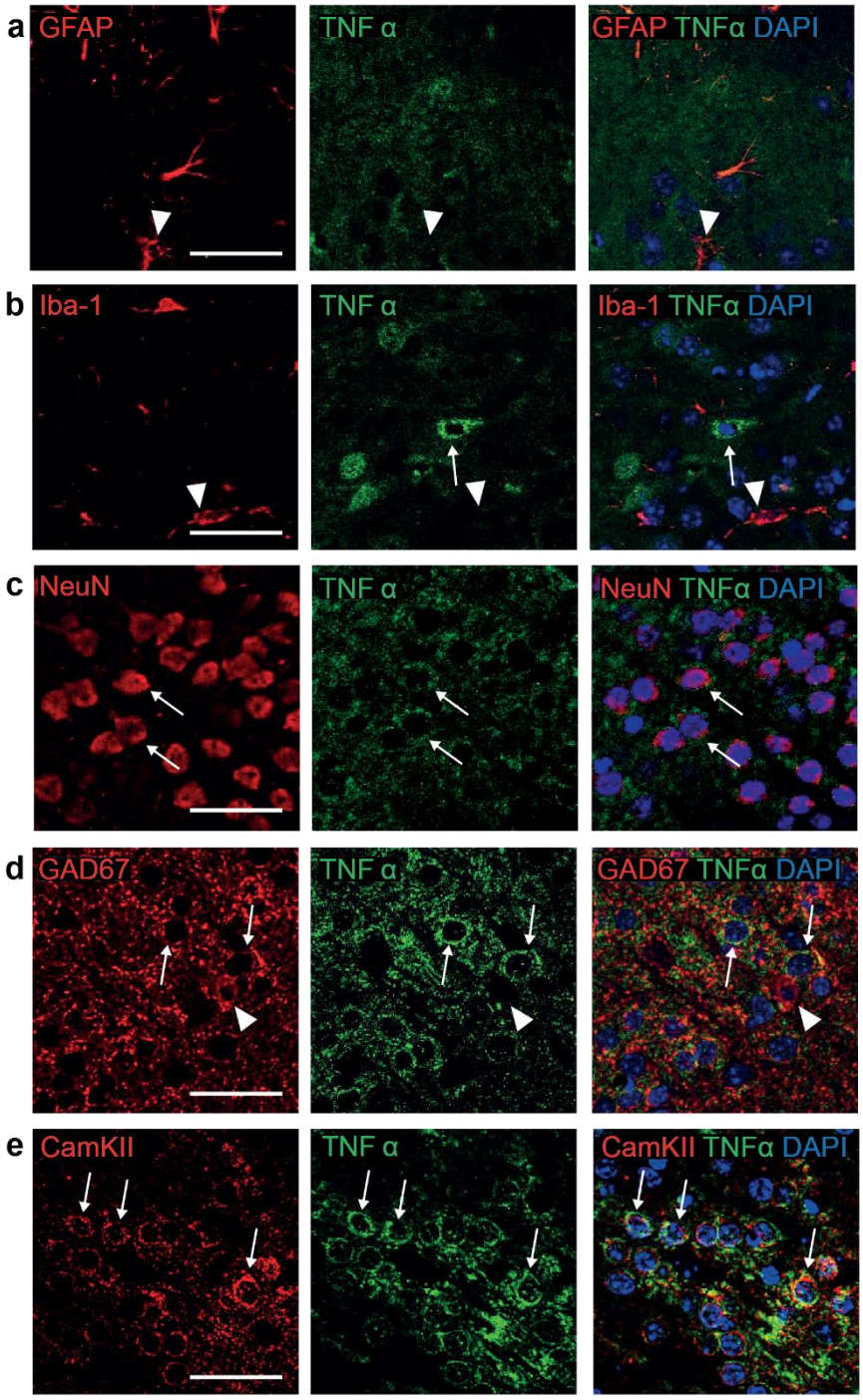


Figure 38: (a - e) Coronal brain sections from remission mice were immunostained and imaged by means of confocal microscopy. Left panels displaying slices stained with anti-GFAP, anti-Iba-1, NeuN, anti-GAD67 and anti-CamKII antibodies, respectively (all red). Middle panels, all micrographs of TNF α staining (green). Right panels, merged images of respective staining are shown (DAPI in blue). Note, clear co-localization observed in NeuN, CamKII and TNF α staining. Scale bars = 30 µm, N=4 mice. Flat white arrows indicate strong TNFα signal.

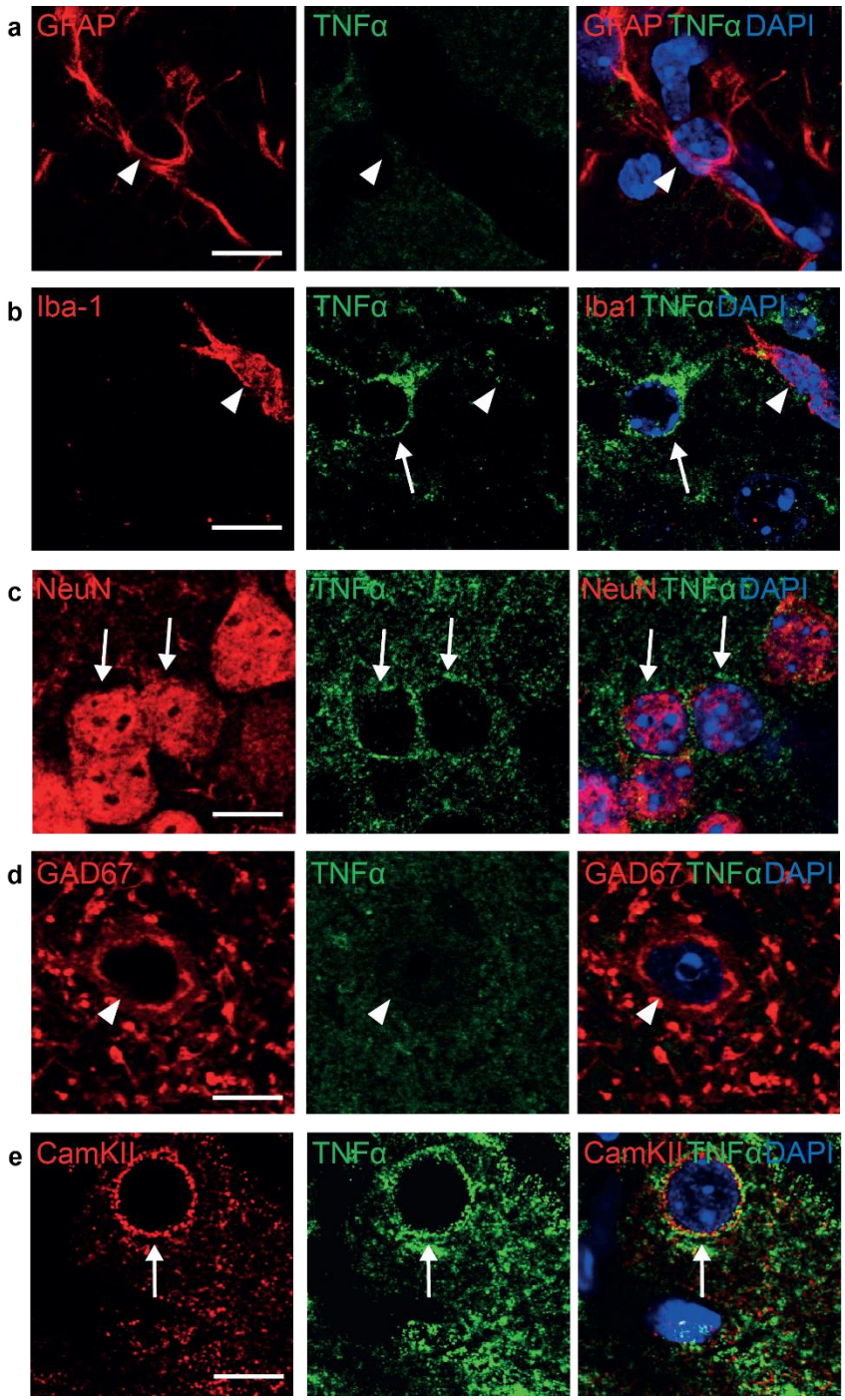


Figure 39: Characterization of the origin of TNF-α release in the remission mice. Higher magnification images are shown here. Left panels display (all in red) anti-GFAP -stained astrocytes (a), anti-Iba-1 stained microglia (b), anti-NeuN stained neurons (c), anti-GAD 67 stained inhibitory neurons (d), and anti-CamKII stained excitatory neurons (e). Middle panels display TNFα staining (green). While merged channels with DAPI (blue) as nuclear staining are shown in right panels. Note, positive signals for co-localization of TNFα, NeuN+ and CamKII+ neurons spotted in (c & e). Flat white arrows indicate strong TNFα signal (Scale bar = 8 µm, N = 4 mice).

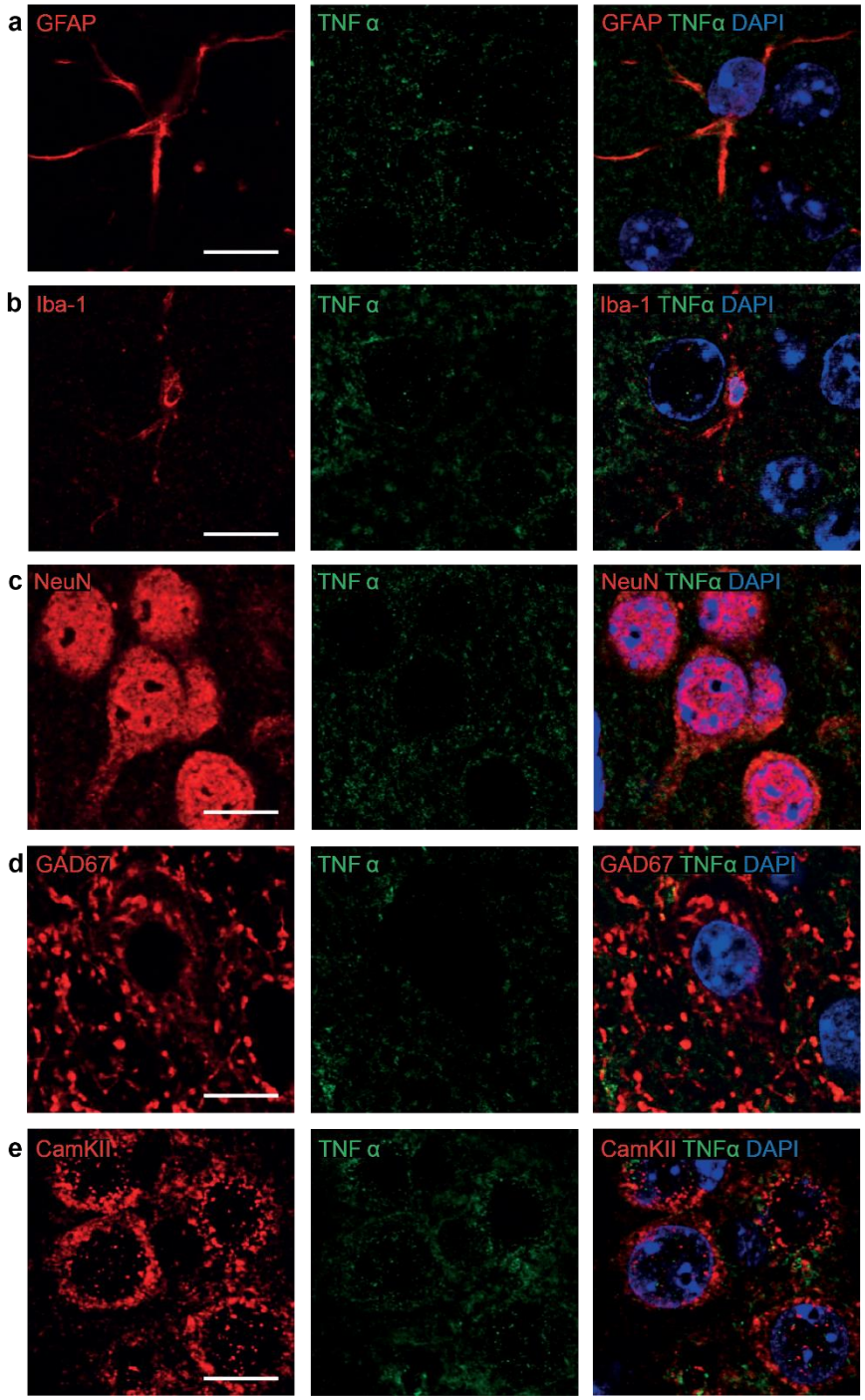


Figure 40: (a - e) Immunofluorescence microscopy for GFAP, Iba-1, NeuN, GAD67, CamKII and TNF α in wild-type control mice. Left, all micrographs display staining against GFAP, Iba-1, NeuN, GAD67 and CamKII (all in red) and center panels show staining TNF α (green), respectively. Right panels show merged imaged from the respective staining (DAPI in blue). Note, no co-localization was spotted in NeuN or CamKII with TNF α staining (Scale bar = 8 µm, N = 4 mice).

# DISCUSSION

This PhD thesis was conceived and designed to understand and characterize cortical network activity in relapse-remitting MS. We addressed two central questions: first, whether and how progressive disease phases of EAE impact on the cortical network functions; and second, what are the molecular mechanism(s) involved in it. In order to answer these questions, we have used several methodological approaches - to study network functions in different cortical areas and immune-pathological activation in the CNS, and further examined behavioral outcomes across all experimental groups. Our study consists of three groups: EAE-relapse or peak of the disease, EAE-remission and same sex, age-matched wild-type controls.

In our work, we described neuronal network activity from both visual and frontal cortices *in vivo* in EAE mice by employing advanced two-photon microscopy towards high-resolution imaging. In addition, we developed a surgical preparation that permits *in vivo* visualization of neuronal activity in both visual and frontal cortices in living animals in EAE. Note that two independent set experiments were carried out in order to visualize network activity in those two different cortical regions (visual and frontal cortices). Our preparation relies extensively on the usage of a synthetic calcium indicator (OGB-1 AM ester) to measure changes in intracellular calcium concentration which closely represents an action potential firing of a cell (Rochefort et al., 2009). The preparation offers the opportunity to directly investigate the mechanisms that underlie cortical network functions in the healthy and diseased brains.

Here, for the first time we demonstrated that the neuronal activity in both visual and frontal cortices were significantly altered in EAE remission mice that had no or mild clinical symptoms as compared with relapse phase (in which clinical symptoms were at peak) or age-matched wild-type control mice. In particular, the fraction of active neurons increased significantly in both cortical regions in EAE remission animals. Additionally, there was a

significant increase of hyperactive fractions observed within the active neuronal population in the visual cortex of EAE remission mice and those hyperactive neurons were randomly distributed across the recording plane. This finding from visual cortex was further corroborated by the result obtained from frontal cortex of remission mice. We observed four-fold increase in activity in the frontal cortex of remission animals suggesting a cortex-wide phenomenon. We also noticed subtle changes in the behavioral tests which might be closely associated with the changes in neuronal activity in the cortex. However, no hyperactive neurons were identified in the frontal cortex. The two-photon data was further substantiated by electrophysiological recordings from remission animals exhibiting increased in sEPSCs frequencies. Surprisingly, there was no sign of cortical demyelination or inflammation or axonal damage(s) observed in those remission animals' brain slices. However, there were some demyelination and mononuclear cells infiltration observed only in lumbar area of the spinal cord, which is in line with few other studies claiming MS as a spinal cord disease (Thorpe et al., 1996, Trop et al., 1998). Additionally, qPCR analysis of remission cortices revealed remarkable increase of TNF-α expression. This was further corroborated by immunostaining where soluble TNF-α were found aggregated around some NeuN+ and particularly CamKII+ excitatory neurons in EAE remission animals. Yet, we demonstrated treating those animals with infliximab (a monoclonal antibody of TNF-α) via intraventricular injections restores normal activity (shown in electrophysiology as well as two-photon recordings). Taken together, we provided direct experimental evidence that the altered activity in remission was causally related to the actions of soluble TNF-α release in the cortex. We also demonstrated that treatment with infliximab completely reverses neuronal hyperactivity in remission.

In conclusion, we characterized the functional changes of cortical network activity *in vivo* by using two-photon calcium imaging in EAE disease model. For the first time, we

reported cortex-wide altered activity pattern of the neuronal networks at very early stage of EAE and such activity pattern is directly associated with the increased expression of soluble TNF-α in the cortex.

### *In vivo* visualization of neuronal activity in the visual and frontal cortices

In the past, most of our knowledge about visual cortex neurons was solely drawn from experiments using either extracellular electrical recordings (recordings of field potentials or neuronal spike patterns) or intracellular recordings (recordings of membrane potential dynamics). For instance, by far the most important tool to study neuronal responses in the visual cortex for physiologists has been the extracellular microelectrodes which unveiled the functional maps of the visual cortex (e.g. visual field position, preferred stimulus orientation and direction, and other receptive field parameters) (Hubener and Bonhoeffer, 2005, Hofer et al., 2006). Recent development of multi-electrode arrays are also used to record activity patterns of visual cortex neurons (Kelly et al., 2007) with sub-milli second temporal resolution (Ito et al., 2014). But such recordings alone are not well suited for elucidating the detailed structure and functional maps at single cell level due to the limitations by a low spatial resolution (>100µm) and a sparse sampling within the recording area. Moreover, it does not truly allow us to identify inactive neurons in case of diseased animals. Hence, extracellular electrical recordings are unable to resolve the spatiotemporal dynamics of large neuronal population with subcellular resolution *in vivo*. On the other hand, intracellular recording methods such as patch clamp recordings provide an unparalleled view into the functional role of individual neuron especially revealing information about its' input and intrinsic cellular properties, spiking output (Long and Lee, 2012, Xie et al., 2012) stimulus-dependent modulation of the spike threshold etc. (Azouz and Gray, 1999, Henze and Buzsaki, 2001, Wilent and Contreras, 2005). However, the technical limitations of this method is its' invasive nature of preparation which permits to record from very few cells simultaneously

and the recording time is limited to a few hours only (Xie et al., 2012) in slices. The *in vivo* preparation for patch recording is still under way of development in disease models. Thus, all electrical recordings are not suitable to resolve the precise spatiotemporal dynamics of large neuronal population with single cell resolution *in vivo*.

Whereas, current development of *in vivo* imaging methods by two-photon microscopy offers several key advantages over electrical recordings such as it provides the ability to map response properties at the single cell level with their precise spatial localization at a high sampling rate. It utilizes near-infrared light source that has longer wavelength enabling deeper penetration depths (Helmchen, 2009) with high signal-to-noise ratio and it allows to visualize and record same neurons over a longer periods of time (Mank et al., 2008, Tian et al., 2009, Andermann et al., 2010, Dombeck et al., 2010). In addition, two-photon imaging allows us to resolve both subcellular structures and functions such as signal transduction and structural plasticity etc. (Dreosti et al., 2009, Shigetomi et al., 2010). Another prime advantage of this method is that it allows for the identification of inactive neurons within the recording area (Busche et al., 2008) and it is less invasive compared with intracellular recordings. Taking those advantages in consideration, we combined two-photon calcium imaging with bolus loading of OGB-1 calcium indicators, to examine activity pattern of visual and frontal cortical neurons in the EAE relapse and remission mice, and compared with wild-type controls *in vivo*.

During cranial window preparation in visual and frontal cortices, we took careful steps not to destroy the dura or any blood vessel as disruption of either one could potentially aggregate erythrocytic layer which could not only make imaging difficult but perhaps impact on physiological states of the respective cortical regions. Hence, the method in general is very sensitive and demands extra care, and expertise for complete *in vivo* preparation.

In principle, our method can be used to address a wide range of questions regarding cortical network function in the developmental phases of EAE and it also opens up new avenues towards other brain diseases such as epilepsy, depression, schizophrenia or Parkinson diseases etc.

## Cortical microcircuit hyperactivity

Our work establishes that neuronal hyperactivity in the cortex is an early pathophysiological indicator in EAE. It is interesting to report in human form of the disease that at the early stage of MS progression , mental fatigue, poor cognitive or executive functions are common (Rao et al., 1991) which are found to be directly associated with increased BOLD responses in the frontal and parietal brain areas as measured by fMRI (Penner et al., 2003). Moreover, some clinical studies show direct link between mental fatigue and hyperactivation in those brain regions including basal ganglia, and thalamus (DeLuca et al., 2008). Such hyperactivation has been interpreted as part of functional reorganization in order to maintain normal performance (Staffen et al., 2002, Genova et al., 2012, Di Filippo et al., 2015, Sundgren et al., 2015) by recruiting additional brain regions (Mainero et al., 2004). In our work, we also observed four-fold increase of network activity to more specific of hyperactivity phenotype emerging from frontal to visual cortex. One might interpret such finding as part of the functional reorganization by recruiting additional cortical areas (associative to sensory cortices or vice-versa). While, recent hypothesis indicate that long-term preservation of brain functional reorganization might contribute to a more favorable course of the disease (Rocca et al., 2010). In addition, several studies reports that in progressive disease phases, steadily increase structural damage and disability limits functional reorganization resulting in reduced cortical information processing capacity, increased metabolic requirements, and recovery needs to further hypoactivation and cognitive impairments (Reddy et al., 2000, Schoonheim et al.,

2010). However, it has been long debated with respect to the neuroimaging studies in human whether such abnormal increase in neuronal activity is compensatory or maladaptive (indicative of dysfunction/neurodegeneration). In that context, our work in mice with EAE provides direct evidence that neuronal hyperactivity is per se a pathophysiological process at early stage of the disease. Additionally, we also show that soluble TNF-α as key responsible factor involved in early disease pathology. Our data suggests binding of soluble TNF-α to excitatory neurons lead to a profound increase in sEPSC frequency, as a clear consequence of presynaptic glutamate release. However, no changes observed in sEPSCs amplitude in our sEPSCs recording which would be indicative of postsynaptic effect of soluble TNF-α by increasing AMPAR trafficking. In the CNS, binding soluble TNF-α to its specific receptor TNFR1 on neurons can mediate glutamate release from synaptic vesicles which can potentiate excitotoxicity by two complementary mechanisms: indirectly, by inhibiting glutamate transport on astrocytes, and directly, by increasing the localization of ionotropic glutamate receptors to synapses (Fig. 41) (Pickering et al., 2005, Pinheiro and Mulle, 2008, Olmos and Llado, 2014).

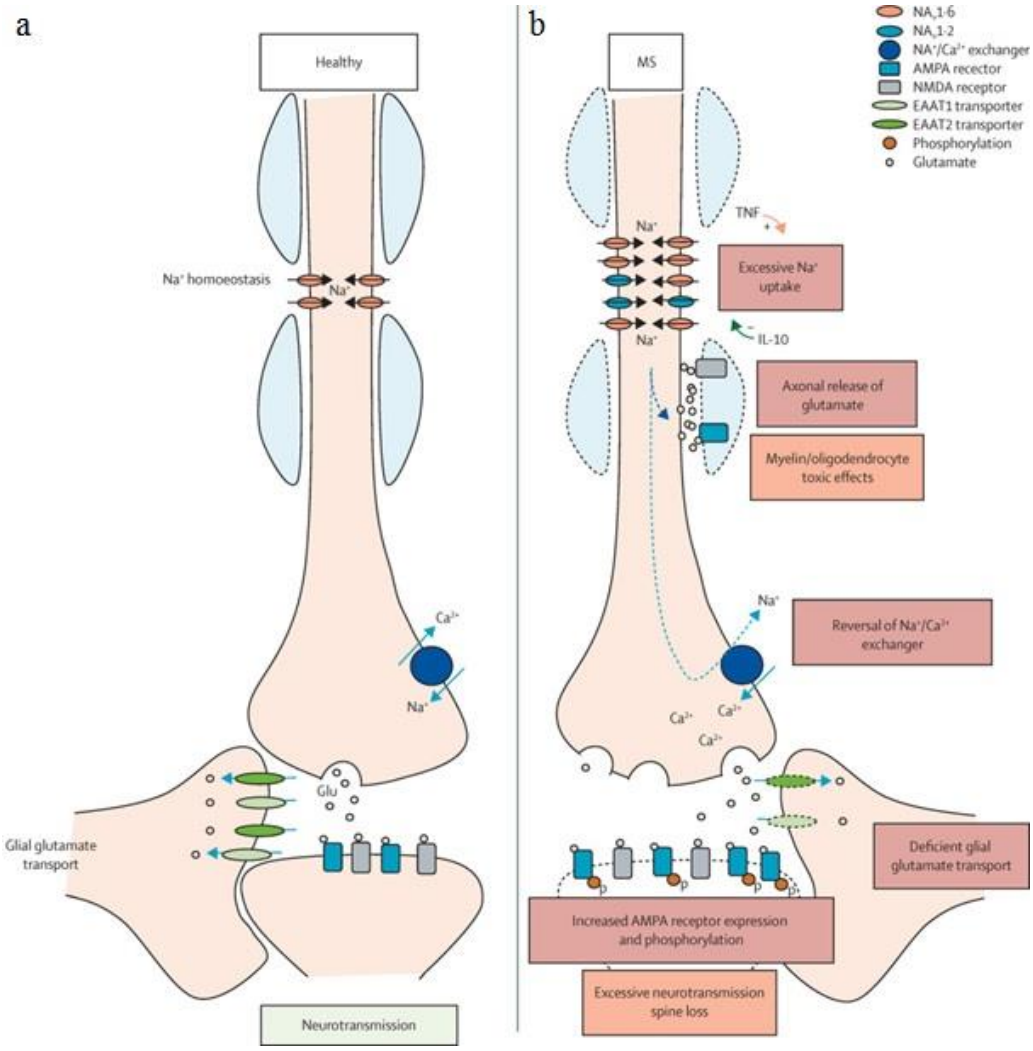


Figure 41: (a) Schematic representation of synaptic glutamate is shown. (b) Proposed mechanism by which glutamate mediated excitotoxicity can occur in the CNS of MS. Modified from (Macrez et al., 2016).

Hence, in our study scenario, increase in neuronal hyperexcitibility is clearly a response to elevation of extracellular glutamate level (Meurs et al., 2008, Park et al., 2011) and from such conditions; one can postulate that those hyperactive neurons might undergo excitotoxic cell death. However, the downstream cellular targets that are involved in TNF-α mediated neuronal hyperexcitibility is not entirely clear yet. It is also largely unknown whether those hyperactive neurons undergo hypoactivation to neuronal silencing (functionally inactive) or neurodegeneration at the later phases of the disease.

If we are to explore further, what would be the functional consequences of neuronal hyperactivity during disease development? In order to understand that we should have understanding of basic cellular processes. First, the intracellular calcium concentration is tightly regulated to ensure coordination among the multiple processes involving calcium that underlie normal cell functioning. But cortical hyperactivity alone may contribute to calcium overload in neurons (Kuchibhotla et al., 2008) and excessive elevation of resting calcium is deleterious to almost all cell types, and may trigger either necrotic or apoptotic cell death (Trump and Berezesky, 1995, Duchen, 2000, LaFerla, 2002). In details, through activity-dependent elevation of intracellular calcium concentration and associated activation of Caspase-3 (D'Amelio et al., 2011), as well as changed in excitation-inhibition ratio (Busche et al., 2008) may causally lead to neuronal silencing and further apoptotic cell death. Several studies have shown hypoactivation in different brain regions in MS patients (Chalah et al., 2015) and hence neuronal silencing in those regions can be more prevalent in those patients at the later stages of the MS. Furthermore, intracellular calcium overload itself can trigger calcineurin activation (Kuchibhotla et al., 2008), which may contribute structural degeneration of dendrites and neuritic beading (Takeuchi et al., 2005, Mahad et al., 2009). In addition, high levels of calcium influx via reversal of $Na^{+}/Ca^{2+}$ exchangers or an abnormal redistribution of pore-forming subunit of neuronal (N)-type voltage gated calcium channels in axons may also perturb axonal transport which might eventually lead to axonal degeneration by the activation of neuronal proteases e.g. calpain (Buki et al., 1999, Kornek et al., 2001, Kurnellas et al., 2007).

Second, hyperactive neurons are more susceptible to epileptiform activity driven by excessive synaptic glutamate release and greater glutamate transmission (During and Spencer, 1993, Meurs et al., 2008), leading to excitotoxic cell death. Clinical studies of EEG recording show spontaneous epileptic activity in the cortex of patients with RRMS (Kelley and

Rodriguez, 2009, Shaygannejad et al., 2013) and significantly increased glutamate levels in the CSF of MS patients (Stover et al., 1997, Srinivasan et al., 2005). More recent data suggests concurrent excitotoxic events are predominant in human prior to neuronal cell death (Kostic et al., 2014). It has also been reported that excessive glutamatergic transmission mediated excitotoxicity often result in cognitive impairments in the early phase of MS pathogenesis (Mandolesi et al., 2010). More recent work suggests that neuronal hyperactivity could potentially initiate CNS residential immune cells activation which has substantial impact on cascade of actions. Indeed, they act as potential source for excessive levels of glutamate release (Ye et al., 2003, Mandolesi et al., 2010, Kostic et al., 2014), participate in the infiltration of immune cell and/or to elevated expression of several proinflammatory cytokines that ultimately affect functional connectivity of the network in later disease stages. Third, neuronal hyperactivity can lead to direct activation of phagocytosis by activating microglia via extracellular ATP signals (Abiega et al., 2016).

Last, some studies in EAE have also reported simultaneous dysfunction of GABA transmission, causing an imbalance between synaptic excitation and inhibition ratio leading to neuronal hyperactivity (Mandolesi et al., 2010). This process can have malicious effect on disease progression by further increase in neuronal hyperactivity throughout the cortex. In line with this, a postmortem study on MS patients revealed significant loss of Parvalbumin positive (PV+) interneurons in normally appearing grey matter from the primary motor cortex (Clements et al., 2008). This loss is supported by the evidence of the impaired cognitive performances in EAE affected animals (Caramia et al., 2004, Mandolesi et al., 2010). Together, in combination with mechanisms related to calcium overloads into the cells could contribute to excitotoxicity mediated neurodegeneration that might become more prominent in advanced disease stages. Finally, the relative contributions of increased vs. decreased neuronal activity remain unknown in the disease pathology of MS, but it is likely that both

hypo- and hyperactivity can lead to network imbalances and thus can negatively impact the disease course.

### Role of TNF-α in neuronal hyperactivity

Elevation of proinflammatory cytokines occurs during early phase of EAE induction (Pollak et al., 2003). Predominantly, TNF-α, and IFN-γ are known to precede infiltration of peripheral immune cells and could have significant impact on neuronal function (Gendron et al., 1991, Leonoudakis et al., 2004). Besides glial cells, TNF-α is also found to be released from neurons (Allan and Rothwell, 2001) and can have direct or indirect effect on glutamate excitotoxicity, notably by excessive glutamate release at the presynaptic nerve terminals. Additionally, soluble form of TNF-α released from reactive astrocytes increases synaptic transmission via AMPA receptor (AMPAR) trafficking at the synaptic cleft (Beattie et al., 2002, Stellwagen et al., 2005). Recently, such TNF-α mediated AMPAR trafficking has been identified in EAE as well (Centonze et al., 2009b, Centonze et al., 2010b). All of these aforementioned events depend on level of soluble TNF-α in the brain. In the striatum, an increase of TNF-α level is a potential mechanism for contributing to a complex behavior such as anxiety. These facts also corroborate our finding in behavioral test battery where we observed changes in anxiety levels in remission animals. Off the note, striatum is emerging as a key brain region in mood regulation in humans and in rodents (Mathew and Ho, 2006, Favilla et al., 2008). This subcortical structure is highly affected in MS and in EAE (Bakshi et al., 2002, Centonze et al., 2009a, Centonze et al., 2009b). Furthermore, resting astrocytes activated by TNF-α can induce apoptotic oligodendroglial cell death (Akassoglou et al., 1998) via caspase-3 activation leading to myelin loss (Pang et al., 2003). TNF-α release can also activate the cerebral endothelium (Centonze et al., 2010a) leading to transendothelial migration of activated leukocytes into the CNS (Alexander et al., 2011).

However, the exerted effects of TNF-α can be prevented by blocking TNF-α with the application of specific monoclonal antibody that inhibits the binding affinity of soluble TNF-α to its receptors TNFR1 and thereby suspending excessive glutamate transmission into the cell. Studies also show controlling TNFR1 expression could potentially ameliorate disease outcome (Brambilla et al., 2011, Williams et al., 2014). Apart from reactive astrocytes, direct release of TNF-α from activated microglia is also a likely candidate for the induction of the synaptic deficits (Mandolesi et al., 2010) in MS. During chronic phase, TNF-α can directly activate microglia in an autocrine/paracrine manner and exert indirect excitotoxic neuronal damage through induction of glutamate release from activated microglia (Fig. 42) (Takeuchi et al., 2006, Shijie et al., 2009). Moreover, increased production of soluble TNF-α readily causes abnormal plasticity of dendritic spines and axonal boutons in presymptomatic EAE mice (Yang et al., 2013). Recent studies have reported that inhibiting TNF-α production reverses hippocampal-dependent cognitive deficits (Belarbi et al., 2012).

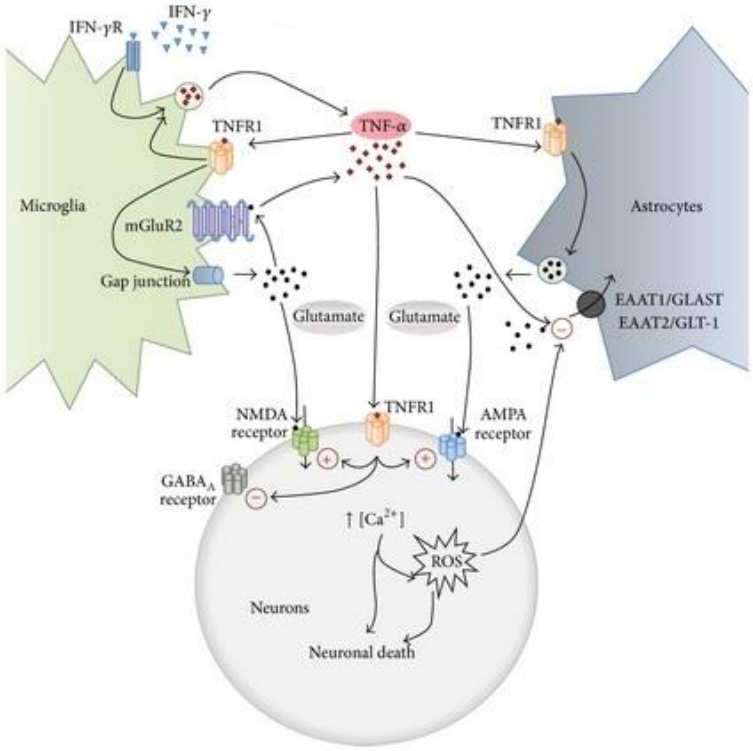


Figure 42: Graphical illustration of TNF-α mediated glial cells activation and neuronal damage. Modified from (Olmos and Llado, 2014)

In addition, blocking soluble TNF-α further decreases downstream expression of several other proinflammatory cytokines including IFN-γ, IL-1β, IL-6 or CCL2 in the CNS (Brambilla et al., 2011). Because IFN-γ and IL-1β are potent regulators of neuronal functions (Gadani et al., 2012). Worth mentioning that TNF-α signaling through TNFR1 is required for VCAM1 expression on astrocytes and could play an important role in facilitating effector T cells infiltration into the CNS parenchyma and causing subsequent neuronal damage in EAE (Gimenez et al., 2004, Bartholomaus et al., 2009). Taken together, it is clear that TNF-α plays a crucial role in alterations of synaptic properties in the cortex and blocking TNF-α may prevent synaptic pathology and associated sensory, as well as cognitive dysfunctions in MS.

## Functional vulnerability of the cortex during MS disease course

Over the past decades, significant amount of studies has been performed in patients using fMRI revealing focal demyelinating lesions in the white matter as well as grey matter degeneration in different brain region in RRMS (Cercignani et al., 2001, Ge et al., 2001). Now, we demonstrate changes in the functional activity with single cell resolution in two different cortical regions in early relapse-remitting EAE. Taking into account of these studies together, a clearer picture emerges about the spatiotemporal sequences of neuronal hyperactivity-to-dysfunction and perhaps cortical degeneration across different brain regions during progressive form of the disease. Our work clearly establishes that increased cortical activity is higher in frontal brain regions compared to sensory areas and such alterations in neuronal activity pattern arise independently of inflammatory cells infiltration, and together this links to the finding of impaired cognitive functions in MS patients at later disease stages. One can anticipate that, with time in progress such increased neuronal activity might become

prominent across the all brain regions. In line with our findings, early manifestation of the cortical network function has been detected in animal models and RRMS patients with and without cognitive impairments (Rocca et al., 2012).

In our study, total network activity in the frontal cortex rises to four fold than in visual cortex and no hyperactive cells present in it which might be due to the local concentration of soluble TNF-α. Note absence of hyperactive neurons in the cortex might be due to the effect of anesthesia. However, these attributes opens up further roadmap of whether direct interaction of soluble TNF-α with excitatory neurons could drive hyperactivity or not? What is the fate of those neurons closely connected to hyperactive neurons; do they turn hyperactive in later disease stage? What kind of activity patterns could be expected from consecutive relapses and remissions? What are additional mechanisms contributing to neurodegeneration in the later disease phases? Noteworthy to mention, some of those outcomes will primarily depend on type of TNF-α because TNF-α is not only released by glial cells but from neurons too (Gahring et al., 1996, Allan and Rothwell, 2001) and its' distinct mechanisms of action on different neuronal populations in the cortex. However, we cannot exclude the contribution of other proinflammatory cytokines (IFN-γ, IL-6) and growth factors (GMCSF, TGF-β) in the disease progression. Thus, it seems the cortical network activity in relapse-remitting EAE depends critically on the abundance of soluble TNF-α in the cortex, their intrinsic vulnerability and the basic network anatomy of the brain areas. It is also possible that differential effects of soluble TNF-α on inhibitory cell play a role in MS.

Hence, elevated level of soluble TNF-α and cortical hyperactivity together can be considered as first and foremost signature of early phase of MS.

## Clinical implications

The precise etiology of MS remains obscure for decades and its clinical course is highly heterogeneous. Patients develop various motor, sensory, cognitive and behavioral symptoms during different disease phases. Currently, most available treatments consist of disease delaying or modifying therapies (e.g. immunomodulators, immunosuppressants etc.) that targets mainly immune system (Wingerchuk and Carter, 2014) in addition to several symptomatic treatments, and work for only a limited time or offer no relief at all in some patients. The development of disease-modifying therapies mainly focuses on inhibition of activated inflammatory cells migration to CNS or by deactivating specific subset of activated immune cells in the brain. However most of these agents have failed in the pivotal phases of therapeutic trials. Few recent failures have been explained by the fact that therapies were evaluated in patients with advanced disease courses, when the focal lesion and irreversible degeneration had already occurred and removal of immune cells or administering immunosuppressant was no longer beneficial (Carvalho and Sa, 2012). Few other studies reported that alteration in biochemical pathways e.g. changes in protein expression thought to lead MS that can precede symptoms by far earlier (Evangelidou et al., 2014). In particular, activated astrocytes and some marker protein expression could trigger microglia activation appearing in the CSF prior to symptoms onset in animals (Miljkovic et al., 2011, Giunti et al., 2014). Moreover, excessive brain activity, presence of activated astrocytes, microglia and reactive oxygen species as measured by PET imaging was considered as biomarker and brain atrophy detected by MRI scans (Katsavos and Anagnostouli, 2013, Housley et al., 2015). Loss of ATP, abnormalities in cerebral glucose metabolism as well as impaired episodic cognitive or motor functions are observed in early disease (Mao and Reddy, 2010, Rahn et al., 2012) and can be expected years earlier than predicted symptoms appear. Hence, these suggest that development of MS therapies need to focus on much earlier time point when neuronal

dysfunction has not already become apparent. This is supported by some recent preclinical studies for the development of immunotherapy. For instance, it has been shown that in a genetic mouse model of EAE, administration of certain monoclonal antibodies reduced localized activation of astrocytes at very young age but not later on. In fact, treatment with TNF-α monoclonal antibody in EAE mice shows recovery in late disease stage but for a restricted period of time (Constantinescu et al., 2011). These important concepts have resulted in diagnostic guidelines improvement by National Multiple Sclerosis Society and the Multiple Sclerosis International Federation. In this regard it is important to mention that most chronic diseases such as ALS, rheumatoid arthritis, diabetes exhibit physiological changes in early disease phases or sometimes asymptomatic phases when treatment is more likely to be effective.

In conclusion, our work identifies soluble TNF-α mediated hyperactivity in the whole cortex in absence of cortical demyelination or inflammatory cells infiltration as an early sign of neuronal dysfunction in relapse-remitting EAE mice. Interestingly, several clinical correlates have been also found where human subjects with increased brain activity at early disease stage and subjects with the highest neuronal activity levels showed the greatest clinical decline (Agosta et al., 2008, Rimkus et al., 2016). Hence, our findings strengthen those clinical data that cortical hyperactivity and increased TNF-α levels might be an early biomarker of MS pathology and might also be a promising target for disease-modifying treatments. Our work provides direct evidence that treatment with Infliximab, TNF-α monoclonal antibody rapidly reverses neuronal hyperactivity in relapse-remitting EAE mice. Although, there is a minimal correlation between cortical hyperactivity and behavioral deficits at the early disease phase, it seems that clinical symptoms and cortical network hyperactivity fall in line. Therefore, it is possible that disease-modifying treatment will be most effective in patients with particularly high neuronal activity levels in addition to elevated cortical TNF-α.

It might be useful to incorporate measuring cortical activity and TNF-α level in future clinical treatment trials.

Most common practice in therapeutic drug development in MS focuses on inhibition of T-cell priming against myelin or preventing inflammatory cells migration to the CNS to decrease demyelination, enhancing remyelination or other immunosuppressants. However, preventing inflammatory cells migration show effectiveness at pre-symptomatic stage of MS and are less or not effective in advanced stages. Unfortunately, treating later stages of MS has been largely unsuccessful due to massive loss of neurons and only few disease-modifying treatments available to delay the consecutive relapses. However, efficacies of those treatments are subject-specific and are often not successful. So far, we have begun to study the network abnormalities in MS with an aim to target these alterations with novel treatment approaches. As mentioned earlier, altered cortical activity along with elevated TNF-α might be a promising target for therapy, perhaps even at the later disease stages. Importantly, while presence of neuronal hyperactivity in the cortex can be correlated with altered sensory and motor deficits in patients, they also show memory deficits which indicate possible alterations of functional activity in the hippocampus region. For example, a recent fMRI study has shown altered hippocampal activity in patients performing memory related task (Finkelmeyer et al., 2016). But a detailed *in vivo* study of hippocampal network activity at the early disease phase is yet to be conducted which might furnish additional evidence for early disease detection. On the other hand, MS brain circuit also comprises hypoactive population which might be very important for the therapeutic development. Yet, the relative contribution of increased vs. decreased neuronal activity in the early disease phase remains unknown, but it is likely that both hyperactive as well as hypoactive networks can negatively impact of MS disease process. Additionally, elevated TNF-α expression is also common in several other diseases including Parkinson's, Alzheimer's, diabetes, etc. but their pattern of differential expression

and their respective sources are not well established. Therefore, relative contribution of TNF-α and its source in addition to altered neuronal network activity can be very crucial to MS pathology.

# REFERENCES

Abiega O, Beccari S, Diaz-Aparicio I, Nadjar A, Laye S, Leyrolle Q, Gomez-Nicola D, Domercq M, Perez-Samartin A, Sanchez-Zafra V, Paris I, Valero J, Savage JC, Hui CW, Tremblay ME, Deudero JJ, Brewster AL, Anderson AE, Zaldumbide L, Galbarriatu L, Marinas A, Vivanco MD, Matute C, Maletic-Savatic M, Encinas JM, Sierra A (2016) Correction: Neuronal Hyperactivity Disturbs ATP Microgradients, Impairs Microglial Motility, and Reduces Phagocytic Receptor Expression Triggering Apoptosis/Microglial Phagocytosis Uncoupling. PLoS Biol 14:e1002508.

Adelsberger H, Garaschuk O, Konnerth A (2005) Cortical calcium waves in resting newborn mice. NatNeurosci 8:988-990.

Agosta F, Valsasina P, Rocca MA, Caputo D, Sala S, Judica E, Stroman PW, Filippi M (2008) Evidence for enhanced functional activity of cervical cord in relapsing multiple sclerosis. Magn Reson Med 59:1035-1042.

Akassoglou K, Bauer J, Kassiotis G, Pasparakis M, Lassmann H, Kollias G, Probert L (1998) Oligodendrocyte apoptosis and primary demyelination induced by local TNF/p55TNF receptor signaling in the central nervous system of transgenic mice: models for multiple sclerosis with primary oligodendrogliopathy. Am J Pathol 153:801-813.

Akirav EM, Bergman CM, Hill M, Ruddle NH (2009) Depletion of CD4(+)CD25(+) T cells exacerbates experimental autoimmune encephalomyelitis induced by mouse, but not rat, antigens. J Neurosci Res 87:3511-3519.

Alexander JS, Zivadinov R, Maghzi AH, Ganta VC, Harris MK, Minagar A (2011) Multiple sclerosis and cerebral endothelial dysfunction: Mechanisms. Pathophysiology 18:3-12.

Alitto HJ, Usrey WM (2003) Corticothalamic feedback and sensory processing. Curr Opin Neurobiol 13:440-445.

Allan SM, Rothwell NJ (2001) Cytokines and acute neurodegeneration. Nat Rev Neurosci 2:734-744.

Andermann ML, Kerlin AM, Reid RC (2010) Chronic cellular imaging of mouse visual cortex during operant behavior and passive viewing. Front Cell Neurosci 4:3.

Anderson JC, Binzegger T, Martin KA, Rockland KS (1998) The connection from cortical area V1 to V5: a light and electron microscopic study. J Neurosci 18:10525-10540.

Arellano G, Ottum PA, Reyes LI, Burgos PI, Naves R (2015) Stage-Specific Role of Interferon-Gamma in Experimental Autoimmune Encephalomyelitis and Multiple Sclerosis. Front Immunol 6:492.

Ascherio A, Munger KL (2007) Environmental risk factors for multiple sclerosis. Part II: Noninfectious factors. Ann Neurol 61:504-513.

Audoin B, Ibarrola D, Ranjeva JP, Confort-Gouny S, Malikova I, Ali-Cherif A, Pelletier J, Cozzone P (2003) Compensatory cortical activation observed by fMRI during a cognitive task at the earliest stage of MS. Hum Brain Mapp 20:51-58.

Azoulay D, Vachapova V, Shihman B, Miler A, Karni A (2005) Lower brain-derived neurotrophic factor in serum of relapsing remitting MS: reversal by glatiramer acetate. J Neuroimmunol 167:215-218.

Azouz R, Gray CM (1999) Cellular mechanisms contributing to response variability of cortical neurons in vivo. J Neurosci 19:2209-2223.

Bakshi R, Benedict RH, Bermel RA, Caruthers SD, Puli SR, Tjoa CW, Fabiano AJ, Jacobs L (2002) T2 hypointensity in the deep gray matter of patients with multiple sclerosis: a quantitative magnetic resonance imaging study. Arch Neurol 59:62-68.

Baranzini SE, Wang J, Gibson RA, Galwey N, Naegelin Y, Barkhof F, Radue EW, Lindberg RL, Uitdehaag BM, Johnson MR, Angelakopoulou A, Hall L, Richardson JC, Prinjha RK, Gass A, Geurts JJ, Kragt J, Sombekke M, Vrenken H, Qualley P, Lincoln RR, Gomez R, Caillier SJ, George MF, Mousavi H, Guerrero R, Okuda DT, Cree BA, Green AJ, Waubant E, Goodin DS, Pelletier D, Matthews PM, Hauser SL, Kappos L, Polman CH, Oksenberg JR (2009) Genome-wide association analysis of susceptibility and clinical phenotype in multiple sclerosis. Hum Mol Genet 18:767-778.

Bartholomaus I, Kawakami N, Odoardi F, Schlager C, Miljkovic D, Ellwart JW, Klinkert WE, Flugel-Koch C, Issekutz TB, Wekerle H, Flugel A (2009) Effector T cell interactions with meningeal vascular structures in nascent autoimmune CNS lesions. Nature 462:94-98.

Bashir K, Whitaker JN (1999) Clinical and laboratory features of primary progressive and secondary progressive MS. Neurology 53:765-771.

Basso DM, Beattie MS, Bresnahan JC (1995) A sensitive and reliable locomotor rating scale for open field testing in rats. J Neurotrauma 12:1-21.

Baxter AG (2007) The origin and application of experimental autoimmune encephalomyelitis. Nat Rev Immunol 7:904-912.

Beattie EC, Stellwagen D, Morishita W, Bresnahan JC, Ha BK, Von Zastrow M, Beattie MS, Malenka RC (2002) Control of synaptic strength by glial TNFalpha. Science 295:2282-2285.

Bechmann I, Galea I, Perry VH (2007) What is the blood-brain barrier (not)? Trends Immunol 28:5-11.

Belarbi K, Jopson T, Tweedie D, Arellano C, Luo W, Greig NH, Rosi S (2012) TNF-alpha protein synthesis inhibitor restores neuronal function and reverses cognitive deficits induced by chronic neuroinflammation. J Neuroinflammation 9:23.

Berridge MJ, Lipp P, Bootman MD (2000) The versatility and universality of calcium signalling. Nat Rev Mol Cell Biol 1:11-21.

Bjartmar C, Trapp BD (2003) Axonal degeneration and progressive neurologic disability in multiple sclerosis. Neurotox Res 5:157-164.

Bjartmar C, Wujek JR, Trapp BD (2003) Axonal loss in the pathology of MS: consequences for understanding the progressive phase of the disease. J Neurol Sci 206:165-171.

Block ML, Hong JS (2005) Microglia and inflammation-mediated neurodegeneration: multiple triggers with a common mechanism. Prog Neurobiol 76:77-98.

Bonhoeffer T, Grinvald A (1991) Iso-orientation domains in cat visual cortex are arranged in pinwheel-like patterns. Nature 353:429-431.

Bour H, Peyron E, Gaucherand M, Garrigue JL, Desvignes C, Kaiserlian D, Revillard JP, Nicolas JF (1995) Major histocompatibility complex class I-restricted CD8+ T cells and class II-restricted CD4+ T cells, respectively, mediate and regulate contact sensitivity to dinitrofluorobenzene. Eur J Immunol 25:3006-3010.

Bozzali M, Spano B, Parker GJ, Giulietti G, Castelli M, Basile B, Rossi S, Serra L, Magnani G, Nocentini U, Caltagirone C, Centonze D, Cercignani M (2013) Anatomical brain connectivity can assess cognitive dysfunction in multiple sclerosis. Mult Scler 19:1161-1168.

Brambilla R, Ashbaugh JJ, Magliozzi R, Dellarole A, Karmally S, Szymkowski DE, Bethea JR (2011) Inhibition of soluble tumour necrosis factor is therapeutic in experimental autoimmune encephalomyelitis and promotes axon preservation and remyelination. Brain 134:2736-2754.

Briggs F, Usrey WM (2008) Emerging views of corticothalamic function. Curr Opin Neurobiol 18:403-407.

Brown JE, Cohen LB, De Weer P, Pinto LH, Ross WN, Salzberg BM (1975) Rapid changes in intracellular free calcium concentration. Detection by metallochromic indicator dyes in squid giant axon. Biophys J 15:1155-1160.

Buchanan SL, Thompson RH, Maxwell BL, Powell DA (1994) Efferent connections of the medial prefrontal cortex in the rabbit. Exp Brain Res 100:469-483.

Buki A, Siman R, Trojanowski JQ, Povlishock JT (1999) The role of calpain-mediated spectrin proteolysis in traumatically induced axonal injury. J Neuropathol Exp Neurol 58:365-375.

Buonanno A, Fields RD (1999) Gene regulation by patterned electrical activity during neural and skeletal muscle development. Curr Opin Neurobiol 9:110-120.

Burman J, Raininko R, Fagius J (2011) Bilateral and recurrent optic neuritis in multiple sclerosis. Acta Neurol Scand 123:207-210.

Burrell AM, Handel AE, Ramagopalan SV, Ebers GC, Morahan JM (2011) Epigenetic mechanisms in multiple sclerosis and the major histocompatibility complex (MHC). Discov Med 11:187-196.

Busche MA, Chen X, Henning HA, Reichwald J, Staufenbiel M, Sakmann B, Konnerth A (2012) Critical role of soluble amyloid-beta for early hippocampal hyperactivity in a mouse model of Alzheimer's disease. Proc Natl Acad Sci U S A 109:8740-8745.

Busche MA, Eichhoff G, Adelsberger H, Abramowski D, Wiederhold KH, Haass C, Staufenbiel M, Konnerth A, Garaschuk O (2008) Clusters of hyperactive neurons near amyloid plaques in a mouse model of Alzheimer's disease. Science 321:1686-1689.

Busche MA, Konnerth A (2015) Neuronal hyperactivity--A key defect in Alzheimer's disease? Bioessays 37:624-632.

Bussey TJ, Padain TL, Skillings EA, Winters BD, Morton AJ, Saksida LM (2008) The touchscreen cognitive testing method for rodents: how to get the best out of your rat. Learn Mem 15:516-523.

Butler MP, O'Connor JJ, Moynagh PN (2004) Dissection of tumor-necrosis factor-alpha inhibition of long-term potentiation (LTP) reveals a p38 mitogen-activated protein kinase-dependent mechanism which maps to early-but not late-phase LTP. Neuroscience 124:319-326.

Byrne JH (1997) Introduction to Neurons and Neuronal Networks.

Calabrese M, Magliozzi R, Ciccarelli O, Geurts JJ, Reynolds R, Martin R (2015) Exploring the origins of grey matter damage in multiple sclerosis. Nat Rev Neurosci 16:147-158.

Caramia MD, Palmieri MG, Desiato MT, Boffa L, Galizia P, Rossini PM, Centonze D, Bernardi G (2004) Brain excitability changes in the relapsing and remitting phases of multiple sclerosis: a study with transcranial magnetic stimulation. Clin Neurophysiol 115:956-965.

Carandini M (2012) From circuits to behavior: a bridge too far? Nat Neurosci 15:507-509.

Carroll RC, Beattie EC, von Zastrow M, Malenka RC (2001) Role of AMPA receptor endocytosis in synaptic plasticity. Nat Rev Neurosci 2:315-324.

Carson MJ (2002) Microglia as liaisons between the immune and central nervous systems: functional implications for multiple sclerosis. Glia 40:218-231.

Carvalho AT, Sa MJ (2012) Switching and escalating therapy in long-lasting multiple sclerosis: not always necessary. ISRN Neurol 2012:451457.

Centonze D, Muzio L, Rossi S, Cavasinni F, De Chiara V, Bergami A, Musella A, D'Amelio M, Cavallucci V, Martorana A (2009a) Inflammation triggers synaptic alteration and degeneration in experimental autoimmune encephalomyelitis. The Journal of Neuroscience 29:3442-3452.

Centonze D, Muzio L, Rossi S, Cavasinni F, De Chiara V, Bergami A, Musella A, D'Amelio M, Cavallucci V, Martorana A, Bergamaschi A, Cencioni MT, Diamantini A, Butti E, Comi G, Bernardi G, Cecconi F, Battistini L, Furlan R, Martino G (2009b) Inflammation triggers synaptic alteration and degeneration in experimental autoimmune encephalomyelitis. J Neurosci 29:3442-3452.

Centonze D, Muzio L, Rossi S, Furlan R, Bernardi G, Martino G (2010a) The link between inflammation, synaptic transmission and neurodegeneration in multiple sclerosis. Cell Death Differ 17:1083-1091.

Centonze D, Muzio L, Rossi S, Furlan R, Bernardi G, Martino G (2010b) The link between inflammation, synaptic transmission and neurodegeneration in multiple sclerosis. Cell Death & Differentiation 17:1083-1091.

Cercignani M, Bozzali M, Iannucci G, Comi G, Filippi M (2001) Magnetisation transfer ratio and mean diffusivity of normal appearing white and grey matter from patients with multiple sclerosis. J Neurol Neurosurg Psychiatry 70:311-317.

Chalah MA, Riachi N, Ahdab R, Creange A, Lefaucheur JP, Ayache SS (2015) Fatigue in Multiple Sclerosis: Neural Correlates and the Role of Non-Invasive Brain Stimulation. Front Cell Neurosci 9:460.

Chang B, Hawes NL, Hurd RE, Davisson MT, Nusinowitz S, Heckenlively JR (2002) Retinal degeneration mutants in the mouse. Vision Res 42:517-525.

Chang KJ, Redmond SA, Chan JR (2016) Remodeling myelination: implications for mechanisms of neural plasticity. Nat Neurosci 19:190-197.

Charo IF, Ransohoff RM (2006) The many roles of chemokines and chemokine receptors in inflammation. N Engl J Med 354:610-621.

Chiaravalloti N, Hillary F, Ricker J, Christodoulou C, Kalnin A, Liu WC, Steffener J, DeLuca J (2005) Cerebral activation patterns during working memory performance in multiple sclerosis using FMRI. J Clin Exp Neuropsychol 27:33-54.

Chiaravalloti ND, DeLuca J (2008) Cognitive impairment in multiple sclerosis. Lancet Neurol 7:1139-1151.

Chichilnisky EJ, Wandell BA (1995) Photoreceptor sensitivity changes explain color appearance shifts induced by large uniform backgrounds in dichoptic matching. Vision Res 35:239-254.

Chino YM, Kaas JH, Smith EL, 3rd, Langston AL, Cheng H (1992) Rapid reorganization of cortical maps in adult cats following restricted deafferentation in retina. Vision Res 32:789-796.

Chung IY, Benveniste EN (1990) Tumor necrosis factor-alpha production by astrocytes. Induction by lipopolysaccharide, IFN-gamma, and IL-1 beta. J Immunol 144:2999-3007.

Clements RJ, McDonough J, Freeman EJ (2008) Distribution of parvalbumin and calretinin immunoreactive interneurons in motor cortex from multiple sclerosis post-mortem tissue. Exp Brain Res 187:459-465.

Cohen JA, Barkhof F, Comi G, Hartung HP, Khatri BO, Montalban X, Pelletier J, Capra R, Gallo P, Izquierdo G, Tiel-Wilck K, de Vera A, Jin J, Stites T, Wu S, Aradhye S, Kappos L, Group TS (2010) Oral fingolimod or intramuscular interferon for relapsing multiple sclerosis. N Engl J Med 362:402-415.

Compston A, Coles A (2008) Multiple sclerosis. Lancet 372:1502-1517.

Constantinescu CS, Farooqi N, O'Brien K, Gran B (2011) Experimental autoimmune encephalomyelitis (EAE) as a model for multiple sclerosis (MS). Br J Pharmacol 164:1079-1106.

Correale J, Farez MF (2015) The Role of Astrocytes in Multiple Sclerosis Progression. Front Neurol 6:180.

Croxford AL, Kurschus FC, Waisman A (2011) Mouse models for multiple sclerosis: historical facts and future implications. Biochim Biophys Acta 1812:177-183.

Cummings JL (1993) Frontal-subcortical circuits and human behavior. Arch Neurol 50:873-880.

Cunningham AJ, Murray CA, O'Neill LA, Lynch MA, O'Connor JJ (1996) Interleukin-1 beta (IL-1 beta) and tumour necrosis factor (TNF) inhibit long-term potentiation in the rat dentate gyrus in vitro. Neurosci Lett 203:17-20.

D'Amelio M, Cavallucci V, Middei S, Marchetti C, Pacioni S, Ferri A, Diamantini A, De Zio D, Carrara P, Battistini L, Moreno S, Bacci A, Ammassari-Teule M, Marie H, Cecconi F (2011) Caspase-3 triggers early synaptic dysfunction in a mouse model of Alzheimer's disease. Nat Neurosci 14:69-76.

Darian-Smith C, Gilbert CD (1994) Axonal sprouting accompanies functional reorganization in adult cat striate cortex. Nature 368:737-740.

De Stefano N, Narayanan S, Francis GS, Arnaoutelis R, Tartaglia MC, Antel JP, Matthews PM, Arnold DL (2001) Evidence of axonal damage in the early stages of multiple sclerosis and its relevance to disability. Arch Neurol 58:65-70.

DeAngelis LM (2009) Natalizumab: a double-edged sword? Ann Neurol 66:262-263.

DeLuca J, Genova HM, Hillary FG, Wylie G (2008) Neural correlates of cognitive fatigue in multiple sclerosis using functional MRI. J Neurol Sci 270:28-39.

Denic A, Johnson AJ, Bieber AJ, Warrington AE, Rodriguez M, Pirko I (2011) The relevance of animal models in multiple sclerosis research. Pathophysiology 18:21-29.

Denk W, Strickler JH, Webb WW (1990) Two-photon laser scanning fluorescence microscopy. Science 248:73-76.

Dhib-Jalbut S, Marks S (2010) Interferon-beta mechanisms of action in multiple sclerosis. Neurology 74 Suppl 1:S17-24.

Di Filippo M, de Iure A, Durante V, Gaetani L, Mancini A, Sarchielli P, Calabresi P (2015) Synaptic plasticity and experimental autoimmune encephalomyelitis: implications for multiple sclerosis. Brain Res 1621:205-213.

Diamond BJ, Johnson SK, Kaufman M, Graves L (2008) Relationships between information processing, depression, fatigue and cognition in multiple sclerosis. Arch Clin Neuropsychol 23:189-199.

Dittel BN (2008) CD4 T cells: Balancing the coming and going of autoimmune-mediated inflammation in the CNS. Brain Behav Immun 22:421-430.

Dogonowski AM, Siebner HR, Sorensen PS, Wu X, Biswal B, Paulson OB, Dyrby TB, Skimminge A, Blinkenberg M, Madsen KH (2013) Expanded functional coupling of subcortical nuclei with the motor resting-state network in multiple sclerosis. Mult Scler 19:559-566.

Dombeck DA, Harvey CD, Tian L, Looger LL, Tank DW (2010) Functional imaging of hippocampal place cells at cellular resolution during virtual navigation. NatNeurosci 13:1433-1440.

Dombrowski SM, Hilgetag CC, Barbas H (2001) Quantitative architecture distinguishes prefrontal cortical systems in the rhesus monkey. Cereb Cortex 11:975-988.

Douglas RJ, Kennedy H, Martin KA (2008) Visual cortex neurons and local circuits. The Encyclopedia of Neuroscience.

Douglas RJ, Martin KA (1998) Neocortex: The synaptic organization of the brain. 459-509.

Dreosti E, Odermatt B, Dorostkar MM, Lagnado L (2009) A genetically encoded reporter of synaptic activity in vivo. Nat Methods 6:883-889.

Droby A, Yuen KS, Muthuraman M, Reitz SC, Fleischer V, Klein J, Gracien RM, Ziemann U, Deichmann R, Zipp F, Groppa S (2015) Changes in brain functional connectivity patterns are driven by an individual lesion in MS: a resting-state fMRI study. Brain Imaging Behav.

Duchen MR (2000) Mitochondria and calcium: from cell signalling to cell death. J Physiol 529 Pt 1:57-68.

Dufour JH, Dziejman M, Liu MT, Leung JH, Lane TE, Luster AD (2002) IFN-gamma-inducible protein 10 (IP-10; CXCL10)-deficient mice reveal a role for IP-10 in effector T cell generation and trafficking. J Immunol 168:3195-3204.

During MJ, Spencer DD (1993) Extracellular hippocampal glutamate and spontaneous seizure in the conscious human brain. Lancet 341:1607-1610.

Dutta R, Chang A, Doud MK, Kidd GJ, Ribaudo MV, Young EA, Fox RJ, Staugaitis SM, Trapp BD (2011) Demyelination causes synaptic alterations in hippocampi from multiple sclerosis patients. Ann Neurol 69:445-454.

Dutta R, McDonough J, Yin X, Peterson J, Chang A, Torres T, Gudz T, Macklin WB, Lewis DA, Fox RJ, Rudick R, Mirnics K, Trapp BD (2006) Mitochondrial dysfunction as a cause of axonal degeneration in multiple sclerosis patients. Ann Neurol 59:478-489.

Dutta R, Trapp BD (2011) Mechanisms of neuronal dysfunction and degeneration in multiple sclerosis. Prog Neurobiol 93:1-12.

Ellis R, Boggild M (2009) Therapy-related acute leukaemia with Mitoxantrone: what is the risk and can we minimise it? Mult Scler 15:505-508.

Ellwardt E, Walsh JT, Kipnis J, Zipp F (2016) Understanding the Role of T Cells in CNS Homeostasis. Trends Immunol 37:154-165.

Engelhardt B, Coisne C (2011) Fluids and barriers of the CNS establish immune privilege by confining immune surveillance to a two-walled castle moat surrounding the CNS castle. Fluids Barriers CNS 8:4.

Engelhardt B, Ransohoff RM (2005) The ins and outs of T-lymphocyte trafficking to the CNS: anatomical sites and molecular mechanisms. Trends Immunol 26:485-495.

Erwin E, Baker FH, Busen WF, Malpeli JG (1999) Relationship between laminar topology and retinotopy in the rhesus lateral geniculate nucleus: results from a functional atlas. J Comp Neurol 407:92-102.

Evangelidou M, Karamita M, Vamvakas SS, Szymkowski DE, Probert L (2014) Altered expression of oligodendrocyte and neuronal marker genes predicts the clinical onset of autoimmune encephalomyelitis and indicates the effectiveness of multiple sclerosis-directed therapeutics. J Immunol 192:4122-4133.

Faivre A, Rico A, Zaaraoui W, Crespy L, Reuter F, Wybrecht D, Soulier E, Malikova I, Confort-Gouny S, Cozzone PJ, Pelletier J, Ranjeva JP, Audoin B (2012) Assessing brain connectivity at rest is clinically relevant in early multiple sclerosis. Mult Scler 18:1251-1258.

Favilla C, Abel T, Kelly MP (2008) Chronic Galphas signaling in the striatum increases anxiety-related behaviors independent of developmental effects. J Neurosci 28:13952-13956.

Fenn AM, Hall JC, Gensel JC, Popovich PG, Godbout JP (2014) IL-4 signaling drives a unique arginase+/IL-1beta+ microglia phenotype and recruits macrophages to the inflammatory CNS: consequences of age-related deficits in IL-4Ralpha after traumatic spinal cord injury. J Neurosci 34:8904-8917.

Finkelmeyer A, Nilsson J, He J, Stevens L, Maller JJ, Moss RA, Small S, Gallagher P, Coventry K, Ferrier IN, McAllister-Williams RH (2016) Altered hippocampal function in major depression despite intact structure and resting perfusion. Psychol Med 46:2157-2168.

Fitzpatrick D, Lund JS, Schmechel DE, Towles AC (1987) Distribution of GABAergic neurons and axon terminals in the macaque striate cortex. J Comp Neurol 264:73-91.

Flachenecker P, Stuke K (2008) National MS registries. J Neurol 255 Suppl 6:102-108.

Flugel A, Odoardi F, Nosov M, Kawakami N (2007) Autoaggressive effector T cells in the course of experimental autoimmune encephalomyelitis visualized in the light of two-photon microscopy. J Neuroimmunol 191:86-97.

Freund J, McDermott D (1942) Sensitization to horse serum by means of adjuvants. Proc Soc Exp Biol Med 49:548–553.

Friese MA, Fugger L (2009) Pathogenic CD8(+) T cells in multiple sclerosis. Ann Neurol 66:132-141.

Fu M, Zuo Y (2011) Experience-dependent structural plasticity in the cortex. Trends Neurosci 34:177-187.

Fu R, Shen Q, Xu P, Luo JJ, Tang Y (2014) Phagocytosis of microglia in the central nervous system diseases. Mol Neurobiol 49:1422-1434.

Fuster JM (1997) Network memory. Trends Neurosci 20:451-459.

Gabbott PL, Somogyi P (1986) Quantitative distribution of GABA-immunoreactive neurons in the visual cortex (area 17) of the cat. Exp Brain Res 61:323-331.

Gadani SP, Cronk JC, Norris GT, Kipnis J (2012) IL-4 in the brain: a cytokine to remember. J Immunol 189:4213-4219.

Gahring LC, Carlson NG, Kulmar RA, Rogers SW (1996) Neuronal expression of tumor necrosis factor alpha in the murine brain. Neuroimmunomodulation 3:289-303.

Gallo A, Bisecco A, Bonavita S, Tedeschi G (2015) Functional plasticity of the visual system in multiple sclerosis. Front Neurol 6:79.

Garaschuk O, Konnerth A (2010) In vivo two-photon calcium imaging using multicell bolus loading. Cold Spring Harb Protoc 2010:pdb prot5482.

Garaschuk O, Milos RI, Grienberger C, Marandi N, Adelsberger H, Konnerth A (2006a) Optical monitoring of brain function in vivo: from neurons to networks. Pflugers Arch 453:385-396.

Garaschuk O, Milos RI, Konnerth A (2006b) Targeted bulk-loading of fluorescent indicators for two-photon brain imaging in vivo. Nat Protoc 1:380-386.

Ge Y, Grossman RI, Udupa JK, Babb JS, Nyul LG, Kolson DL (2001) Brain atrophy in relapsing-remitting multiple sclerosis: fractional volumetric analysis of gray matter and white matter. Radiology 220:606-610.

Gendron RL, Nestel FP, Lapp WS, Baines MG (1991) Expression of tumor necrosis factor alpha in the developing nervous system. Int J Neurosci 60:129-136.

Genova HM, Lengenfelder J, Chiaravalloti ND, Moore NB, DeLuca J (2012) Processing speed versus working memory: contributions to an information-processing task in multiple sclerosis. Appl Neuropsychol Adult 19:132-140.

Gilliet M, Liu YJ (2002) Human plasmacytoid-derived dendritic cells and the induction of T-regulatory cells. Hum Immunol 63:1149-1155.

Gimenez MA, Sim JE, Russell JH (2004) TNFR1-dependent VCAM-1 expression by astrocytes exposes the CNS to destructive inflammation. J Neuroimmunol 151:116-125.

Giunti D, Parodi B, Cordano C, Uccelli A, Kerlero de Rosbo N (2014) Can we switch microglia's phenotype to foster neuroprotection? Focus on multiple sclerosis. Immunology 141:328-339.

Gobel W, Helmchen F (2007) In vivo calcium imaging of neural network function. Physiology (Bethesda) 22:358-365.

Gold R, Linington C, Lassmann H (2006) Understanding pathogenesis and therapy of multiple sclerosis via animal models: 70 years of merits and culprits in experimental autoimmune encephalomyelitis research. Brain 129:1953-1971.

Golding NL, Spruston N (1998) Dendritic sodium spikes are variable triggers of axonal action potentials in hippocampal CA1 pyramidal neurons. Neuron 21:1189-1200.

Goldstein K (1999) The mental changes due to frontal lobe damage. J Psychol 17:187-208.

Goodin DS, Frohman EM, Garmany GP, Jr., Halper J, Likosky WH, Lublin FD, Silberberg DH, Stuart WH, van den Noort S, Therapeutics, Technology Assessment Subcommittee of the American Academy of N, the MSCfCPG (2002) Disease modifying therapies in multiple sclerosis: report of the Therapeutics and Technology Assessment Subcommittee of the American Academy of Neurology and the MS Council for Clinical Practice Guidelines. Neurology 58:169-178.

Graler MH, Goetzl EJ (2004) The immunosuppressant FTY720 down-regulates sphingosine 1-phosphate G-protein-coupled receptors. FASEB J 18:551-553.

Greenwood J, Heasman SJ, Alvarez JI, Prat A, Lyck R, Engelhardt B (2011) Review: leucocyte-endothelial cell crosstalk at the blood-brain barrier: a prerequisite for successful immune cell entry to the brain. Neuropathol Appl Neurobiol 37:24-39.

Greter M, Heppner FL, Lemos MP, Odermatt BM, Goebels N, Laufer T, Noelle RJ, Becher B (2005) Dendritic cells permit immune invasion of the CNS in an animal model of multiple sclerosis. Nat Med 11:328-334.

Grienberger C, Konnerth A (2012) Imaging calcium in neurons. Neuron 73:862-885.

Groom AJ, Smith T, Turski L (2003) Multiple sclerosis and glutamate. Ann N Y Acad Sci 993:229-275; discussion 287-228.

Guenova E, Skabytska Y, Hoetzenecker W, Weindl G, Sauer K, Tham M, Kim KW, Park JH, Seo JH, Ignatova D, Cozzio A, Levesque MP, Volz T, Koberle M, Kaesler S, Thomas P, Mailhammer R, Ghoreschi K, Schakel K, Amarov B, Eichner M, Schaller M, Clark RA, Rocken M, Biedermann T (2015) IL-4 abrogates T(H)17 cell-mediated inflammation by selective silencing of IL-23 in antigen-presenting cells. Proc Natl Acad Sci U S A 112:2163-2168.

Haak S, Croxford AL, Kreymborg K, Heppner FL, Pouly S, Becher B, Waisman A (2009) IL-17A and IL-17F do not contribute vitally to autoimmune neuro-inflammation in mice. J Clin Invest 119:61-69.

Haines JD, Inglese M, Casaccia P (2011) Axonal damage in multiple sclerosis. Mt Sinai J Med 78:231-243.

Hamm RJ, Pike BR, O'Dell DM, Lyeth BG, Jenkins LW (1994) The rotarod test: an evaluation of its effectiveness in assessing motor deficits following traumatic brain injury. J Neurotrauma 11:187-196.

Haussleiter IS, Brune M, Juckel G (2009) Psychopathology in multiple sclerosis: diagnosis, prevalence and treatment. Ther Adv Neurol Disord 2:13-29.

Helekar SA, Shin JC, Mattson BJ, Bartley K, Stosic M, Saldana-King T, Montague PR, Hutton GJ (2010) Functional brain network changes associated with maintenance of cognitive function in multiple sclerosis. Front Hum Neurosci 4:219.

Helmchen F (2009) Two-Photon Functional Imaging of Neuronal Activity. In: In Vivo Optical Imaging of Brain Function (Frostig, R. D., ed) Boca Raton (FL).

Helmchen F, Denk W (2005) Deep tissue two-photon microscopy. Nat Methods 2:932-940.

Helmchen F, Imoto K, Sakmann B (1996) Ca2+ buffering and action potential-evoked Ca2+ signaling in dendrites of pyramidal neurons. Biophys J 70:1069-1081.

Helmchen F, Waters J (2002) Ca2+ imaging in the mammalian brain in vivo. Eur J Pharmacol 447:119-129.

Hendrickson AE, Wilson JR, Ogren MP (1978) The neuroanatomical organization of pathways between the dorsal lateral geniculate nucleus and visual cortex in Old World and New World primates. J Comp Neurol 182:123-136.

Hendry SH, Schwark HD, Jones EG, Yan J (1987) Numbers and proportions of GABA-immunoreactive neurons in different areas of monkey cerebral cortex. J Neurosci 7:1503-1519.

Henze DA, Buzsaki G (2001) Action potential threshold of hippocampal pyramidal cells in vivo is increased by recent spiking activity. Neuroscience 105:121-130.

Hirase H, Qian L, Bartho P, Buzsaki G (2004) Calcium dynamics of cortical astrocytic networks in vivo. PLoS Biol 2:E96.

Hofer SB, Mrsic-Flogel TD, Bonhoeffer T, Hubener M (2006) Prior experience enhances plasticity in adult visual cortex. Nat Neurosci 9:127-132.

Hofman FM, Hinton DR, Johnson K, Merrill JE (1989) Tumor necrosis factor identified in multiple sclerosis brain. J Exp Med 170:607-612.

Hofstetter HH, Shive CL, Forsthuber TG (2002) Pertussis toxin modulates the immune response to neuroantigens injected in incomplete Freund's adjuvant: induction of Th1 cells and experimental autoimmune encephalomyelitis in the presence of high frequencies of Th2 cells. J Immunol 169:117-125.

Hoglund RA, Maghazachi AA (2014) Multiple sclerosis and the role of immune cells. World J Exp Med 4:27-37.

Housley WJ, Pitt D, Hafler DA (2015) Biomarkers in multiple sclerosis. Clin Immunol 161:51-58.

Hubel DH, Wiesel TN (1968) Receptive fields and functional architecture of monkey striate cortex. J Physiol 195:215-243.

Hubener M, Bonhoeffer T (2005) Visual cortex: two-photon excitement. Curr Biol 15:R205-208.

Huber AK, Wang L, Han P, Zhang X, Ekholm S, Srinivasan A, Irani DN, Segal BM (2014) Dysregulation of the IL-23/IL-17 axis and myeloid factors in secondary progressive MS. Neurology 83:1500-1507.

Huseby ES, Huseby PG, Shah S, Smith R, Stadinski BD (2012) Pathogenic CD8 T cells in multiple sclerosis and its experimental models. Front Immunol 3:64.

Ito S, Yeh FC, Hiolski E, Rydygier P, Gunning DE, Hottowy P, Timme N, Litke AM, Beggs JM (2014) Large-scale, high-resolution multielectrode-array recording depicts functional network differences of cortical and hippocampal cultures. PLoS One 9:e105324.

Jadidi-Niaragh F, Mirshafiey A (2011) Th17 cell, the new player of neuroinflammatory process in multiple sclerosis. Scand J Immunol 74:1-13.

Jenkins TM, Toosy AT, Ciccarelli O, Miszkiel KA, Wheeler-Kingshott CA, Henderson AP, Kallis C, Mancini L, Plant GT, Miller DH, Thompson AJ (2010) Neuroplasticity predicts outcome of optic neuritis independent of tissue damage. Ann Neurol 67:99-113.

Johansen JP, Cain CK, Ostroff LE, LeDoux JE (2011) Molecular mechanisms of fear learning and memory. Cell 147:509-524.

Jolivel V, Luessi F, Masri J, Kraus SH, Hubo M, Poisa-Beiro L, Klebow S, Paterka M, Yogev N, Tumani H, Furlan R, Siffrin V, Jonuleit H, Zipp F, Waisman A (2013) Modulation of dendritic cell properties by laquinimod as a mechanism for modulating multiple sclerosis. Brain 136:1048-1066.

Jones JL, Anderson JM, Phuah CL, Fox EJ, Selmaj K, Margolin D, Lake SL, Palmer J, Thompson SJ, Wilkins A, Webber DJ, Compston DA, Coles AJ (2010) Improvement in disability after alemtuzumab treatment of multiple sclerosis is associated with neuroprotective autoimmunity. Brain 133:2232-2247.

Kaas JH, Krubitzer LA, Chino YM, Langston AL, Polley EH, Blair N (1990) Reorganization of retinotopic cortical maps in adult mammals after lesions of the retina. Science 248:229-231.

Kandel ER, Schwartz JH, Jessell TM, Siegelbaum SA, Hudspeth (2013) Principles of Neural Science. 229.

Kang J, Kang N, Yu Y, Zhang J, Petersen N, Tian GF, Nedergaard M (2010) Sulforhodamine 101 induces long-term potentiation of intrinsic excitability and synaptic efficacy in hippocampal CA1 pyramidal neurons. Neuroscience 169:1601-1609.

Kanki T, Ban T (1997) The PFC: Anatomy, physiology and neuropsychology of the frontal lobe. The PFC: Anatomy, physiology and neuropsychology of the frontal lobe.

Kappos L, Radue EW, O'Connor P, Polman C, Hohlfeld R, Calabresi P, Selmaj K, Agoropoulou C, Leyk M, Zhang-Auberson L, Burtin P, Group FS (2010) A placebo-controlled trial of oral fingolimod in relapsing multiple sclerosis. N Engl J Med 362:387-401.

Katsavos S, Anagnostouli M (2013) Biomarkers in Multiple Sclerosis: An Up-to-Date Overview. Mult Scler Int 2013:340508.

Katz LC, Shatz CJ (1996) Synaptic activity and the construction of cortical circuits. Science 274:1133-1138.

Kelley BJ, Rodriguez M (2009) Seizures in patients with multiple sclerosis: epidemiology, pathophysiology and management. CNS Drugs 23:805-815.

Kelly RC, Smith MA, Samonds JM, Kohn A, Bonds AB, Movshon JA, Lee TS (2007) Comparison of recordings from microelectrode arrays and single electrodes in the visual cortex. J Neurosci 27:261-264.

Kerlin AM, Andermann ML, Berezovskii VK, Reid RC (2010) Broadly tuned response properties of diverse inhibitory neuron subtypes in mouse visual cortex. Neuron 67:858-871.

Kerr JN, Greenberg D, Helmchen F (2005) Imaging input and output of neocortical networks in vivo. ProcNatlAcadSciUSA 102:14063-14068.

Killestein J, Polman CH (2005) Current trials in multiple sclerosis: established evidence and future hopes. Curr Opin Neurol 18:253-260.

Komiyama Y, Nakae S, Matsuki T, Nambu A, Ishigame H, Kakuta S, Sudo K, Iwakura Y (2006) IL-17 plays an important role in the development of experimental autoimmune encephalomyelitis. J Immunol 177:566-573.

Kornek B, Storch MK, Bauer J, Djamshidian A, Weissert R, Wallstroem E, Stefferl A, Zimprich F, Olsson T, Linington C, Schmidbauer M, Lassmann H (2001) Distribution of a calcium channel subunit in dystrophic axons in multiple sclerosis and experimental autoimmune encephalomyelitis. Brain 124:1114-1124.

Kornek B, Storch MK, Weissert R, Wallstroem E, Stefferl A, Olsson T, Linington C, Schmidbauer M, Lassmann H (2000) Multiple sclerosis and chronic autoimmune encephalomyelitis: a comparative quantitative study of axonal injury in active, inactive, and remyelinated lesions. Am J Pathol 157:267-276.

Kossut M, Juliano SL (1999) Anatomical correlates of representational map reorganization induced by partial vibrissectomy in the barrel cortex of adult mice. Neuroscience 92:807-817.

Kostic M, Dzopalic T, Zivanovic S, Zivkovic N, Cvetanovic A, Stojanovic I, Vojinovic S, Marjanovic G, Savic V, Colic M (2014) IL-17 and glutamate excitotoxicity in the pathogenesis of multiple sclerosis. Scand J Immunol 79:181-186.

Kuchibhotla KV, Goldman ST, Lattarulo CR, Wu HY, Hyman BT, Bacskai BJ (2008) Abeta plaques lead to aberrant regulation of calcium homeostasis in vivo resulting in structural and functional disruption of neuronal networks. Neuron 59:214-225.

Kurnellas MP, Donahue KC, Elkabes S (2007) Mechanisms of neuronal damage in multiple sclerosis and its animal models: role of calcium pumps and exchangers. Biochem Soc Trans 35:923-926.

Kuruvilla AP, Shah R, Hochwald GM, Liggitt HD, Palladino MA, Thorbecke GJ (1991) Protective effect of transforming growth factor beta 1 on experimental autoimmune diseases in mice. Proc Natl Acad Sci U S A 88:2918-2921.

LaFerla FM (2002) Calcium dyshomeostasis and intracellular signalling in Alzheimer's disease. Nat Rev Neurosci 3:862-872.

Langkilde AR, Frederiksen JL, Rostrup E, Larsson HB (2002) Functional MRI of the visual cortex and visual testing in patients with previous optic neuritis. Eur J Neurol 9:277-286.

Lassmann H (2007) Experimental models of multiple sclerosis. Rev Neurol (Paris) 163:651-655.

Leonoudakis D, Braithwaite SP, Beattie MS, Beattie EC (2004) TNFalpha-induced AMPA-receptor trafficking in CNS neurons; relevance to excitotoxicity? Neuron Glia Biol 1:263-273.

Leray E, Yaouanq J, Le Page E, Coustans M, Laplaud D, Oger J, Edan G (2010) Evidence for a two-stage disability progression in multiple sclerosis. Brain 133:1900-1913.

Leyhe T, Laske C, Buchkremer G, Wormstall H, Wiendl H (2005) [Dementia as a primary symptom in late onset multiple sclerosis. Case series and review of the literature]. Nervenarzt 76:748-755.

Liang B, Workman C, Lee J, Chew C, Dale BM, Colonna L, Flores M, Li N, Schweighoffer E, Greenberg S, Tybulewicz V, Vignali D, Clynes R (2008) Regulatory T cells inhibit dendritic cells by lymphocyte activation gene-3 engagement of MHC class II. J Immunol 180:5916-5926.

Liblau RS, Gonzalez-Dunia D, Wiendl H, Zipp F (2013) Neurons as targets for T cells in the nervous system. Trends Neurosci 36:315-324.

Lieberman AP, Pitha PM, Shin HS, Shin ML (1989) Production of tumor necrosis factor and other cytokines by astrocytes stimulated with lipopolysaccharide or a neurotropic virus. Proc Natl Acad Sci U S A 86:6348-6352.

Lin BJ, Chen TW, Schild D (2007) Cell type-specific relationships between spiking and [Ca2+]i in neurons of the Xenopus tadpole olfactory bulb. J Physiol 582:163-175.

Lipscomb MF, Masten BJ (2002) Dendritic cells: immune regulators in health and disease. Physiol Rev 82:97-130.

Liu MT, Keirstead HS, Lane TE (2001) Neutralization of the chemokine CXCL10 reduces inflammatory cell invasion and demyelination and improves neurological function in a viral model of multiple sclerosis. J Immunol 167:4091-4097.

Lodish H, Berk A, Zipursky SL (2000) Overview of Neuron Structure and Function. Molecular Cell Biology 4th edition.

Long MA, Lee AK (2012) Intracellular recording in behaving animals. Curr Opin Neurobiol 22:34-44.

Lovas G, Szilagyi N, Majtenyi K, Palkovits M, Komoly S (2000) Axonal changes in chronic demyelinated cervical spinal cord plaques. Brain 123 ( Pt 2):308-317.

Lovett-Racke AE, Yang Y, Racke MK (2011) Th1 versus Th17: are T cell cytokines relevant in multiple sclerosis? Biochim Biophys Acta 1812:246-251.

Lublin FD, Reingold SC (1996) Defining the clinical course of multiple sclerosis: results of an international survey. National Multiple Sclerosis Society (USA) Advisory

Committee on Clinical Trials of New Agents in Multiple Sclerosis. Neurology 46:907-911.

Lucchinetti CF, Popescu BF, Bunyan RF, Moll NM, Roemer SF, Lassmann H, Bruck W, Parisi JE, Scheithauer BW, Giannini C, Weigand SD, Mandrekar J, Ransohoff RM (2011) Inflammatory cortical demyelination in early multiple sclerosis. N Engl J Med 365:2188-2197.

Lull ME, Block ML (2010) Microglial activation and chronic neurodegeneration. Neurotherapeutics 7:354-365.

Macrez R, Stys PK, Vivien D, Lipton SA, Docagne F (2016) Mechanisms of glutamate toxicity in multiple sclerosis: biomarker and therapeutic opportunities. Lancet Neurol 15:1089-1102.

Mahad D, Lassmann H, Turnbull D (2008a) Review: Mitochondria and disease progression in multiple sclerosis. Neuropathol Appl Neurobiol 34:577-589.

Mahad D, Ziabreva I, Lassmann H, Turnbull D (2008b) Mitochondrial defects in acute multiple sclerosis lesions. Brain 131:1722-1735.

Mahad DJ, Ziabreva I, Campbell G, Lax N, White K, Hanson PS, Lassmann H, Turnbull DM (2009) Mitochondrial changes within axons in multiple sclerosis. Brain 132:1161-1174.

Mainero C, Caramia F, Pozzilli C, Pisani A, Pestalozza I, Borriello G, Bozzao L, Pantano P (2004) fMRI evidence of brain reorganization during attention and memory tasks in multiple sclerosis. Neuroimage 21:858-867.

Mandolesi G, Grasselli G, Musumeci G, Centonze D (2010) Cognitive deficits in experimental autoimmune encephalomyelitis: neuroinflammation and synaptic degeneration. Neurol Sci 31:S255-259.

Mangalam A, Rodriguez M, David C (2006) Role of MHC class II expressing CD4+ T cells in proteolipid protein(91-110)-induced EAE in HLA-DR3 transgenic mice. Eur J Immunol 36:3356-3370.

Mank M, Santos AF, Direnberger S, Mrsic-Flogel TD, Hofer SB, Stein V, Hendel T, Reiff DF, Levelt C, Borst A, Bonhoeffer T, Hubener M, Griesbeck O (2008) A genetically encoded calcium indicator for chronic in vivo two-photon imaging. NatMethods 5:805-811.

Mao P, Reddy PH (2010) Is multiple sclerosis a mitochondrial disease? Biochim Biophys Acta 1802:66-79.

Markram H, Helm PJ, Sakmann B (1995) Dendritic calcium transients evoked by single back-propagating action potentials in rat neocortical pyramidal neurons. J Physiol 485 ( Pt 1):1-20.

Mars LT, Saikali P, Liblau RS, Arbour N (2011) Contribution of CD8 T lymphocytes to the immuno-pathogenesis of multiple sclerosis and its animal models. Biochim Biophys Acta 1812:151-161.

Martins TB, Rose JW, Jaskowski TD, Wilson AR, Husebye D, Seraj HS, Hill HR (2011) Analysis of proinflammatory and anti-inflammatory cytokine serum concentrations in patients with multiple sclerosis by using a multiplexed immunoassay. Am J Clin Pathol 136:696-704.

Masterman DL, Cummings JL (1997) Frontal-subcortical circuits: the anatomic basis of executive, social and motivated behaviors. J Psychopharmacol 11:107-114.

Mathew SJ, Ho S (2006) Etiology and neurobiology of social anxiety disorder. J Clin Psychiatry 67 Suppl 12:9-13.

Matloubian M, Lo CG, Cinamon G, Lesneski MJ, Xu Y, Brinkmann V, Allende ML, Proia RL, Cyster JG (2004) Lymphocyte egress from thymus and peripheral lymphoid organs is dependent on S1P receptor 1. Nature 427:355-360.

McCarthy DP, Richards MH, Miller SD (2012) Mouse models of multiple sclerosis: experimental autoimmune encephalomyelitis and Theiler's virus-induced demyelinating disease. Methods Mol Biol 900:381-401.

McFarland HF, Martin R (2007) Multiple sclerosis: a complicated picture of autoimmunity. Nat Immunol 8:913-919.

Meurs A, Clinckers R, Ebinger G, Michotte Y, Smolders I (2008) Seizure activity and changes in hippocampal extracellular glutamate, GABA, dopamine and serotonin. Epilepsy Res 78:50-59.

Miljkovic D, Spasojevic I (2013) Multiple sclerosis: molecular mechanisms and therapeutic opportunities. Antioxid Redox Signal 19:2286-2334.

Miljkovic D, Timotijevic G, Mostarica Stojkovic M (2011) Astrocytes in the tempest of multiple sclerosis. FEBS Lett 585:3781-3788.

Miller SD, Karpus WJ (2007) Experimental autoimmune encephalomyelitis in the mouse. Curr Protoc Immunol Chapter 15:Unit 15 11.

Miller SD, Karpus WJ, Davidson TS (2010) Experimental autoimmune encephalomyelitis in the mouse. Curr Protoc Immunol Chapter 15:Unit 15 11.

Minsky M (1988) Memoir on inventing the confocal scanning microscope. Scanning 10:128-138.

Minta A, Kao JP, Tsien RY (1989) Fluorescent indicators for cytosolic calcium based on rhodamine and fluorescein chromophores. J Biol Chem 264:8171-8178.

Mishra MK, Yong VW (2016) Myeloid cells - targets of medication in multiple sclerosis. Nat Rev Neurol 12:539-551.

Morecraft RJ, Herrick JL, Stilwell-Morecraft KS, Louie JL, Schroeder CM, Ottenbacher JG, Schoolfield MW (2002) Localization of arm representation in the corona radiata and internal capsule in the non-human primate. Brain 125:176-198.

Morganti-Kossman MC, Lenzlinger PM, Hans V, Stahel P, Csuka E, Ammann E, Stocker R, Trentz O, Kossmann T (1997) Production of cytokines following brain injury: beneficial and deleterious for the damaged tissue. Mol Psychiatry 2:133-136.

Nakajima H, Hosokawa T, Sugino M, Kimura F, Sugasawa J, Hanafusa T, Takahashi T (2010) Visual field defects of optic neuritis in neuromyelitis optica compared with multiple sclerosis. BMC Neurol 10:45.

Neumann M, Wang Y, Kim S, Hong SM, Jeng L, Bilgen M, Liu J (2009) Assessing gait impairment following experimental traumatic brain injury in mice. J Neurosci Methods 176:34-44.

Nimmerjahn A, Helmchen F (2012) In vivo labeling of cortical astrocytes with sulforhodamine 101 (SR101). Cold Spring Harb Protoc 2012:326-334.

Nimmerjahn A, Kirchhoff F, Kerr JN, Helmchen F (2004) Sulforhodamine 101 as a specific marker of astroglia in the neocortex in vivo. Nat Methods 1:31-37.

Ntziachristos V (2010) Going deeper than microscopy: the optical imaging frontier in biology. Nat Methods 7:603-614.

Olmos G, Llado J (2014) Tumor necrosis factor alpha: a link between neuroinflammation and excitotoxicity. Mediators Inflamm 2014:861231.

Onger D, Price JL (2000) Organization of networks in the orbital and medial PFC of rats, monkeys and humans. Cereb Cortex 10:206-219.

Ozenci V, Kouwenhoven M, Link H (2002) Cytokines in multiple sclerosis: methodological aspects and pathogenic implications. Multiple Sclerosis 8:396-404.

Ozenci V, Kouwenhoven M, Teleshova N, Pashenkov M, Fredrikson S, Link H (2000) Multiple sclerosis: pro- and anti-inflammatory cytokines and metalloproteinases are affected differentially by treatment with IFN-beta. J Neuroimmunol 108:236-243.

Pang Y, Cai Z, Rhodes PG (2003) Disturbance of oligodendrocyte development, hypomyelination and white matter injury in the neonatal rat brain after intracerebral injection of lipopolysaccharide. Brain Res Dev Brain Res 140:205-214.

Panitch HS, Hirsch RL, Schindler J, Johnson KP (1987) Treatment of multiple sclerosis with gamma interferon: exacerbations associated with activation of the immune system. Neurology 37:1097-1102.

Paredes RM, Etzler JC, Watts LT, Zheng W, Lechleiter JD (2008) Chemical calcium indicators. Methods 46:143-151.

Park CK, Lu N, Xu ZZ, Liu T, Serhan CN, Ji RR (2011) Resolving TRPV1- and TNF-alpha-mediated spinal cord synaptic plasticity and inflammatory pain with neuroprotectin D1. J Neurosci 31:15072-15085.

Paterka M, Voss JO, Werr J, Reuter E, Franck S, Leuenberger T, Herz J, Radbruch H, Bopp T, Siffrin V, Zipp F (2016) Dendritic cells tip the balance towards induction of regulatory T cells upon priming in experimental autoimmune encephalomyelitis. J Autoimmun.

Patrikios P, Stadelmann C, Kutzelnigg A, Rauschka H, Schmidbauer M, Laursen H, Sorensen PS, Bruck W, Lucchinetti C, Lassmann H (2006) Remyelination is extensive in a subset of multiple sclerosis patients. Brain 129:3165-3172.

Patterson GH, Piston DW (2000) Photobleaching in two-photon excitation microscopy. Biophys J 78:2159-2162.

Paxinos G, Franklin KBJ (2012) Paxinos and Franklin's the Mouse Brain in Stereotaxic Coordinates: Elsevier Academic Press.

Penner IK, Rausch M, Kappos L, Opwis K, Radu EW (2003) Analysis of impairment related functional architecture in MS patients during performance of different attention tasks. J Neurol 250:461-472.

Perry VH, Teeling J (2013) Microglia and macrophages of the central nervous system: the contribution of microglia priming and systemic inflammation to chronic neurodegeneration. Semin Immunopathol 35:601-612.

Petermann F, Korn T (2011) Cytokines and effector T cell subsets causing autoimmune CNS disease. FEBS Lett 585:3747-3757.

Pickering M, Cumiskey D, O'Connor JJ (2005) Actions of TNF-alpha on glutamatergic synaptic transmission in the central nervous system. Exp Physiol 90:663-670.

Pinheiro PS, Mulle C (2008) Presynaptic glutamate receptors: physiological functions and mechanisms of action. Nat Rev Neurosci 9:423-436.

Pitt D, Werner P, Raine CS (2000) Glutamate excitotoxicity in a model of multiple sclerosis. Nat Med 6:67-70.

Podojil JR, Kohm AP, Miller SD (2006) CD4+ T cell expressed CD80 regulates central nervous system effector function and survival during experimental autoimmune encephalomyelitis. J Immunol 177:2948-2958.

Polazzi E, Levi G, Minghetti L (1999) Human immunodeficiency virus type 1 Tat protein stimulates inducible nitric oxide synthase expression and nitric oxide production in microglial cultures. J Neuropathol Exp Neurol 58:825-831.

Pollak Y, Ovadia H, Orion E, Weidenfeld J, Yirmiya R (2003) The EAE-associated behavioral syndrome: I. Temporal correlation with inflammatory mediators. J Neuroimmunol 137:94-99.

Pollinger B, Krishnamoorthy G, Berer K, Lassmann H, Bosl MR, Dunn R, Domingues HS, Holz A, Kurschus FC, Wekerle H (2009) Spontaneous relapsing-remitting EAE in the SJL/J mouse: MOG-reactive transgenic T cells recruit endogenous MOG-specific B cells. J Exp Med 206:1303-1316.

Purves D, Augustine GJ, Fitzpatrick D (2001) Excitatory and Inhibitory Postsynaptic Potentials. Neuroscience 2nd edition.

Quintana FJ, Yeste A, Mascanfroni ID (2015) Role and therapeutic value of dendritic cells in central nervous system autoimmunity. Cell Death Differ 22:215-224.

Rahn K, Slusher B, Kaplin A (2012) Cognitive impairment in multiple sclerosis: a forgotten disability remembered. Cerebrum 2012:14.

Raivich G (2005) Like cops on the beat: the active role of resting microglia. Trends Neurosci 28:571-573.

Rao SM, Leo GJ, Ellington L, Nauertz T, Bernardin L, Unverzagt F (1991) Cognitive dysfunction in multiple sclerosis. II. Impact on employment and social functioning. Neurology 41:692-696.

Rasmussen R, Nedergaard M, Petersen NC (2016) Sulforhodamine 101, a widely used astrocyte marker, can induce cortical seizure-like activity at concentrations commonly used. Sci Rep 6:30433.

Rasouli J, Ciric B, Imitola J, Gonnella P, Hwang D, Mahajan K, Mari ER, Safavi F, Leist TP, Zhang GX, Rostami A (2015) Expression of GM-CSF in T Cells Is Increased in Multiple Sclerosis and Suppressed by IFN-beta Therapy. J Immunol 194:5085-5093.

Reddy H, Narayanan S, Arnoutelis R, Jenkinson M, Antel J, Matthews PM, Arnold DL (2000) Evidence for adaptive functional changes in the cerebral cortex with axonal injury from multiple sclerosis. Brain 123 ( Pt 11):2314-2320.

Rimkus Cd, Steenwijk MD, Barkhof F (2016) Causes, effects and connectivity changes in MS-related cognitive decline. Dementia & Neuropsychologia 10.

Roberts AC, Robbins TW, Weiskrantz L (2000) Prefontal cortex-executive and cognitive function. New York: Oxford University Press 51-66.

Roberts RJ, Hager L, Heron C (1994) Prefrontal cognitive processes, working memory and inhibition of antisaccade task. 265–282.

Rocca MA, Ceccarelli A, Rodegher M, Misci P, Riccitelli G, Falini A, Comi G, Filippi M (2010) Preserved brain adaptive properties in patients with benign multiple sclerosis. Neurology 74:142-149.

Rocca MA, Valsasina P, Martinelli V, Misci P, Falini A, Comi G, Filippi M (2012) Large-scale neuronal network dysfunction in relapsing-remitting multiple sclerosis. Neurology 79:1449-1457.

Rochefort NL, Garaschuk O, Milos RI, Narushima M, Marandi N, Pichler B, Kovalchuk Y, Konnerth A (2009) Sparsification of neuronal activity in the visual cortex at eye-opening. Proc Natl Acad Sci U S A 106:15049-15054.

Rombouts SA, Lazeron RH, Scheltens P, Uitdehaag BM, Sprenger M, Valk J, Barkhof F (1998) Visual activation patterns in patients with optic neuritis: an fMRI pilot study. Neurology 50:1896-1899.

Ross WN, Nakamura T, Watanabe S, Larkum M, Lasser-Ross N (2005) Synaptically activated ca2+ release from internal stores in CNS neurons. Cell Mol Neurobiol 25:283-295.

Rowland NE (2007) Food or fluid restriction in common laboratory animals: balancing welfare considerations with scientific inquiry. Comp Med 57:149-160.

Runyan CA, Schummers J, Van Wart A, Kuhlman SJ, Wilson NR, Huang ZJ, Sur M (2010) Response features of parvalbumin-expressing interneurons suggest precise roles for subtypes of inhibition in visual cortex. Neuron 67:847-857.

Saxena A, Martin-Blondel G, Mars LT, Liblau RS (2011) Role of CD8 T cell subsets in the pathogenesis of multiple sclerosis. FEBS Lett 585:3758-3763.

Scheuss V, Yasuda R, Sobczyk A, Svoboda K (2006) Nonlinear [Ca2+] signaling in dendrites and spines caused by activity-dependent depression of Ca2+ extrusion. J Neurosci 26:8183-8194.

Schmolesky M (1995) The Primary Visual Cortex. In: Webvision: The Organization of the Retina and Visual System (Kolb, H. et al., eds) Salt Lake City (UT).

Schoonheim MM, Geurts JJ, Barkhof F (2010) The limits of functional reorganization in multiple sclerosis. Neurology 74:1246-1247.

Scott LJ, Figgitt DP (2004) Mitoxantrone: a review of its use in multiple sclerosis. CNS Drugs 18:379-396.

Sega S, Wraber B, Mesec A, Horvat A, Ihan A (2004) IFN-beta1a and IFN-beta1b have different patterns of influence on cytokines. Clin Neurol Neurosurg 106:255-258.

Shaygannejad V, Ashtari F, Zare M, Ghasemi M, Norouzi R, Maghzi H (2013) Seizure characteristics in multiple sclerosis patients. J Res Med Sci 18:S74-77.

Sherman SM, Guillery RW (1998) On the actions that one nerve cell can have on another: distinguishing "drivers" from "modulators". Proc Natl Acad Sci U S A 95:7121-7126.

Shigetomi E, Kracun S, Sofroniew MV, Khakh BS (2010) A genetically targeted optical sensor to monitor calcium signals in astrocyte processes. Nat Neurosci 13:759-766.

Shijie J, Takeuchi H, Yawata I, Harada Y, Sonobe Y, Doi Y, Liang J, Hua L, Yasuoka S, Zhou Y, Noda M, Kawanokuchi J, Mizuno T, Suzumura A (2009) Blockade of glutamate release from microglia attenuates experimental autoimmune encephalomyelitis in mice. Tohoku J Exp Med 217:87-92.

Shortman K, Heath WR (2001) Immunity or tolerance? That is the question for dendritic cells. Nat Immunol 2:988-989.

Siddiqui SV, Chatterjee U, Kumar D, Siddiqui A, Goyal N (2008) Neuropsychology of prefrontal cortex. Indian J Psychiatry 50:202-208.

Skulina C, Schmidt S, Dornmair K, Babbe H, Roers A, Rajewsky K, Wekerle H, Hohlfeld R, Goebels N (2004) Multiple sclerosis: brain-infiltrating CD8+ T cells persist as clonal expansions in the cerebrospinal fluid and blood. Proc Natl Acad Sci U S A 101:2428-2433.

Smith KJ, McDonald WI (1999) The pathophysiology of multiple sclerosis: the mechanisms underlying the production of symptoms and the natural history of the disease. Philos Trans R Soc Lond B Biol Sci 354:1649-1673.

Soderstrom M, Hillert J, Link J, Navikas V, Fredrikson S, Link H (1995) Expression of IFN-gamma, IL-4, and TGF-beta in multiple sclerosis in relation to HLA-Dw2 phenotype and stage of disease. Mult Scler 1:173-180.

Sohya K, Kameyama K, Yanagawa Y, Obata K, Tsumoto T (2007) GABAergic neurons are less selective to stimulus orientation than excitatory neurons in layer II/III of visual

cortex, as revealed by in vivo functional Ca2+ imaging in transgenic mice. J Neurosci 27:2145-2149.

Sospedra M, Martin R (2005) Immunology of multiple sclerosis. Annu Rev Immunol 23:683-747.

Spitzer NC, Root CM, Borodinsky LN (2004) Orchestrating neuronal differentiation: patterns of Ca2+ spikes specify transmitter choice. Trends Neurosci 27:415-421.

Sprent J (2005) Direct stimulation of naive T cells by antigen-presenting cell vesicles. Blood Cells Mol Dis 35:17-20.

Srinivasan R, Sailasuta N, Hurd R, Nelson S, Pelletier D (2005) Evidence of elevated glutamate in multiple sclerosis using magnetic resonance spectroscopy at 3 T. Brain 128:1016-1025.

Staffen W, Mair A, Zauner H, Unterrainer J, Niederhofer H, Kutzelnigg A, Ritter S, Golaszewski S, Iglseder B, Ladurner G (2002) Cognitive function and fMRI in patients with multiple sclerosis: evidence for compensatory cortical activation during an attention task. Brain 125:1275-1282.

Stasiolek M, Bayas A, Kruse N, Wieczarkowiecz A, Toyka KV, Gold R, Selmaj K (2006) Impaired maturation and altered regulatory function of plasmacytoid dendritic cells in multiple sclerosis. Brain 129:1293-1305.

Stellwagen D, Beattie EC, Seo JY, Malenka RC (2005) Differential regulation of AMPA receptor and GABA receptor trafficking by tumor necrosis factor-α. The Journal of Neuroscience 25:3219-3228.

Stellwagen D, Malenka RC (2006a) Synaptic scaling mediated by glial TNF-alpha. Nature 440:1054-1059.

Stellwagen D, Malenka RC (2006b) Synaptic scaling mediated by glial TNF-α. Nature 440:1054-1059.

Stern JN, Keskin DB, Kato Z, Waldner H, Schallenberg S, Anderson A, von Boehmer H, Kretschmer K, Strominger JL (2010) Promoting tolerance to proteolipid protein-induced experimental autoimmune encephalomyelitis through targeting dendritic cells. Proc Natl Acad Sci U S A 107:17280-17285.

Stosiek C, Garaschuk O, Holthoff K, Konnerth A (2003) In vivo two-photon calcium imaging of neuronal networks. Proc Natl Acad Sci U S A 100:7319-7324.

Stover JF, Lowitzsch K, Kempski OS (1997) Cerebrospinal fluid hypoxanthine, xanthine and uric acid levels may reflect glutamate-mediated excitotoxicity in different neurological diseases. Neurosci Lett 238:25-28.

Stroh A, Adelsberger H, Groh A, Ruhlmann C, Fischer S, Schierloh A, Deisseroth K, Konnerth A (2013) Making waves: initiation and propagation of corticothalamic ca(2+) waves in vivo. Neuron 77:1136-1150.

Stromnes IM, Goverman JM (2006) Active induction of experimental allergic encephalomyelitis. Nat Protoc 1:1810-1819.

Stys PK, Waxman SG, Ransom BR (1992) Ionic mechanisms of anoxic injury in mammalian CNS white matter: role of Na+ channels and Na(+)-Ca2+ exchanger. J Neurosci 12:430-439.

Su KG, Banker G, Bourdette D, Forte M (2009) Axonal degeneration in multiple sclerosis: the mitochondrial hypothesis. Curr Neurol Neurosci Rep 9:411-417.

Sundgren M, Wahlin A, Maurex L, Brismar T (2015) Event related potential and response time give evidence for a physiological reserve in cognitive functioning in relapsing-remitting multiple sclerosis. J Neurol Sci 356:107-112.

Svoboda K, Yasuda R (2006) Principles of two-photon excitation microscopy and its applications to neuroscience. Neuron 50:823-839.

Takano T, Tian GF, Peng W, Lou N, Libionka W, Han X, Nedergaard M (2006) Astrocyte-mediated control of cerebral blood flow. Nat Neurosci 9:260-267.

Takeuchi H, Jin S, Wang J, Zhang G, Kawanokuchi J, Kuno R, Sonobe Y, Mizuno T, Suzumura A (2006) Tumor necrosis factor-alpha induces neurotoxicity via glutamate release from hemichannels of activated microglia in an autocrine manner. J Biol Chem 281:21362-21368.

Takeuchi H, Mizuno T, Zhang G, Wang J, Kawanokuchi J, Kuno R, Suzumura A (2005) Neuritic beading induced by activated microglia is an early feature of neuronal dysfunction toward neuronal death by inhibition of mitochondrial respiration and axonal transport. J Biol Chem 280:10444-10454.

Tamamaki N, Yanagawa Y, Tomioka R, Miyazaki J, Obata K, Kaneko T (2003) Green fluorescent protein expression and colocalization with calretinin, parvalbumin, and somatostatin in the GAD67-GFP knock-in mouse. J Comp Neurol 467:60-79.

Thome C, Kelly T, Yanez A, Schultz C, Engelhardt M, Cambridge SB, Both M, Draguhn A, Beck H, Egorov AV (2014) Axon-carrying dendrites convey privileged synaptic input in hippocampal neurons. Neuron 83:1418-1430.

Thorpe JW, Kidd D, Moseley IF, Thompson AJ, MacManus DG, Compston DA, McDonald WI, Miller DH (1996) Spinal MRI in patients with suspected multiple sclerosis and negative brain MRI. Brain 119 ( Pt 3):709-714.

Thrane AS, Rappold PM, Fujita T, Torres A, Bekar LK, Takano T, Peng W, Wang F, Rangroo Thrane V, Enger R, Haj-Yasein NN, Skare O, Holen T, Klungland A, Ottersen OP, Nedergaard M, Nagelhus EA (2011) Critical role of aquaporin-4 (AQP4) in astrocytic Ca2+ signaling events elicited by cerebral edema. Proc Natl Acad Sci U S A 108:846-851.

Tian L, Hires SA, Mao T, Huber D, Chiappe ME, Chalasani SH, Petreanu L, Akerboom J, McKinney SA, Schreiter ER, Bargmann CI, Jayaraman V, Svoboda K, Looger LL (2009) Imaging neural activity in worms, flies and mice with improved GCaMP calcium indicators. NatMethods 6:875-881.

Tomassini V, Matthews PM, Thompson AJ, Fuglo D, Geurts JJ, Johansen-Berg H, Jones DK, Rocca MA, Wise RG, Barkhof F, Palace J (2012) Neuroplasticity and functional recovery in multiple sclerosis. Nat Rev Neurol 8:635-646.

Toosy AT, Hickman SJ, Miszkiel KA, Jones SJ, Plant GT, Altmann DR, Barker GJ, Miller DH, Thompson AJ (2005) Adaptive cortical plasticity in higher visual areas after acute optic neuritis. Ann Neurol 57:622-633.

Trapp BD, Peterson J, Ransohoff RM, Rudick R, Mork S, Bo L (1998) Axonal transection in the lesions of multiple sclerosis. N Engl J Med 338:278-285.

Trop I, Bourgouin PM, Lapierre Y, Duquette P, Wolfson CM, Duong HD, Trudel GC (1998) Multiple sclerosis of the spinal cord: diagnosis and follow-up with contrast-enhanced MR and correlation with clinical activity. AJNR Am J Neuroradiol 19:1025-1033.

Trump BF, Berezesky IK (1995) Calcium-mediated cell injury and cell death. FASEB J 9:219-228.

Tsien RW, Tsien RY (1990) Calcium channels, stores, and oscillations. Annu Rev Cell Biol 6:715-760.

Tsien RY (1981) A non-disruptive technique for loading calcium buffers and indicators into cells. Nature 290:527-528.

Tsien RY, Harootunian AT (1990) Practical design criteria for a dynamic ratio imaging system. Cell Calcium 11:93-109.

Ulges A, Witsch EJ, Pramanik G, Klein M, Birkner K, Buhler U, Wasser B, Luessi F, Stergiou N, Dietzen S, Bruhl TJ, Bohn T, Bundgen G, Kunz H, Waisman A, Schild H, Schmitt E, Zipp F, Bopp T (2016) Protein kinase CK2 governs the molecular decision between encephalitogenic TH17 cell and Treg cell development. Proc Natl Acad Sci U S A 113:10145-10150.

Valenzuela RM, Costello K, Chen M, Said A, Johnson KP, Dhib-Jalbut S (2007) Clinical response to glatiramer acetate correlates with modulation of IFN-gamma and IL-4 expression in multiple sclerosis. Mult Scler 13:754-762.

Valsasina P, Rocca MA, Absinta M, Sormani MP, Mancini L, De Stefano N, Rovira A, Gass A, Enzinger C, Barkhof F, Wegner C, Matthews PM, Filippi M (2011) A multicentre study of motor functional connectivity changes in patients with multiple sclerosis. Eur J Neurosci 33:1256-1263.

van Horssen J, Witte ME, Schreibelt G, de Vries HE (2011) Radical changes in multiple sclerosis pathogenesis. Biochim Biophys Acta 1812:141-150.

Verkhratsky A, Butt A (2007) Glial Neurobilogy: A Textbook.

Wasser B, Pramanik G, Hess M, Klein M, Luessi F, Dornmair K, Bopp T, Zipp F, Witsch E (2016) Increase of Alternatively Activated Antigen Presenting Cells in Active Experimental Autoimmune Encephalomyelitis. J Neuroimmune Pharmacol.

Wekerle H, Kojima K, Lannes-Vieira J, Lassmann H, Linington C (1994) Animal models. Ann Neurol 36 Suppl:S47-53.

Wilent WB, Contreras D (2005) Stimulus-dependent changes in spike threshold enhance feature selectivity in rat barrel cortex neurons. J Neurosci 25:2983-2991.

Williams SK, Maier O, Fischer R, Fairless R, Hochmeister S, Stojic A, Pick L, Haar D, Musiol S, Storch MK, Pfizenmaier K, Diem R (2014) Antibody-mediated inhibition of TNFR1 attenuates disease in a mouse model of multiple sclerosis. PLoS One 9:e90117.

Wingerchuk DM, Carter JL (2014) Multiple sclerosis: current and emerging disease-modifying therapies and treatment strategies. Mayo Clin Proc 89:225-240.

Wojtowicz MA, Ishigami Y, Mazerolle EL, Fisk JD (2014) Stability of intraindividual variability as a marker of neurologic dysfunction in relapsing remitting multiple sclerosis. J Clin Exp Neuropsychol 36:455-463.

Wong AA, Brown RE (2006) Visual detection, pattern discrimination and visual acuity in 14 strains of mice. Genes Brain Behav 5:389-403.

Wu GF, Laufer TM (2007) The role of dendritic cells in multiple sclerosis. Curr Neurol Neurosci Rep 7:245-252.

Xie C, Lin Z, Hanson L, Cui Y, Cui B (2012) Intracellular recording of action potentials by nanopillar electroporation. Nat Nanotechnol 7:185-190.

Xu N, Li X, Zhong Y (2015) Inflammatory cytokines: potential biomarkers of immunologic dysfunction in autism spectrum disorders. Mediators Inflamm 2015:531518.

Yamahachi H, Marik SA, McManus JN, Denk W, Gilbert CD (2009) Rapid axonal sprouting and pruning accompany functional reorganization in primary visual cortex. Neuron 64:719-729.

Yang G, Parkhurst CN, Hayes S, Gan WB (2013) Peripheral elevation of TNF-alpha leads to early synaptic abnormalities in the mouse somatosensory cortex in experimental autoimmune encephalomyelitis. Proc Natl Acad Sci U S A 110:10306-10311.

Ye ZC, Wyeth MS, Baltan-Tekkok S, Ransom BR (2003) Functional hemichannels in astrocytes: a novel mechanism of glutamate release. J Neurosci 23:3588-3596.

Yuste R, Denk W (1995) Dendritic spines as basic functional units of neuronal integration. Nature 375:682-684.

Yuste R, MacLean J, Vogelstein J, Paninski L (2011) Imaging action potentials with calcium indicators. Cold Spring Harb Protoc 2011:985-989.

Zarei M, Chandran S, Compston A, Hodges J (2003) Cognitive presentation of multiple sclerosis: evidence for a cortical variant. J Neurol Neurosurg Psychiatry 74:872-877.

Zozulya AL, Ortler S, Lee J, Weidenfeller C, Sandor M, Wiendl H, Fabry Z (2009) Intracerebral dendritic cells critically modulate encephalitogenic versus regulatory immune responses in the CNS. J Neurosci 29:140-152.

Zuccato C, Cattaneo E (2009) Brain-derived neurotrophic factor in neurodegenerative diseases. Nat Rev Neurol 5:311-322.

## PUBLICATIONS IN PEER REVIEWED JOURNALS

**Pramanik G**, Ellwardt E, Jubal ER, Novkovic T, Vogt J, Luchtman D, Schmalz M, Berger Z, Kuhlmann T, Mittmann T, Zipp F, Stroh A (2016). Cortical hyperactivity beyond the immune attack: starting point of neurodegeneration. In revision – *Nature Neuroscience.*

Ulges A, Witsch EJ, **Pramanik G**, Klein M, Birkner K, Bühler U, Wasser B, Luessi F, Stergiou N, Dietzen S, Brühl TJ, Bohn T, Bündgen G, Kunz H, Waisman A, Schild H, Schmitt E, Zipp F, Bopp T (2016) Protein kinase CK2 governs the molecular decision between encephalitogenic Th17 cell and Treg cell development. *Proceedings of the National Academy of Science of the United States of America* 113:10145-10150.

Wasser B, **Pramanik G**, Hess M, Klein M, Luessi F, Dornmair K, Bopp T, Zipp F, Witsch E (2016) Increase of alternatively activated antigen presenting cells in active experimental autoimmune encephalomyelitis. *Journal of Neuroimmune Pharmacology* 11:721-732.

Schmid F, Wachsmuth L, Schwalm M, Prouvot PH, Jubal ER, Fois C, **Pramanik G**, Zimmer C, Faber C, Stroh A (2015) Assessing sensory versus optogenetic network activation by combining (o)fMRI with optical $Ca^{2+}$ recordings. *Journal of Cerebral Blood Flow & Metabolism* 36:1885-1900.

# DECLARATION

I hereby declare that the present thesis is my original work and that it has not been previously presented in this or any other university for any degree. I have appropriately acknowledged and referenced all text passages that are derived literally from or are based on the content of published or unpublished work of others, and all information that relates to verbal communications. I have abided by the principles of good scientific conduct laid down in the charter of Johannes-Gutenberg University of Mainz in carrying out the investigations described in the dissertation.

Gautam Kumar Pramanik

Mainz, Germany